How low can you go?: Implications of biological nutrient removal under low dissolved oxygen conditions in pilot-scale systems

By

Rachel Denise Stewart

A dissertation submitted in partial fulfillment of the requirements for the degree of

Doctor of Philosophy
(Civil and Environmental Engineering)

at the

UNIVERSITY OF WISCONSIN – MADISON

2023

Date of final oral examination: 05/11/2023

The dissertation is approved by the following members of the final oral committee:
Daniel R. Noguera, Professor, Civil and Environmental Engineering
Katherine D. McMahon, Professor, Civil and Environmental Engineering and Bacteriology
Timothy Donohue, Professor, Bacteriology
Mohan Qin, Assistant Professor, Civil and Environmental Engineering
Matt Seib, PhD, PE, Process Engineer, Madison Metropolitan Sewerage District

Abstract

How low can you go?: Implications of biological nutrient removal under low dissolved oxygen conditions in pilot-scale systems

By Rachel D. Stewart

Increasing energy costs and climate change necessitate an optimization of energy use at wastewater treatment plants for a sustainable future. Aeration within the biological nutrient removal (BNR) process accounts for a large portion of energy consumption at a wastewater treatment plant. As such, reducing the aeration input is considered a primary solution to reducing the energy required for wastewater treatment. While successful BNR at lower than conventional dissolved oxygen (DO) concentrations has been demonstrated, challenges remain before reduced aeration can be implemented at full-scale.

In Chapter 1, we first compared two automated aeration control strategies under low-DO conditions in two pilot-scale treatment systems. We showed that effective, year-round BNR can be achieved with both strategies by increasing the solids retention time. However, both pilot-scale processes experienced poor solids settleability during the winter. While settleability was recovered during warmer temperatures, improving settling quality under low-DO remains a challenged to be resolved. In Chapter 2, we investigated the short- and long-term effect of DO reductions on the production and emission of nitrous oxide, a potent greenhouse gas. We found that while increases in nitrous oxide production and emission immediately followed DO reductions, long-term emissions decreased after prolonged operation under low-DO conditions. Process nuisances and performance deviations (e.g. nitrite accumulation) also corresponded with increased emissions. Finally, in Chapter 3, we used genome-resolved metagenomics and metatranscriptomics to explore

the diversity and dynamics of the *Candidatus* Accumlibacter lineage, key organisms contributing to phosphorus removal from wastewater. We found that Accumulibacter community was highly diverse across time in multiple pilot-scale low-DO systems, supporting evidence that most members of this lineage have a high affinity for oxygen. The information gained in these studies expands on the feasibility and implications of low-DO wastewater treatment at full-scale and adds to our understanding of the microbial community carrying out BNR under these conditions.

Acknowledgments

We've finally made it to this moment! I say "we" because this PhD journey couldn't have been made without the countless people who have mentored, worked alongside, supported, and encouraged me. I've done my best to mention you all by name but to those whose names I have forgotten, forgive me. I'm so thankful for you all!

I first want to thank my advisors Dan Noguera and Trina McMahon. I reached out to Trina on a recommendation, as she was the "EBPR expert", super intimidated and a bit nervous. I soon found out Trina is one of the most welcoming and encouraging advisors I could have gotten. Thank you so much for your feedback, support, and patience! I thought I'd be coming to UW Madison to work on cute, small EBPR reactors, but Dan approached me with another opportunity to work on big, messy, sometimes smelly and worm-infested pilot-scale plants, and I couldn't have gotten luckier. It has been a pleasure to work with you, Dan. I have grown so much as an all-around thinker from your mentorship, feedback, and support. Thanks to you both, I feel more confident in my abilities and thoughts.

To Matt Seib, who has essentially served as a third advisor, thank you for your insight, feedback, and encouragement. I've learned so much about the entire wastewater treatment process and problem solving from you. Also, big thank you for fixing all the things!! I also have to thank other staff at the Madison Metropolitan Sewerage District. To the lab, Carol Mielke, Bill Hughes, Josh LeMoine, Jessica Schwark, Jessica McMammon, Sonia Druskill, Jenny Faust, you all have made a huge impact on the work I got to do, as your sample analyses were invaluable. Thank you for your patience as we changed our sampling plan "just one more time". Thank you to other MMSD staff that played a role in the pilot projects.

I would also like to thank the other members of my committee (Timothy Donohue and Mohan Qin) for providing feedback on my work, and the number of great professors I have had the pleasure of learning from at UW Madison.

To the many lab members that I have had the pleasure of working with and learning from, thank you. My first introduction to the Noguera and McMahon labs with Matt Scarborough and Chris Lawson pretty much sealed the deal. Thanks, you two for picking me up from the airport and sharing gummies with me, but mostly for your insight, encouragement, and conversation. Thank you to Natalie Keene Beach for leaving lab supplies to me and your insight. You were an amazing example of what it takes to manage a project as demanding as the pilots. I look forward to crossing paths again with you in the water/wastewater world! Thank you to Patricia Tran, who I consider a good friend, for your help, encouragement, and conversation over these years. And also your patience on my many questions. You are an amazing scientist and I've learned so much from you. See you on the climbing wall this weekend?.. Carly Amstadt, you were the first undergraduate student that I spoke to about working with the pilots and were amazing to work with. Thank you sooo much for your patience as I figured things out. It was amazing to see you flourish into a great engineer and someone who I learned from. Thank you, Abel Ingle and Kevin Walters, for your help and our many laughs and conversations. I'll miss you both. Thank you, Diana Mendez and Coty Weathersby, for your friendship and for making so many of my days feel more enjoyable. I missed you both when you graduated. Thank you, Elizabeth McDaniel and Ben Peterson, for continuing to answer my bioinformatics questions and being great examples for me to follow. Thank you to Amber White (for literally saving our lives that one time with your winter driving skills), Charles Olmstead, Krys Kibler, Riley Hale, Kathryn Smith, Angie Magness, Pancho Moya, Alex Linz, Robin Rohwer, Rania Bashar, and Gustavo Uribe-Santos for being great

people to work with. Thank you to the Donohue Lab members who I had an opportunity to learn from for a short time and would always help me in the lab. Thanks, Kevin Myers, for answering so many of my questions. Thank you to the many, many undergraduate research assistants that put their time and effort into the pilot projects. Morgan Keck, James Alvin, Lucas Lobreglio, Michael Liu, Trenton Weiss, Kailey Devault, Sara Neufcourt, Claire Steines, Maddie Douglas, Ellen Feigl, Anthony Radicia, Brennan Ellis, and Lillian Glacklin you all were great to work with. Finally, thank you to the Ehall lab manager, Jackie Cooper. Literally, nothing gets done without you. Thank you for being so encouraging.

I would be remiss if I didn't thank the folks at Tennessee Tech University that guided and encouraged me to this PhD path. Thank you to Tania Datta and Grace McClellan Tinker for everything! You two are a huge reason why I made it to grad school. You taught and inspired me so much.

Thank you to my friends that I have made over the years for your encouragement. Thank you to the crew I met in Madison (Theo, Alesia, Ruby, Ali, Kela, Angel, Devon, Jon, Marquel, and others that I know I'm forgetting). My time in Madison would've been a lot less enjoyable without you. Thank you to Maddie and Stephen for being great people and inviting me to go climbing; it turned into a real hobby and new way to get moving. Thank you to my "Ratchets", Chloe, Courtney, Cydnee, Danielle, and Tema, for being my sisters since middle school. Thank you to Dove for being a great friend. Your surprise mail always brought a smile to my face and gave me motivation to keep pushing.

To my SCUBA diving family, thank you all for your encouragement and support over the past 10+ years. Kamau Sadiki, Kramer Wimberly, Rebecca Hunter-Wimberly, Jay Haigler, Ernie Franklin, Chris Searles, Melody Garrett, Shirikiana Gerima, Gerald Jones, Michelle Lampkin, and

countless others I appreciate you. To the one and only Mr. Kenneth Stewart, thank you for all you have done for me and others. Your dedication to youth empowerment has inspired me so much. I hope to pay it forward and have as much of an impact on the youth as you have. You are also the reason I have such a passion for a cleaner environment.

To my family, I love and appreciate y'all so much. I would need a quite a few pages to thank you for raising me with love. To my many Aunts and Uncles, thank you for being my second, third, fourth, etc. parents. To my cousins, who I consider my siblings, thanks for your love and support. To my family that has passed on and is not with me physically for this moment, I miss you and your spirits live with me.

To my loving partner, Jasenia, thank you for supporting me. You made me feel I could do anything, even when I wasn't sure of myself. Thank you for all our laughs and being a shoulder to cry on. Also thanks for all the good (and sometimes too spicy.. haha) food. Can't wait for our next chapter!

Finally, to my parents, Janet and Paul Stewart, thank you for your love and the sacrifices you made for me. Thank you for instilling values such as hard-work and perseverance in me. Thank you all for providing a life for me that I can look back upon fondly. I love and miss you, Dad, and I know you're bragging about me. I love you Mom and look forward to our many more diving adventures to come. You're my favorite dive buddy.

Table of Contents

Abstract ..... *i*

Acknowledgments ..... *iii*

List of Figures ..... *x*

List of Supplementary Figures ..... *xii*

List of Tables ..... *xiv*

List of Supplementary Tables ..... *xv*

1 Introduction *1*

1.1 Motivation **1**

1.2 Conventional biological nutrient removal **2**

1.3 Nitrogen removal through nitrogen cycling organisms **3**

1.4 Phosphorus removal through EBPR **5**

1.5 Low-DO aeration control strategies for energy-efficient BNR **6**

1.6 Research objectives and dissertation outline **8**

1.7 References **10**

2 Pilot-scale Comparison of Biological Nutrient Removal (BNR) using Intermittent and Continuous Ammonia-Based Low Dissolved Oxygen Aeration Control Systems *12*

2.1 ABSTRACT **13**

2.2 KEYWORDS **13**

2.3 HIGHLIGHTS: **14**

2.4 INTRODUCTION **15**

2.5 MATERIALS AND METHODS **16**

2.5.1 Pilot-scale reactor operation and control 16

2.5.2 Analytical methods 23

2.5.3 Statistical analysis 24

2.6 RESULTS AND DISCUSSION **24**

2.6.1 Nutrient removal was better in the AOia than in the UCTca process 25

2.6.2 Oxygen, nitrogen species, and phosphate dynamics during intermittent aeration 29

2.6.3 Oxygen and ammonium dynamics during continuous aeration 34

2.7 CONCLUSIONS **37**

2.8 SUPPLEMENTARY MATERIAL **39**

2.9 ACKNOWLEDGMENTS **47**

2.10 REFERENCES **47**

3 Nitrous oxide (N_2O) measurements in pilot-scale plants operated under low dissolved oxygen conditions *50*

3.1 INTRODUCTION **51**

3.2 METHODS **53**

3.2.1 Pilot-scale plant operations 53
3.2.2 Solids retention time (SRT) control 55
3.2.3 DO control 56
3.2.4 Analytical Methods 57
3.3 RESULTS 59
3.3.1 Nitrification performance 59
3.3.2 Total nitrogen removal and SND 61
3.3.3 N_2O production and emissions 63
3.4 DISCUSSION 66
3.4.1 N_2O emissions immediately following DO reductions and during performance upsets 67
3.4.2 Long-term impact of low-DO on N_2O emissions 68
3.5 CONCLUSIONS 69
3.6 ACKNOWLEDGMENTS 70
3.7 REFERENCES 70
4 Metagenomic Analysis of the Candidatus Accumulibacter Genus in Biological Nutrient Removal (BNR) Pilot-Scale Plants Operated with Minimal Aeration 73
4.1 ABSTRACT 74
4.2 IMPORTANCE 75
4.3 KEY WORDS 75
4.4 INTRODUCTION 76
4.5 METHODS 78
4.5.1 Operation of pilot-scale plants 78
4.5.2 Metagenomic sequencing 82
4.5.3 Metatranscriptomic sequencing 84
4.5.4 Metagenome assembly, binning, and annotation 85
4.5.5 Phylogenetic analysis and relative abundance 86
4.5.6 *ppk1* gene phylogenetic analysis 87
4.5.7 Tetrasphaera relative abundance analysis 87
4.5.8 Metatranscriptomic data analysis 87
4.6 RESULTS AND DISCUSSION 88
4.6.1 Pilot-scale EBPR performance 88
4.6.2 Assembly of Ca. Accumulibacter draft genomes 89
4.6.3 Phylogeny of recovered Accumulibacter MAGs 94
4.6.4 Accumulibacter diversity and dynamics 98
4.6.5 Tetrasphaera abundance and diversity 103
4.6.6 Denitrification and aerobic respiration potential of the Accumulibacter population 105
4.6.7 Activity under low-DO conditions 110
4.7 CONCLUSIONS 111
4.8 Supplementary Figures 113
4.9 Acknowledgments 121
4.10 References 122
5 Conclusions and Future Directions 126
5.1 Summary 126
5.2 Explore the limit to which DO does not impact sludge settleability 127

5.3 Improve nitrous oxide sampling campaigns 128
5.4 Further analysis of BNR microbial community dynamics under low-DO conditions 128
5.5 References 129

List of Figures

Figure 1-1 Modified University of Cape Town activated sludge process. 3

Figure 1-2 The biochemical transformations which comprise the nitrogen cycle. 3

Figure 1-3 Enhanced biological phosphorus removal and canonical *Candidatus* Accumulibacter metabolism. 6

Figure 2-1 AOia pilot-scale treatment train configuration. 18

Figure 2-2 UCT-type pilot-scale treatment train configuration (UCTca). 22

Figure 2-3 Comparison of nutrient removal performance between the two pilot-scale systems. 26

Figure 2-4 Total nitrogen removal efficiency between the two pilot-scale systems. 28

Figure 2-5 Sensor recordings on days 273-279 in the AOia pilot plant. 31

Figure 2-6 Sensor NH4+ recordings on days 273-279 in tank UCT4 of the UCTca pilot plant 35

Figure 2-7 Effect of stepwise SRT changes on (A) mixed liquor total suspended solids (MLTSS) concentrations and (B) sludge volume index. 36

Figure 3-1 Biologically mediated nitrous oxide (N2O) production pathways 52

Figure 3-2 AO-G pilot-scale treatment train configuration. 54

Figure 3-3 AO-FF pilot-scale treatment train configuration. 55

Figure 3-4 Air pumping set up for measurement of N_2O gaseous emissions measurements. 58

Figure 3-5 Nitrogen removal in the AO-G pilot. 60

Figure 3-6 Nitrogen removal in the AO-FF pilot. 61

Figure 3-7 Bristle worms that were found in the mixed liquor and attached to reactor surfaces. 61

Figure 3-8 Total nitrogen removal of both pilot plants throughout the entire operation. 63

Figure 3-9 Dissolved N_2O versus the N_2O emission rate in each aerated tank of both pilot plants. 64

Figure 3-10 Effluent NO2- versus the emission factor (EF) in each of the pilot plants across DO phases 3-6 68
Figure 4-1 UCTca, AOia, AO-G, and AO-FF pilot-scale treatment train configurations 80
Figure 4-2 Maximum-likelihood genome tree of the non-redundant Accumulibacter species set97
Figure 4-3 Accumulibacter relative abundance throughout the operation of the (A) UCTca and (B) AOia pilot-scale systems..... 100
Figure 4-4 Accumulibacter relative abundance throughout operation of the (A) AO-G and (B) AO-FF pilots 101
Figure 4-5 Average abundance of MAGs in the non-redundant Accumulibacter species set relative to the total Accumulibacter population. 102
Figure 4-6 Tetrasphaera relative abundance in the (A) UCTca and (B) AOia pilots..... 104
Figure 4-7 Tetrasphaera relative abundance in the (A) AO-G and (B) AO-FF pilots. 105
Figure 4-8 Denitrification gene neighborhoods of Accumulibacter MAGs assembled in this study. 108
Figure 4-9 Relative abundance and average expression of MAG within the non-redundant Accumulibacter species set. 111

List of Supplementary Figures

Supplementary Figure 2-1Aeration control cascading loops in the AOia and UCTca pilot-scale treatment trains. 39

Supplementary Figure 2-2 Biosolids and HRT management in pilot-scale plants. 41

Supplementary Figure 2-3 Historical effluent TKN, SRT, and temperature of previous pilot plant operations at Nine Springs WWTP (Madison, WI) before the reconstruction of the two pilot plants described in this study. 42

Supplementary Figure 2-4 Nitrate sensor recordings from days 273-279 43

Supplementary Figure 2-5 Monthly average of the percent of time the intermittently aerated zones of the AOia pilot system spent in air-off mode. 44

Supplementary Figure 2-6 In-situ chemical profiles in the AOia pilot during one air-on/air-off cycle. 45

Supplementary Figure 4-1 Maximum-liklihood genome tree of all Accumulibacter MAGs assembled in this study and from Petriglieri et al. (2022) 113

Supplementary Figure 4-2 Pairwise genome-wide ANI comparisons made with fastANI 114

Supplementary Figure 4-3 Clusters of all Accumulibacter MAGs that were assembled from all 34 metagenomes and the 36 HQ MAGs compiled by Petriglieri et al. (2022). 115

Supplementary Figure 4-4 Phylogenetic tree of non-redundant *ppk1* sequences from a database compiled by McDaniel, Moya-Flores, et al. (2021), supplemented with sequences from Petriglieri et al. (2022) and Accumulibacter MAGs assembled in this study. 116

Supplementary Figure 4-5 Phylogenetic tree of all copies of the 16S rRNA sequences from the assembled Accumulibacter MAGs. 117

Supplementary Figure 4-6 Time-series relative abundance of each non-redundant Accumulibacter species in the AOia and UCTca pilot-scale plants..... 121

List of Tables

Table 3-1 SRT management throughout operation of both pilot-scale plants. 56

Table 3-2 DO control phases throughout operation of both pilot-scale plants. 57

Table 3-3 Average nitrification performance in each pilot throughout each DO operational phase. 60

Table 3-4 Extent of SND in each pilot during each DO phase. 62

Table 3-5 Average dissolved concentrations and emission rates of N_2O in the individual tanks of each pilot plant throughout operation..... 64

Table 3-6 Average emission factor from each pilot during each DO phase. 65

Table 4-1 Summary of DNA and RNA sampling. 82

Table 4-2 Pilot-scale reactor BNR performance summary 89

Table 4-3 Assembled Accumulibacter MAG statistics. 91

Table 4-4 Presence/absence of denitrification and aerobic respiration genes in MAGs assembled in this study. 106

List of Supplementary Tables

Supplementary Table 1 Pairwise comparison of TKN, TP, and TN removal efficiency before and after the installation of the variable spped influent pump on day 175. 46

1 Introduction

1.1 Motivation

Biological nutrient removal (BNR) is one of the oldest biotechnological processes used by wastewater treatment plants (WWTPs) to treat 34 billion gallons of wastewater generated, on average, every day in the U.S. [1]. BNR relies on a self-assembled microbial community to remove key nutrients such as nitrogen (N) and phosphorus (P) from wastewater. Traditional wastewater treatment has focused primarily on nutrient removal for pollutant control without much consideration of energy use. As such, conventional BNR treatment methods have a substantial energy footprint that accounts for ~3% of the total electricity load in the U.S. [2]. As society's grand challenges now include combating climate change in addition to pollution control, increasingly more WWTPs are embracing energy neutral and even energy production goals, answering the industry's call to become water resource recovery facilities (WRRFs), instead of mere WWTPs. To achieve this goal, new treatment strategies to carry out BNR effectively, efficiently, and at lower costs are necessary. Reducing the aeration inputs into the BNR process is considered a primary solution to lowering energy requirements for BNR, and successful treatment has been demonstrated under low dissolved oxygen conditions. However, practical challenges and unintended consequences remain to be solved before this strategy can be implemented. Furthermore, an understanding of the microbial community performing BNR under minimal aeration will aid in process modelling for better operation. This work aimed to understand the implications of minimal aeration strategies on the overall BNR treatment performance and the microorganisms carrying out BNR *in situ.*

1.2 Conventional biological nutrient removal

Municipal and industrial wastewater streams contain nutrients, such as N and P, that pose a risk to human and environmental health if released in excess into the environment. Eutrophication, caused by an accumulation of N and P, is one such risk that results in harmful algal blooms, fish kills, and "dead zones" in freshwater and coastal surface water bodies. In addition to eutrophication, N, P, and organic pollutants exert an oxygen demand in water as microorganisms consume these compounds, depleting the water of dissolved oxygen (DO) needed for other forms of life. By providing optimal conditions for microbial growth, WWTPs take advantage of the natural metabolism of these microorganisms to remove or transform dissolved pollutants. The activated sludge process refers to the treatment of wastewater using an enrichment culture of microorganisms, some of which are involved in BNR. Activated sludge processes can take on several different configurations to carry out BNR. One of these configurations is known as the modified University of Cape Town (UCT) process without an internal nitrate recycle which is used at the Nine Springs WWTP at the Madison Metropolitan Sewerage District in Madison, WI who have supported this research (Figure 1-1). In this configuration, the microorganisms and influent wastewater are exposed to designated anaerobic, anoxic, and aerobic zones. In each of these zones, various biochemical conversions take place to facilitate N and P removal, which are described below.

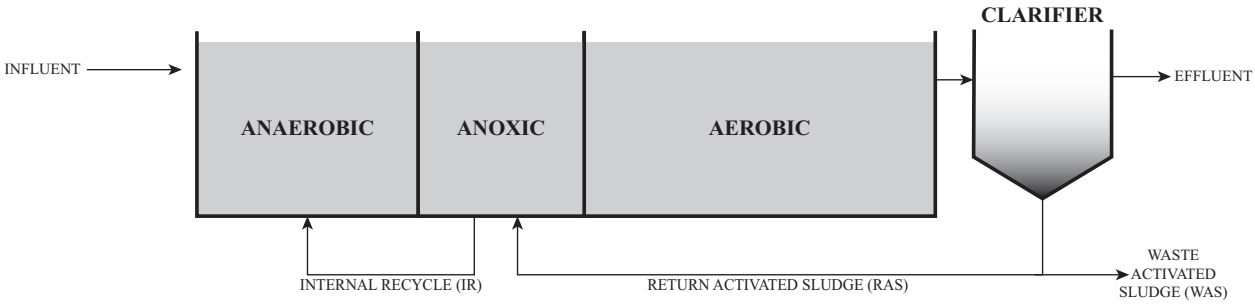

Figure 1-1 Modified University of Cape Town without internal nitrate recycle activated sludge process. The modified University of Cape Town (UCT) process without nitrate recycle configuration includes dedicated anaerobic, anoxic, and aerobic zones followed by the clarifier. In this configuration influent wastewater is sent first to the anaerobic zone along with mixed liquor recycled from the anoxic zone. The combined mixed liquor flow then enters the anoxic zone along with the return activated sludge (RAS) from the clarifier. Next, the mixed liquor enters the aerobic zone and finally enters the clarifier where the suspended solids are separated from the treated water. Most of the separated solids are pumped back into the anoxic zone as RAS, and some are removed from the system as waste activated sludge (WAS).

1.3 Nitrogen removal through nitrogen cycling organisms

Nitrogen removal in WWTPs is achieved through several biologically mediated pathways (Figure 1-2). Aerobic nitrification is typically described as a sequential biochemical process, beginning with

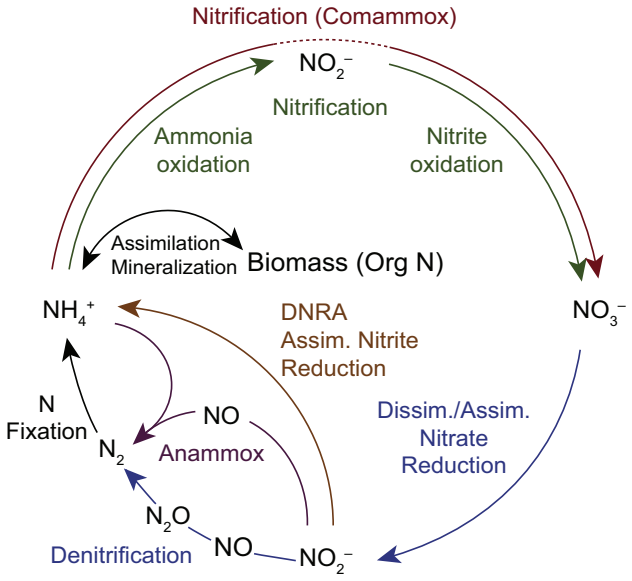

Figure 1-2 The biochemical transformations which comprise the nitrogen cycle. NH_4^+, ammonium; NO_2^-, nitrite; NO_3^-, nitrate; NO, nitric oxide; N_2O, nitrous oxide; N_2, nitrogen gas

the oxidation of ammonia to nitrite by ammonia oxidizing bacteria (AOB), followed by the oxidation of nitrite to nitrate by nitrite oxidizing bacteria (NOB). Nitrifying organisms are chemolithoautotrophs that use carbon dioxide as their carbon source, ammonia or nitrite as their energy source, and oxygen as the terminal electron acceptor for energy conservation. Genera within *Nitrosomonas* and *Nitrosospira* are commonly identified as dominant AOBs within WWTPs [3], while canonical NOBs include *Nitrobacter, Nitrospira*, and *Nitrotoga* [4, 5]. Ammonia oxidizing archaea (AOA) can also perform the first step of nitrification and have been found in wastewater treatment systems [6]. The discovery of complete ammonia oxidizing (comammox) bacteria has further challenged our conceptual understanding of N transformations in WWTPs [7, 8]. Comammox bacteria are able to perform both steps of nitrification within a single cell as their genetic content includes machinery for both ammonia and nitrite oxidation. Known comammox bacteria belong to the genus *Nitrospira* [9], and until recently remained unidentified as ammonia oxidizers because established polymerase chain reaction (PCR) primers used to identify AOB did not detect the genetic markers which were phylogenetically distinct from those of canonical ammonia oxidizers. These organisms also cannot be distinguished from *Nitrospira*-NOB based off their 16S rRNA gene or marker genes for nitrite oxidation [7, 10]. The role of comammox bacteria as ammonia oxidizers in conventional WWTPs is still being explored.

Anoxic denitrification is the process in which nitrate/nitrite is reduced to N gas through a series of sequential steps. Within BNR systems, denitrification conventionally occurs in a designated zone where nitrate/nitrite are the only electron acceptors present. Denitrification within BNR systems is carried out by ordinary heterotrophic bacteria using readily biodegradable organic carbon as the electron donor and carbon source. Because carbon is often limited in municipal wastewater influent, facilities may opt to externally add organic carbon sources such as methanol

to supplement carbon requirements. This added cost to meet treatment standards necessitates a more efficient way to remove total N. Denitrification metabolism is widespread amongst organisms, and common bacterial strains isolated from denitrifying WWTPs belong to Proteobacteria [11]. However, the dominant denitrifying population varies between systems depending upon influent characteristics and operational conditions (e.g. carbon sources).

While BNR systems are typically designed to achieve total N removal via aerobic nitrification and anoxic denitrification, new treatment configurations are being used to facilitate another bacterial N transformation pathway known as anaerobic ammonium oxidation (anammox). Anammox is a biochemical process in which ammonium is oxidized to N_2 gas using nitrite as a terminal electron acceptor in the absence of oxygen [12]. Because anammox bacteria do not require oxygen or an organic carbon source, biotechnological advancement has rapidly been made to take advantage of this energy-efficient and cost-saving N removal pathway [13].

1.4 Phosphorus removal through EBPR

Biological P removal is typically promoted under cyclic anaerobic-aerobic conditions through enhanced biological phosphorus removal (EBPR) by polyphosphate accumulating organisms (PAOs). PAOs possess the ability to accumulate and intracellularly store P in excess. One of the most detected and commonly studied PAOs in BNR systems designed for EBPR is *Candidatus* Accumulibacter phosphatis (hereinafter referred to as Accumulibacter) [14, 15]. Figure 1-2 provides a summary of the metabolism of Accumulibacter in which phosphorus removal is facilitated. Under anaerobic conditions Accumulibacter generate internal energy and reducing equivalents through the use of intracellularly stored polyphosphate and glycogen. This energy is used to take up volatile fatty acids (VFAs) and convert them into internally stored polyhydroxyalkanoate

(PHA). As polyphosphate is degraded, it is released from the cell as orthophosphate. In the presence of oxygen, the stored PHA drives growth and is used by Accumulibacter as an energy source to take up polyphosphate and replenish intracellular glycogen stores. Through these oscillations of anaerobic-aerobic conditions net P removal from the bulk liquid is achieved [16, 17].

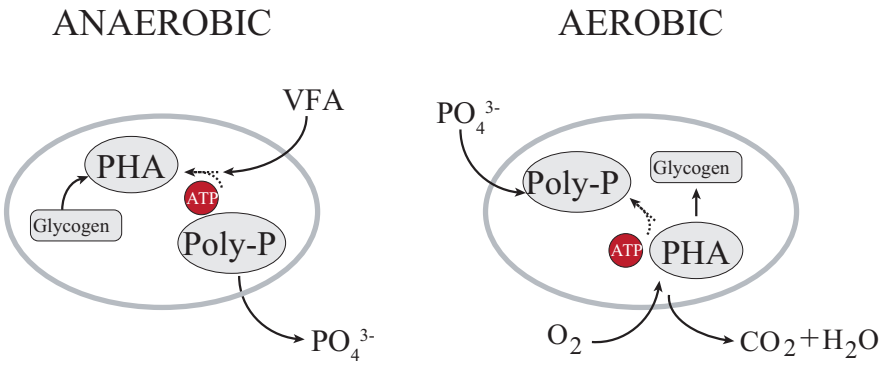

Figure 1-3 Enhanced biological phosphorus removal and canonical *Candidatus* Accumulibacter metabolism. Under anaerobic conditions, Accumulibacter uptakes volatile fatty acids (VFAs), such as acetate and convert and stores them as polyhydroxalkanoates (PHAs). Polyphosphate (poly-P) stored within the cell is used to generate ATP in order to carry out the anaerobic metabolism. Under aerobic conditions, PAOs use PHAs as a carbon an energy source to take up orthophosphate (PO_4^{3-}) and replenish poly-P and glycogen reserves.

1.5 Low-DO aeration control strategies for energy-efficient BNR

Conventional BNR systems operate at elevated levels of DO (>2.0 mg/L) in aerobic zones to ensure complete nitrification and EBPR. Because of this, aeration can account for as much as 60% of total energy consumption at a WWTP [18]. Previous research has demonstrated that this energy demand can be reduced through aeration reduction, thus decreasing the DO concentrations within the aerobic zones of the BNR process. Even further, automated process design through the use of sensor technology offers the ability to aerate as needed to meet effluent quality standards [19]. Ammonia-based aeration control (ABAC) is one such method that regulates airflow to meet the oxygen required for ammonia oxidation and has been implemented under continuous and intermittent aeration in the aerobic zone [20-22]. Combined, automated aeration under low-DO

conditions offers the potential for energy and cost savings [23], however, its application under various operational conditions remains to be refined.

While new treatment methods are being developed to minimize aeration, facilities must also strategize combining aeration reductions with meeting stricter effluent quality standards. Favorably, N and P removal has been demonstrated in studies at low-DO (<1.0 mg/L) under continuous and intermittent aeration ranging from lab- to full-scale systems [24-26]. The success of BNR under low-DO has been attributed to the ability of the microbial community to adapt to these conditions. Stable nitrification has been well documented under low-DO conditions (as low as 0.3 mg/L), and total N removal has been demonstrated to improve under low-DO as nitrification and denitrification can occur simultaneously in the same reactor, termed simultaneous nitrification-denitrification (SND) [27].

EBPR has also been successfully demonstrated under low-DO and even anoxic conditions. It has been shown that the PAOs in these systems have a high affinity for oxygen, and some possess the ability to uptake P using nitrate/nitrite as an electron acceptor. PAOs carrying out simultaneous P uptake and denitrification have been termed denitrifying PAOs (DPAOs) and provide an added benefit of carbon savings in addition to aeration savings.

While successful BNR performance has been demonstrated at low-DO conditions, the activated sludge microbial community remains to be elucidated. For example, it is not clear how the community transitions from a high- to low-DO environment or how community dynamics in low-DO systems change over time, particularly outside of highly controlled lab-scale reactors. Furthermore, DO is an important parameter that can affect the production and emission of nitrous oxide, a potent greenhouse gas. Nitrous oxide emission is a result of an imbalance between microbial production and consumption of nitrous oxide and DO has been shown to affect these

microbial pathways. In order for a reduced carbon footprint to be realized at WWTPs as a result of minimal aeration, nitrous oxide emissions must be minimized.

1.6 Research objectives and dissertation outline

This work aims to address the feasibility and implications of BNR under low-DO conditions. Specifically, this dissertation seeks to address the following research objectives:

1. Compare BNR performance using intermittent and continuous ammonia-based aeration control under low-DO in pilot-scale BNR treatment trains.
2. Assess the effectiveness of increased solids retention time to maintain nitrification during cold-water temperatures.
3. Evaluate nitrous oxide emissions when transitioning a pilot-scale BNR system from high- to low-DO and long-term effects of low-DO on nitrous oxide emissions
4. Characterize the Accumulibacter population and dynamics performing EBPR in low-DO pilot-scale BNR systems.

In **Chapter 2**, we built upon low-DO pilot-scale studies conducted under the UW-Madison and Madison Metropolitan Sewerage District cooperative agreement. We operated and compared the performance of two pilot-scale treatment trains operated with intermittent and continuous ammonia-based low-DO control. We show that both aeration control strategies are effective at BNR. While increasing solids retention time aids in nitrification during cold water operation, the settleability of the solids is negatively impacted.

In **Chapter 3**, we evaluated the effect of decreasing the DO on nitrous oxide emissions, and the long-term consequences of low-DO operation. We reconfigured the pilot-scale treatment trains and reseeded them with fresh activated sludge acclimatized to high-DO conditions from the full-

scale process. We used a stepwise reduction in DO approach and measured dissolved and gaseous nitrous oxide concentrations from the systems. We found that while immediate reductions in DO resulted in an increase in nitrous oxide production and emission, long-term operation at reduced DO concentrations is followed with reduced emissions.

In **Chapter 4**, we use metagenomics to explore the Accumulibacter population in all four pilot-scale systems operated under low-DO. Using long-read sequencing technology, we were able to assemble medium- to high-quality Accumulibacter MAGs, expanding the existing database of this lineage's genomes. We also use metatranscriptomics to investigate the populations activity under changing DO conditions.

Finally, in **Chapter 5**, we summarize the main findings from this work and outline recommendations for future research.

The research described in this dissertation was made possible through funding from the Madison Metropolitan Sewerage District, the National Science Foundation, the Graduate Engineering Research Scholars at the University of Wisconsin-Madison, and the Great Lakes Bioenergy Research Center.

1.7 References

1. EPA, U., *The Sources and Solutions: Wastewater*. 2023.
2. EPRI, *Water and Sustainability (Volume 4): US Electricity Consumption for Water Supply and Treatment—The Next Half Century.* Technical report 1006787, 2002. **4**.
3. Purkhold, U., et al., *Phylogeny of all recognized species of ammonia oxidizers based on comparative 16S rRNA and amoA sequence analysis: implications for molecular diversity surveys.* Applied and environmental microbiology, 2000. **66**(12): p. 5368-5382.
4. Lucker, S., et al., *Nitrotoga-like bacteria are previously unrecognized key nitrite oxidizers in full-scale wastewater treatment plants.* ISME J, 2015. **9**(3): p. 708-20.
5. Saunders, A.M., et al., *The activated sludge ecosystem contains a core community of abundant organisms.* ISME J, 2016. **10**(1): p. 11-20.
6. Park, H.D., et al., *Occurrence of ammonia-oxidizing archaea in wastewater treatment plant bioreactors.* Appl Environ Microbiol, 2006. **72**(8): p. 5643-7.
7. Daims, H., et al., *Complete nitrification by Nitrospira bacteria.* Nature, 2015. **528**(7583): p. 504-9.
8. van Kessel, M.A., et al., *Complete nitrification by a single microorganism.* Nature, 2015. **528**(7583): p. 555-9.
9. Daims, H., S. Lucker, and M. Wagner, *A New Perspective on Microbes Formerly Known as Nitrite-Oxidizing Bacteria.* Trends Microbiol, 2016. **24**(9): p. 699-712.
10. Pinto, A.J., et al., *Metagenomic Evidence for the Presence of Comammox Nitrospira-Like Bacteria in a Drinking Water System.* mSphere, 2016. **1**(1).
11. Lu, H., K. Chandran, and D. Stensel, *Microbial ecology of denitrification in biological wastewater treatment.* Water Res, 2014. **64**: p. 237-254.
12. Van de Graaf, A.A., et al., *Anaerobic oxidation of ammonium is a biologically mediated process.* Applied and environmental microbiology, 1995. **61**(4): p. 1246-1251.
13. Ali, M. and S. Okabe, *Anammox-based technologies for nitrogen removal: advances in process start-up and remaining issues.* Chemosphere, 2015. **141**: p. 144-153.
14. Zilles, J.L., et al., *Involvement of Rhodocyclus-related organisms in phosphorus removal in full-scale wastewater treatment plants.* Applied and environmental microbiology, 2002. **68**(6): p. 2763-2769.
15. He, S. and K.D. McMahon, *Microbiology of 'Candidatus Accumulibacter' in activated sludge.* Microb Biotechnol, 2011. **4**(5): p. 603-19.
16. McMahon, K.D., S. He, and A. Oehmen, *The microbiology of phosphorus removal by activated sludge*, in *Microbial ecology of activated sludge*. 2010, IWA Publishers. p. 281-319.
17. Seviour, R.J., T. Mino, and M. Onuki, *The microbiology of biological phosphorus removal in activated sludge systems.* FEMS microbiology reviews, 2003. **27**(1): p. 99-127.
18. Appelbaum, B., *Water and sustainability: US electricity consumption for water supply and treatment-The next half century, 2002.* Palo Alto, CA.
19. Åmand, L., G. Olsson, and B. Carlsson, *Aeration control – a review.* Water Science and Technology, 2013. **67**(11): p. 2374-2398.
20. Rieger, L., et al., *Ammonia-based feedforward and feedback aeration control in activated sludge processes.* Water Environ Res, 2014. **86**(1): p. 63-73.
21. Regmi, P., et al., *Control of aeration, aerobic SRT and COD input for mainstream nitritation/denitritation.* Water Res, 2014. **57**: p. 162-71.

22. Regmi, P., et al., *Ammonia-based intermittent aeration control optimized for efficient nitrogen removal.* Biotechnol Bioeng, 2015. **112**(10): p. 2060-7.
23. Medinilla, V.R., et al., *Impact of Ammonia-Based Aeration Control (ABAC) on Energy Consumption.* Applied Sciences, 2020. **10**(15).
24. Keene, N.A., et al., *Pilot plant demonstration of stable and efficient high rate biological nutrient removal with low dissolved oxygen conditions.* Water Res, 2017. **121**: p. 72-85.
25. Camejo, P.Y., et al., *Candidatus Accumulibacter phosphatis clades enriched under cyclic anaerobic and microaerobic conditions simultaneously use different electron acceptors.* Water Res, 2016. **102**: p. 125-137.
26. Jimenez, J., et al., *Nitrite-shunt and biological phosphorus removal at low dissolved oxygen in a full-scale high-rate system at warm temperatures.* Water Environment Research, 2020. **92**(8): p. 1111-1122.
27. Münch, E.V., P. Lant, and J. Keller, *Simultaneous nitrification and denitrification in bench-scale sequencing batch reactors.* Water Research, 1996. **30**(2): p. 277-284.

2 Pilot-scale Comparison of Biological Nutrient Removal (BNR) using Intermittent and Continuous Ammonia-Based Low Dissolved Oxygen Aeration Control Systems

This chapter has been published under the same title as:

Rachel D. Stewart, Rania Bashar, Carly Amstadt, Gustavo A. Uribe-Santos, Katherine D. McMahon, Matt Seib, Daniel R. Noguera. *Water Sci Technol.* 15 January 2022; 85 (2): 578–590. doi: https://doi.org/10.2166/wst.2021.630

Author contributions

RDS, RB, MS, DRN developed the research plan. RB performed process modelling for improved year-round treatment. RDS, RB, CA, GUS, and MS operated and collected samples from the pilot-scale plants. RDS performed data analyses. RDS, MS, and DRN wrote the manuscript with input from all authors.

2.1 ABSTRACT

Sensor driven aeration control strategies have recently been developed as a means to efficiently carry out biological nutrient removal (BNR) and reduce aeration costs in wastewater treatment plants. Under load-based aeration control, often implemented as ammonia-based aeration control (ABAC), airflow is regulated to meet desired effluent standards without specifically setting dissolved oxygen (DO) targets. Another approach to reduce aeration requirements is to constantly maintain low-DO conditions and allow the microbial community to adapt to the low-DO environment. In this study, we compared the performance of two pilot-scale BNR treatment trains that simultaneously used ABAC and low-DO operation to evaluate the combination of these two strategies. One pilot plant was operated with continuous ABAC while the other one used intermittent ABAC. Both processes achieved greater than 90% total Kjehldal nitrogen (TKN) removal, 60% total nitrogen removal, and nearly 90% total phosphorus removal. Increasing the solids retention time (SRT) during the period of cold (~ 12 ^{o}C) water temperatures helped maintain ammonia removal performance under low-DO conditions. However, both processes experienced poor solids settling characteristics during winter. While settling was recovered under warmer temperatures, improving settling quality remains a challenge under low-DO operation.

2.2 KEYWORDS

Aeration Control, Biological nutrient removal, Dissolved Oxygen, Enhanced biological phosphorus removal, Nitrification, Solids volume index

2.3 HIGHLIGHTS:

- The performance of two pilot-scale reactors operated under continuous and intermittent low-DO aeration were compared.
- A stepwise increase in SRT led to improved nitrification during cold water periods.
- Intermittent aeration led to improved total nitrogen removal without a loss in EBPR.
- Deteriorated sludge settleability under low-DO remains a challenge to be solved.

2.4 INTRODUCTION

Nitrogen (N) and phosphorus (P) are key nutrients that must be removed from wastewater as they can cause eutrophication when introduced into surface waters. Traditional biological nutrient removal (BNR) systems employed at wastewater treatment plants (WWTPs) typically remove N through a two-stage process consisting of aerobic nitrification and anoxic denitrification [1]. P is removed under cyclic anaerobic-aerobic conditions through enhanced biological phosphorus removal (EBPR) by polyphosphate accumulating organisms (PAOs) [2]. Conventionally, extensive aeration is implemented for both processes, and in some cases, supplemental carbon is added to reach treatment requirements. These requirements are driving efforts to modify operating configurations with the goal of reducing energy and carbon requirements in BNR systems [3-5].

Automated process control through the use of online sensors has gained interest as a means to reduce aeration energy consumption while meeting effluent quality standards [6-8]. One such control strategy is ammonia-based aeration control (ABAC) where airflow is regulated to satisfy oxygen requirements for biological ammonia oxidation. ABAC has been implemented through continuous and intermittent aeration and has been shown to decrease aeration energy demands and increase total N removal in both aeration methods [9, 10]. Intermittent ABAC was originally employed as a strategy to achieve nitrite shunt, which may result in up to a 25% and 40% reduction in oxygen and chemical oxygen demand (COD) requirements, respectively [9]. However, recent research has shown nitrite shunt may not be achieved in all intermittently aerated BNR systems [11, 12]. In general, continuous or intermittent ABAC has been implemented to maintain high dissolved oxygen (DO) conditions during the aerated periods [9]. In contrast, we are interested in the use of ABAC in combination with intermittent and continuous aeration in systems aimed at

maintaining low-DO conditions (≤ 0.7 mg/L) during aerated periods. This combination of operational conditions could achieve ecological stability and further reduce aeration energy requirements.

In this study we investigated the use of continuous and intermittent ABAC to control aeration in low-DO BNR systems. We used two pilot-scale plants that received primary effluent from the full-scale Nine Springs WWTP at the Madison Metropolitan Sewerage District (MMSD) in Madison, WI, USA. Both of these pilot plants had multiple tanks in series to simulate plug-flow conditions which are not often studied, yet are the most common process used to treat municipal wastewater. We were particularly interested in process performance during the winter period, when wastewater temperature in Madison, WI, USA, can reach below 12° C and maintaining nitrification during low-DO operation is of concern [13]. We were also interested in evaluating pilot plant results with influent flow rates that mimicked full-scale flow variations since most pilot plant research to date does not consider flow variations in the operation of reactors given the intrinsic complexities of implementing this option.

2.5 MATERIALS AND METHODS

2.5.1 Pilot-scale reactor operation and control

2.5.1.1 Anoxic-oxic (AO) reactor with intermittent aeration (AOia)

A pilot-scale treatment train, operated at the Nine Springs WWTP (Madison WI), is configured as an anoxic-oxic with intermittent aeration (AOia) process (**Figure 1-1**). The AOia pilot plant was seeded with activated sludge from the full-scale plant (configured as a University of Cape Town process without internal nitrate recycle) in October 2018 and initially operated at conditions aimed at achieving nitrite shunt. The plant was converted to the intermittent aeration

operational strategy on May 1st, 2019 (day 0 in this study) and was evaluated for 483 days, until August 25th, 2020. Between days 0 and 341 the pilot plant system (**Figure 2-1A**) consisted of a non-aerated tank, three intermittently aerated tanks that maintained low-DO conditions (≤ 0.7 mg/L) when aerated, and a high DO polishing aerated tank with a combined total volume of 2,080 L. On day 342, the system was reconfigured to achieve better plug-flow conditions by replacing the one unaerated 473 L tank with four 140-L tanks (**Figure 2-1B)**. The high DO polishing aerated tank was also replaced by a larger volume tank for a total pilot reactor volume of 2,280 L. Throughout the entire operation the system also included a 1,210 L secondary clarifier. Primary effluent from the full-scale WWTP was used as influent to the pilot-scale reactor. Influent flow rates were aimed to maintain a hydraulic retention time (HRT) comparable to that of the full-scale plant. To achieve this, during the first five months of operation (days 0 – 174), the influent flow rate was manually controlled and adjusted daily; afterwards, the plant was equipped with a variable speed influent pump that was automatically controlled to mimic real-time changes in full-scale influent flows. During the entire operational period, the daily average influent flow rates were between 2.50 – 6.80 m^3/day (**Supplementary Figure 2-2A)**, corresponding to daily average HRT of 13.1 ± 3.0 hours (**Supplementary Figure 2-2B**).

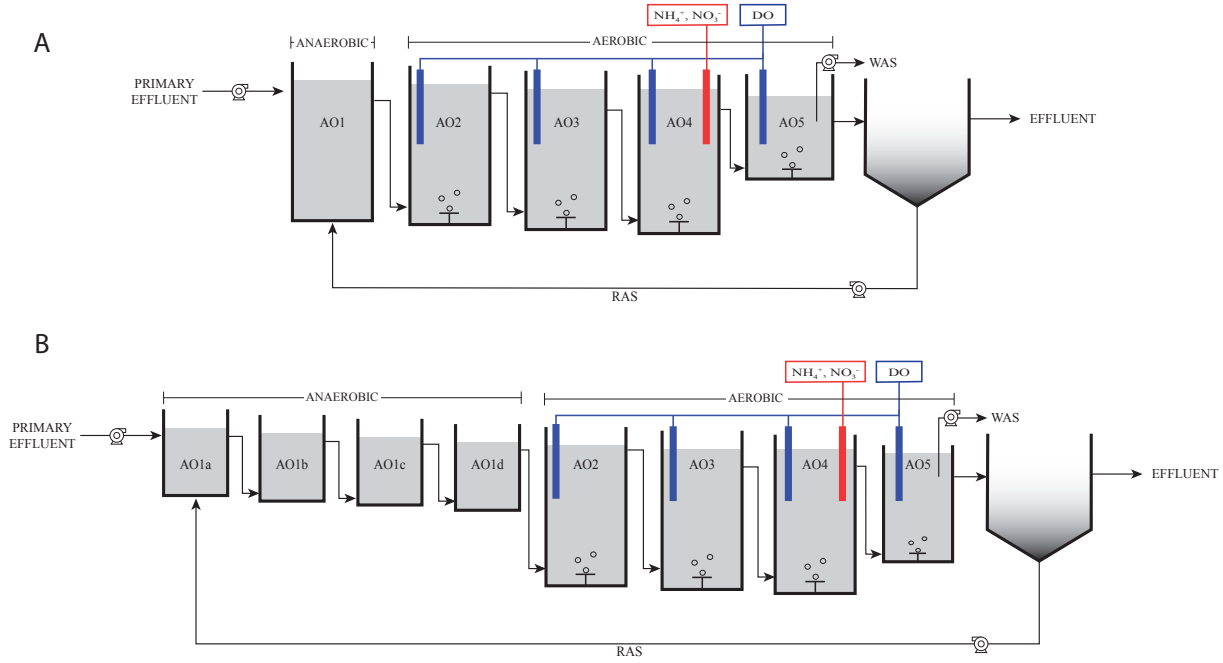

Figure 2-1 AOia pilot-scale treatment train configuration. AOia pilot-scale treatment train configuration showing anaerobic and aerobic tanks, and the clarifier. Return activated sludge (RAS) was pumped from the bottom of the clarifier into the first unaerated tank. Waste activated sludge (WAS) was pumped out of tank AO5. Sensors (NH_4^+, NO_3^-, NO_2^- and DO) and aeration control details are shown in **Figure S1A**. (A) During the first 341 days of operation the system included an unaerated tank (AO1), three tanks under the intermittent ABAC regime (AO2, AO3, and AO4), and one high-DO polishing tank (AO5). (B) AOia reconfiguration after day 341. Tank AO1 was replaced by four smaller tanks.

Return activated sludge (RAS) was recycled back into the first non-aerated tank at an average of 1.7 m^3/day between days 0 – 158, 3.2 m^3/day between days 159 – 287, and 5.9 m^3/day between days 288 – 483 (**Supplementary Figure 2-2C**). The increase in RAS flow rate throughout the study was implemented in response to the development of poor settling sludge that required faster pumping out of the clarifier to prevent solids overflow into the effluent.

2.5.1.1.1 Solids retention time (SRT) variation for winter operation

The SRT was controlled by implementing waste activated sludge (WAS) removal from the last aerated tank and calculating the sludge exiting the plant via the WAS, the effluent, and in

any accumulated foam that was manually removed from tank water surfaces. WAS flow rates were adjusted daily using a target SRT and measurements (three times per week) of suspended solids in WAS, effluent, and removed foam.

We implemented a stepwise increase to the SRT starting in fall 2019 by reducing the WAS flow rate (**Supplementary Figure 2-2E**). This was carried out over the course of 6 weeks to bring the SRT from about 10 days to 16 days (day 161 – day 203). Then, a stepwise SRT decrease began in February 2020 (day 292) to bring the plant back to 10 days SRT by April 2020, for warmer weather operation.

2.5.1.1.2 Aeration control loops and sensors

Intermittent aeration in the AOia pilot reactor occurred in the three middle aerated tanks (AO2, AO3, and AO4 in **Figure 2-1**) by using proportional-integral (PI) control according to cascading control loops (**Supplementar Figure 2-1A**). The primary control loop, NH_4^+ Loop 1, determines aerated and un-aerated periods using NH_4^+ and NO_3^- concentrations as input variables. NH_4^+ Loop 1 initiates "air-on" mode until a minimum operator-specified NH_4^+ concentration within tank AO4 has been reached, at which point the "air-off" mode is initiated by automatically closing the air valve in tanks AO2, AO3, and AO4. The air-on mode resumes once an operator-defined maximum NH_4^+ setpoint has been reached, the NO_3^- concentration has reached a maximum allowable decrease, or NO_3^- is at a concentration of zero. By this control logic, nitrification is prioritized over denitrification by setting a maximum allowable NH_4^+ concentration and limiting the unaerated periods based on amount of NO_3^- denitrified. The NH_4^+ and NO_3^- sensors were placed in the last intermittently aerated tank to perform feedback control which enacts system control based on the difference in a measured variable and a desired setpoint [8] For the majority of the operation the high and low NH_4^+ concentration limits were set

at 2 and 5 mg NH_4^+-N/L, respectively. These setpoints were established to ensure NH_4^+ removal in the final high-DO polishing tank and to also operate the sensor in an environment with sufficient NH_4^+ to ensure reliable signal. The maximum allowable NO_3^- concentration decrease was set at 3.5 mg NO_3^--N /L to achieve optimal conditions for denitrification while also maintaining sufficient aerated periods for nitrification and phosphorus removal. While in air-on mode the control loop selects a user-defined DO setpoint that is to be achieved in each of the intermittently aerated tanks. The DO setpoint was 0.7 mg/L.

The secondary control loops (DO Loop 2, DO Loop 3, and DO Loop 4) are used to maintain the DO setpoint determined from the NH_4^+ Loop 1 by adjusting the air flow rate to each tank using motorized proportional air valves. If the DO concentration is above the DO setpoint, the air valve position is reduced, and vice versa. During aerated periods, compressed air was provided though a fine-bubble membrane diffuser (Sanitaire, Brown Deer, WI) installed at the base of each aerobic tank. The final high-DO polishing aerated tank, intended to remove any residual NH_4^+ from the prior intermittently aerated tank, is aerated to maintain a DO concentration of 2.0 mgO_2/L using an on/off air solenoid valve.

Online sensors used for the control loops included an ion selective electrode to record NH_4^+ (AmmoLyt Plus 700 IQ, YSI, Yellow Springs, OH), UV-vis sensor for NO_3^- and NO_2^- (NiCaVis 701 IQ, YSI, Yellow Springs, OH), and optical DO sensors (IQ SensorNet FDO 701, YSI, Yellow Springs, OH).

2.5.1.2 University of Cape Town (UCT)-type reactor with continuous aeration (UCTca)

A pilot-scale system simulating the configuration of the full-scale process at MMSD but operated with continuous low-DO conditions (**Figure 2-2A**) was also operated, for comparison with the AOia pilot plant. This process, referred to as the UCTca pilot plant, is a modification of

the UCT configuration that does not use internal recycle [3, 14]. The pilot plant was seeded in September of 2018 with activated sludge from the full-scale process. However, most results reported here correspond to May 1st, 2019 (day 0) thru August 25th, 2020 (day 483). The anaerobic, anoxic, and aerated portions of this pilot plant initially consisted of 5 tanks for a combined total volume of 2,180 L. The anaerobic portion of the plant was reconfigured on day 446 to achieve better plug-flow conditions by replacing a 284-L tank with three 140-L tanks (**Figure 2-2B**). In addition, the volume of the anoxic portion was decreased from 473 L to 140 L for a total pilot reactor volume of 1,980 L. A 1,010 L secondary clarifier was also included for the entire operation. Similar to the operation of the AOia pilot plant, influent flow rates were initially adjusted manually in the UCTca and starting at day 174 they were controlled using variable speed influent pumping that automatically changed flow rates to mimic real-time changes in full-scale influent flows (**Supplementar Figure 2-2A**). The influent flow rate into the UCTca reactor varied between 2.14 and 7.90 m^3/day resulting in an average HRT of 14.0 ± 2.1 hours. As with the AOia pilot plant, the RAS flow rate was increased in response to poor sludge settling characteristics (**Supplementar Figure 2-2B**) and stepwise SRT adjustments were implemented to achieve a higher SRT during the low temperature period (**Supplementar Figure 2-2C**) as described above for the AOia pilot plant.

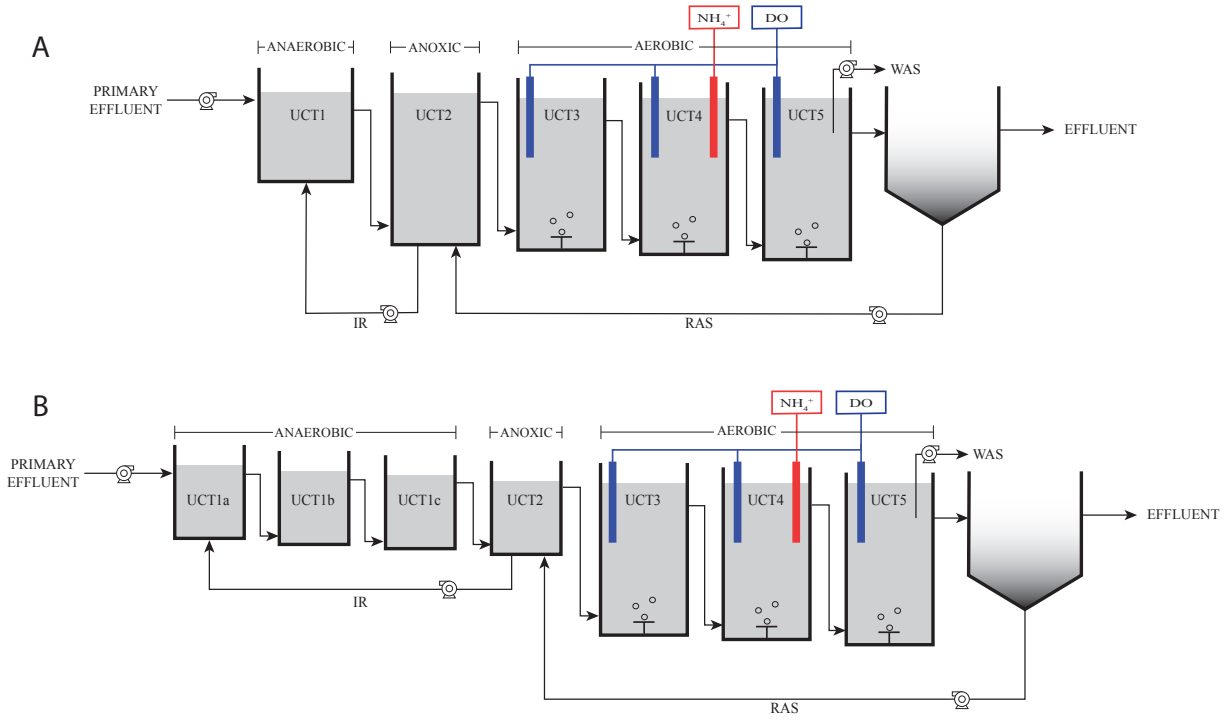

Figure 2-2 UCT-type pilot-scale treatment train configuration (UCTca). UCT-type pilot-scale treatment train configuration (UCTca) showing anaerobic, anoxic, and aerobic tanks, the clarifier, the return activated sludge (RAS) line from the bottom of the clarifier and into the anoxic tank, and an internal recycle (IR) line from the anoxic tank into the first anaerobic tank. Waste activated sludge (WAS) was pumped out from the last aerobic tank. Sensors (NH_4^+ and DO) and aeration control details are shown in **Supplementary Figure 2-1B**. (A) During 446 days of operation the UCTca system included one anaerobic tank (UCT1), one anoxic tank (UCT2), two aerobic tanks under continuous ABAC (UCT3 and UCT4) and one higher DO polishing tank (UCT5). (B) After 446 days of operation, the anaerobic tank was replaced with 3 smaller anaerobic tanks and the anoxic tank was reduced in size to better represent plug flow conditions.

Aeration in this pilot plant was also controlled based on NH_4^+ concentration. An NH_4^+ online sensor (described above) was installed in the second aerated tank of the UCTca treatment train (tank UCT4 in **Figure 2-2**). Each of the three aerated tanks was equipped with a DO sensor (described above).

Similar to the AOia configuration, aeration control within the UCTca pilot plant was executed using a PI control loop based on NH_4^+ concentration. However, aeration was

continuous and a single NH_4^+ concentration was targeted (**Supplementary Figure 2-1B**). The first loop, NH_4^+ Loop 1, adjusts the DO setpoint (allowed to be between 0.1 and 0.6 mg/L) in the two middle aerated tanks to maintain an operator-defined NH_4^+ setpoint in the second aerated tank (tank UCT4). If NH_4^+ concentration decreases past the setpoint, the DO setpoint also decreases, and vice versa. Throughout the operation described in this study, an NH_4^+ concentration of 5 mg NH_4^+-N/L in tank UCT4 was targeted. The secondary control loops (DO Loop 2 and DO Loop 3) adjust the position of the proportional air valve to achieve the DO setpoint (in tanks UCT3 and UCT4) defined by the primary NH_4^+-based loop. The last aerated tank (UCT5) was operated under a separate control loop to initially maintain a DO of 0.6 mg/L through day 218, at which point it was switched to maintain a DO concentration of 1.0 mgO_2/L to slow denitrification in the clarifier.

2.5.2 Analytical methods

Filtered influent and effluent grab samples from both pilot plants were collected 3 and 6 times per week, respectively. Grab samples from each tank in both pilots were collected once per week. Grab samples from the influent, effluent, AO5, LD1a (or LD1), and LD5 were also collected for solids analysis. For analyses of soluble components, samples were immediately filtered through a 0.45-micron filter (Nitrocellulose Membrane Filters, EMD Millipore Corp., Darmstadt, Germany) and stored at 4°C until further analysis. Unfiltered samples were used for solids measurements.

Total suspended solids (TSS), volatile suspended solids (VSS), filtered total Kjeldahl nitrogen (TKN), and filtered total phosphorus (TP) were measured according to standard methods [15]. Nitrite (NO_2^- -N) and nitrate (NO_3^--N) were measured using high performance liquid chromatography (HPLC) as described elsewhere [3].

2.5.3 Statistical analysis

Statistical significance analyses to compare the performance between the AOia and UCTca systems were performed in R [16]. A Shapiro-Wilk test was performed to determine whether a dataset was normally distributed. For normally and non-normally distributed data a *t* test and a Wilcoxon rank-sum test were performed, respectively. A p-value less than 0.05 suggests the difference in variables is statistically significant.

2.6 RESULTS AND DISCUSSION

Experimentation at the pilot-scale is intended to provide experimental observations to determine whether a process is ready for full-scale implementation. Ideally, wastewater treatment research at the pilot-scale should consider the expected variations in organic and nutrient loadings and the fluctuations in flow rates and temperatures. In addition, testing wastewater treatment processes at the pilot-scale provide opportunities for evaluating other potential challenges to full-scale implementation, such as sludge bulking and foaming. Our pilot-scale research program has considered variations in wastewater characteristics and water temperature by tapping directly into primary effluent from the full-scale WWTP and housing the pilot plants in locations that are not temperature controlled [3, 17].

Since the demonstration that nitrification can be successfully implemented using low-DO conditions [18] and the recognition that BNR operated under low-DO is a feasible approach to reduce energy use during wastewater treatment, approaches to control aeration using sensor technology have emerged [7, 11]. Aeration control based on NH_4^+ concentrations has gained momentum as a practical approach for automating aeration while maintaining desirable water quality standards [19]. The recent attention to ABAC with continuous or intermittent aeration [11,

[20] prompted us to perform a comparison of these two aeration control technologies in pilot plants that simulate the general layout of common full-scale plug flow BNR systems operated in a temperate climate and under low-DO conditions. The most important observations in this comparison are described and discussed below.

2.6.1 Nutrient removal was better in the AOia than in the UCTca process

The AOia and UCTca pilot plant performance was assessed over a period of time that included summer and winter water temperatures (minimum below 12 ºC and maximum above 25.0 ºC) (**Supplementary Figure 2-2A)**. Under the different aeration modes employed, both plants exhibited effective nitrification, although, the extent of TKN removal was slightly better in the AOia plant than in the UCTca plant (**Figure 2-3A**). Influent filtered TKN was 34.3 ± 6.5 mg TKN/L. The AOia system achieved an average effluent TKN of 1.82 ± 1.34 mg TKN/L, equivalent to a 95% removal efficiency. The UCTca reactor experienced a higher average effluent TKN of 2.16 ± 1.09 mg TKN/L, a significantly different result ($p = 8.4e-06$) that corresponds to a removal efficiency of 93%. This TKN removal efficiency was consistent throughout the operational period, indicating that the practice of increasing SRT as winter approaches was effective and eliminated earlier problems with nitrification when the SRT was not preventively increased (**Supplementary Figure 2-3**). The better nitrification observed in the AOia plant could be due to the polishing tank in the AOia operated at a higher DO concentration (2 mg/L) than the tank in the UCTca plant (1 mg/L).

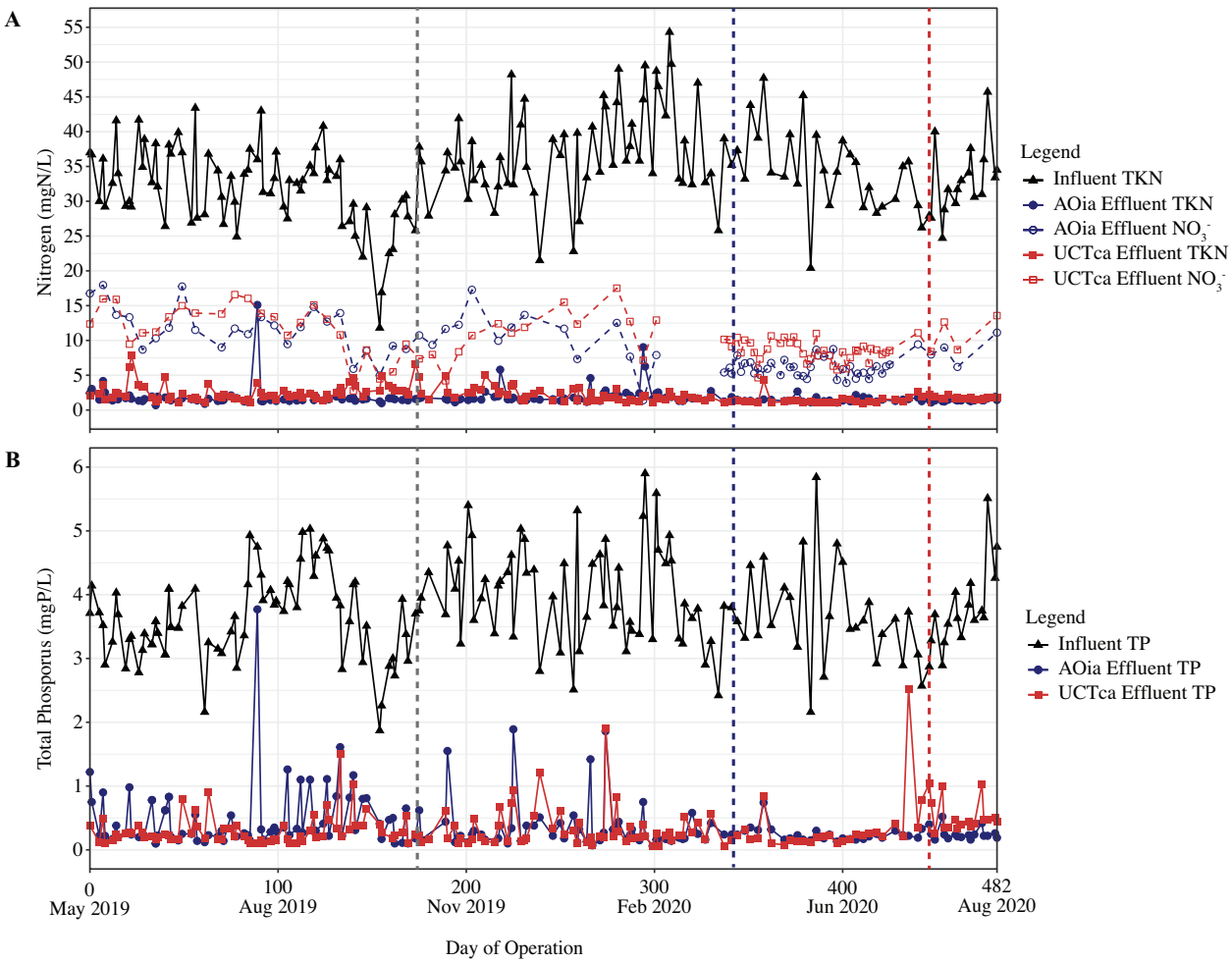

Figure 2-3 Comparison of nutrient removal performance between the two pilot-scale systems. Comparison of nutrient removal performance between the two pilot-scale systems. Blue and red dashed vertical lines indicate the AOia and UCTca configuration change, respectively. The grey dashed vertical line indicates the change to variable influent flows, and the blue and red lines indicate when the reactor configurations were changed in the AOia and the UCTca plants, respectively. (A) Influent and effluent total Kjehldal nitrogen (TKN) and effluent nitrate (NO_3^-) in filtered samples. To simplify the figure, nitrite was (NO_2^-) was not plotted, but concentrations on average were less than 1.0 mg/L. Note that the lack of nitrate data for 36 days after Feb 2020 was due to the inability to perform these tests due to the covid-19 pandemic. (B) Total phosphorus (TP) in filtered samples.

Effluent nitrate concentrations (**Figure 2-3A**) were also statistically different (p = 1.7e-03) in both plants, averaging 8.60 ± 3.57 mg N/L in the AOia and 10.06 ± 3.09 mg N/L in the UCTca, respectively. While there was not a clear difference in effluent nitrate concentrations during the first half of pilot plant operation, effluent nitrate concentrations in the AOia became

consistently lower than in the UCTca after 231 days of operation. Neither pilot plant showed nitrite accumulation in the effluent. In the AOia plant, effluent nitrite was 0.23 ± 0.16 mg N/L, and in the UCTca it was 0.30 ± 0.23 mg N/L, results that are not statistically different ($p = 0.38$).

With better TKN removal and lower effluent nitrate concentrations in the AOia, total nitrogen [21] removal was also statistically different in the two pilot plants. The AOia treatment train achieved an average TN removal efficiency of 68%, compared to 63% in the UCTca train ($p = 0.004$) (**Figure 2-4A**). With the configuration of these pilot plants, denitrification occurs in two different locations: the unaerated zones at the head of each plant and either the continuously aerated low-DO zone in UCTca or the intermittently aerated zone in the AOia. Using a mass balance approach (i.e., the difference between TN in the influent, unaerated zones, and the effluent), we evaluated the extent of denitrification in the unaerated and aerated zones on a mass per day basis. Total denitrification within the AOia (105 ± 34 gN/day) was greater than in the UCTca (94 ± 33 gN/day) pilot plant, a statistically insignificant difference ($p = 0.074$). The contribution of unaerated and aerated zones to denitrification was also estimated (**Figure 2-4B**). In this case, denitrification in the unaerated zones was statistically higher ($p = 2.0e\text{-}12$) in the UCTca pilot (47 ± 14 gN/day) than in the AOia pilot (29 ± 12 gN/day). The difference in the unaerated zone denitrification could be attributed to RAS flow rates, since they were higher in the UCTca pilot system for most of the operational period (**Supplementary Figure 2-2B**). Conversely, the opposite was true for denitrification attributed to the low-DO (47 ± 32 gN/day) or intermittent zones (76 ± 32 gN/day), likely because the cyclic anoxic periods experienced during intermittent aeration in the AOia pilot create more opportunity for denitrification than the low-DO conditions in the UCTca. Denitrification in the aerated zones varied widely in both pilots, with minimal to no SND occurring in the UCTca pilot on some days, although

denitrification in these zones substantially increased when the flows into the pilot plants were set to mimic the flow variations observed in the full-scale plant (**Figure 2-4B**).

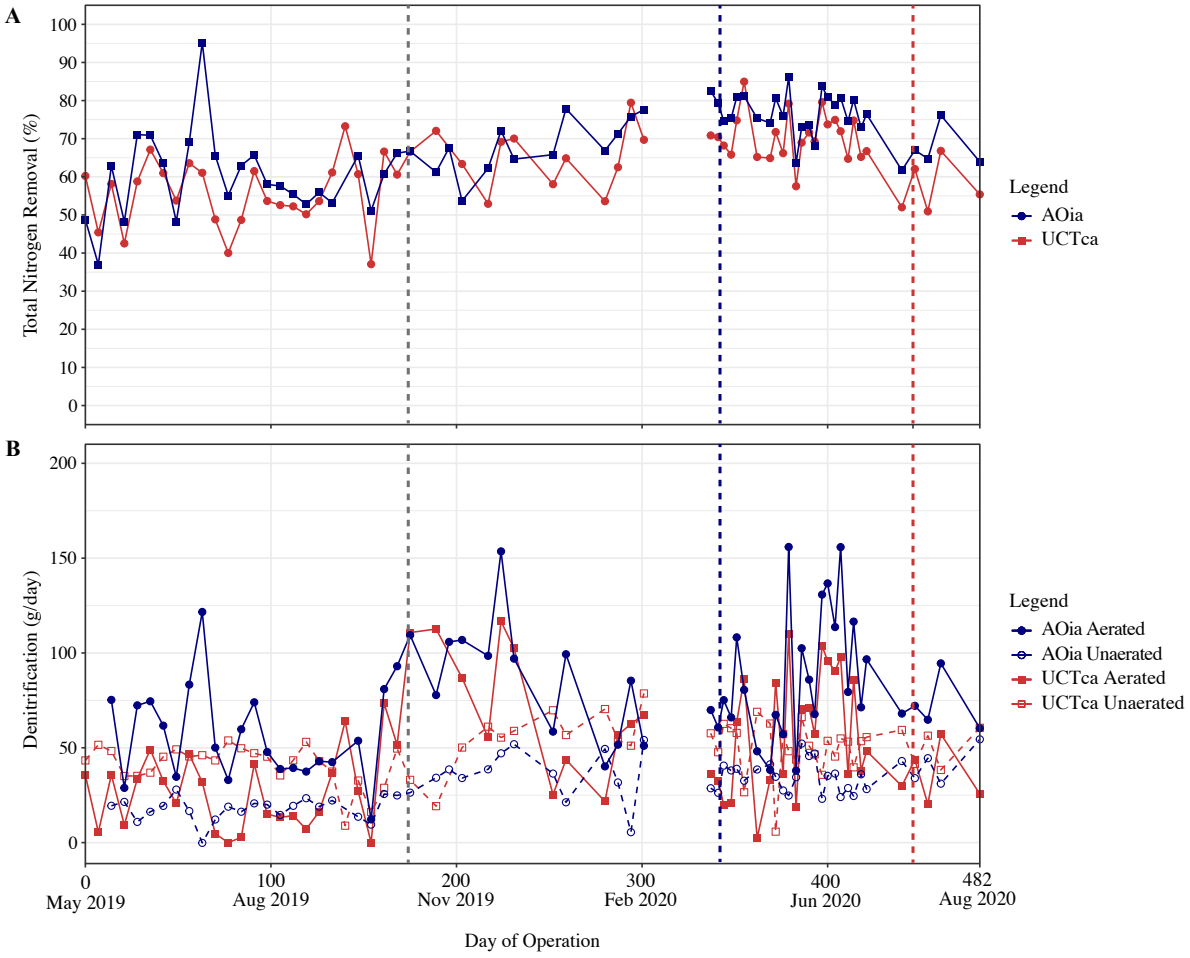

Figure 2-4 Total nitrogen removal efficiency between the two pilot-scale systems. Total nitrogen removal efficiency between the two pilot-scale systems reveals the AOia pilot plant achieves better TN removal than the UCTca pilot plant. Dashed vertical lines indicate the change to variable flow rates in both plants (grey) and configuration changes in AOia (blue) and UCTca (red). (A) Comparison of TN removal efficiency, (B) Comparison of denitrification in unaerated and aerated zones. Note that the lack of data for 36 days after Feb 2020 was due to the inability to perform nitrite and nitrate these tests due to the covid-19 pandemic.

Biological P removal, which is known not to be affected by low-DO conditions [3], was statistically similar in both plants (**Figure 2-3B**). Influent filtered TP throughout the course of

operation was 3.8 ± 0.7 mg/L. Effluent filtered TP for the AOia and UCTca reactors were statistically similar, at 0.4 ± 0.4 mg TP/L and 0.3 ± 0.3 mg TP/L, respectively ($p = 0.24$).

A final observation regarding nutrient removal is that the implementation of flow variability in the middle of the research period did not appear to negatively affect N or P removal efficiencies. Pairwise comparisons of TKN, TN, and P removal efficiencies before and after implementation of flow variability shows no significant statistical decrease in efficiency after flow variability implementation (**Supplementary Table 2-1**). Rather, the comparisons show either no statistically significant differences, or statistically significant improvements in efficiency. This result is reassuring since most pilot plant research to date does not consider the flow variations in the operation of reactors given the intrinsic complexities of implementing this option.

2.6.2 Oxygen, nitrogen species, and phosphate dynamics during intermittent aeration

Online chemical analysis sensors were used to carry out intermittent ABAC and gather additional high-frequency data in the AOia pilot. A plot of sensor recordings taken from day 273 to day 279 is shown in **Figure 2-5**, which is typical of daily trends after the flow rate was switched to mimic flow changes in the full-scale plant. Several important characteristics of the intermittent ABAC control strategy are depicted in **Figure 2-5**. First, the reported HRT from the sensor control unit represents the fluctuations in flow experienced by the pilot plant including the expected diurnal cycles and sudden flow fluctuations when pumping stations turn on and off (**Figure 2-5A**). Second, the sensor readings for NH_4^+ in tank AO4 show consistent cyclic NH_4^+ concentrations between the setpoints of 2 and 5 mg/L (**Figure 2-5B**), which effectively sets the aeration on/off cycles in tanks AO2, AO3, and AO4. Throughout the entire operation the average DO during air-on periods in tanks AO2, AO3, and AO4 were 0.55, 0.58, 0.64 mgO_2/L,

respectively. The final high-DO polishing tank maintained average DO concentration of 1.78 mg/L throughout the operation. Third, nitrate concentrations fluctuate not only in response to the air-on/off pattern, but also experience diurnal cycles (**Figure 2-5B**), with higher concentrations during the evenings each day. The figure shows that during high loading periods NH_4^+ concentrations remain controlled, but nitrate concentrations tend to increase as the plant spends more time in the air-on mode than the air-off mode. The latter is evident on the slopes and length of the NH_4^+ cycles. During the nitrate peaks, the average durations of air-on and air-off periods were 84 min and 59 min respectively, whereas during the nitrate valleys, the averages were 64 min and 61 min, respectively (**Supplementary Figure 2-4**). Fourth, during the periods of low nitrogen loading into the plant, nitrate concentration can be remarkably low, as observed for day 276. Finally, small fluctuations in nitrite concentration are observable, which increase in magnitude during high loading periods, but in general they remain low throughout the different cycles.

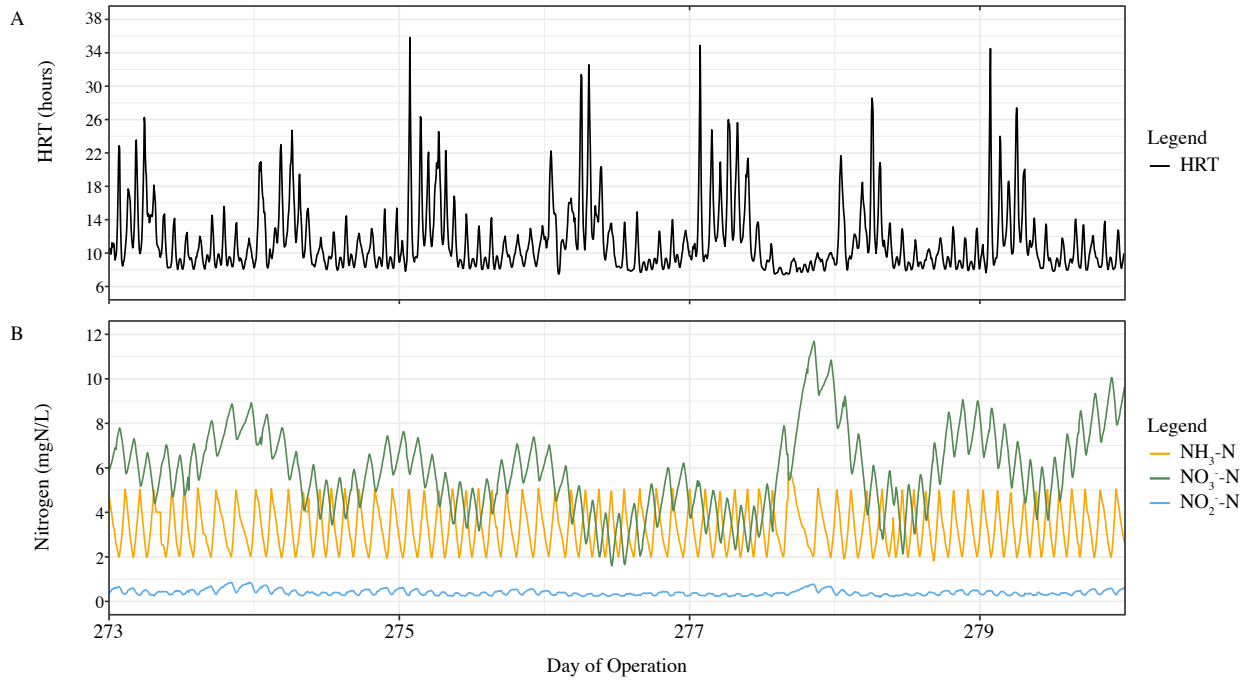

Figure 2-5 Sensor recordings on days 273-279 in the AOia pilot plant. Sensor recordings on days 273-279 in the AOia pilot plant. (A) HRT variation in both pilot plants implemented to mimic flow variability in full-scale plant. (B) Sensor recordings of NH_4^+, NO_3^-, and NO_2^- in tank AO4 show NH_4^+ oscillates between the allowable limits without a diurnal pattern. NO_3^- fluctuates in response to air-on/air-off periods, diurnal flows, and periods of high and low loadings. Significant NO_2^- accumulation was not observed.

It is noteworthy that the sensor-measured nitrate concentrations in the AOia process exhibited the described superimposed fluctuations. Although these measurements were taken before a continuously aerated tank (i.e., a polishing AO5 tank), some of these fluctuations may carry on and affect effluent characteristics at a level of resolution that was not captured with the schedule used for collecting effluent grab samples. Nevertheless, effluent nitrate concentrations in the AOia plant were consistently lower than the effluent concentrations from the UCTca, especially after implementing the flow variations that mimic flow variations in full-scale. Thus, from a perspective of TN removal, our results show that intermittent ABAC is better than continuous ABAC because the intermittent aeration created the anoxic periods that strongly favored denitrification.

The reduction in aeration requirements during the intermittent ABAC operation can be assessed at a larger scale by calculating the amount of time that the plant was in air-on mode versus air-off throughout the 483-day operation (**Supplementary Figure 2-5**). Overall, the AOia pilot plant spent 42% of the time in the air-off mode (i.e., a cumulative total of 202 days out of 483 days). However, the amount of time spent in air-off mode fluctuated widely throughout the operation, with some periods being as low as 28% of the time, and other periods as high as 61% throughout the operation (**Supplementary Figure 2-5**). Using a standard aeration design guide [22] an estimate of energy savings can be calculated. Under a volume-weighted average DO concentration across all aerated zones measured in the AOia pilot process of 0.6 mg/L and the average time spent in air-on mode, an energy saving of 51% can be realized when compared to a continuously aerated process achieving a DO concentration of 2.0mg/L, the current conditions at Nine Springs Wastewater Treatment Plant. It should be noted that actual energy usage to turn on/off high-power blowers used to provide aeration full-scale is not captured in this estimate, and operating blowers in such a manner may not be practical given constraints of current aeration technology.

We were particularly interested in EBPR performance in the intermittently aerated pilot plant, since the cyclic aeration creates anoxic conditions in a section of the conventional anaerobic/aerobic EBPR process where phosphorus uptake is expected to take place because oxygen is present and can serve as the external electron acceptor. In the absence of a sensor to detect the P concentration dynamics during air-on and air-off periods, we measured PO_4^{3-}—P concentrations every 10 minutes during an intermittent ABAC aeration cycle in tank AO2 (**Supplementary Figure 2-6A**). P increases during the air-off periods and decreases during the air-on periods, consistent with P removing activity by PAOs when oxygen is available. Samples

for this test were taken early in the treatment train (tank AO2) to best capture P dynamics since similar measurements in downstream tanks (e.g., AO4) show very low P concentrations (**Supplementary Figure 2-6B**). During the air-on period in tank AO2, P decreased at a rate of 21.7 mgPO_4^{3-}P/L-hr, while P increased at a rate of 16.0 mgPO_4^{3-}P/L-hr during the air-off period. To determine if the observed rate of P increase was due solely to advection or included P release from PAOs during intermittent aeration, the expected rate of P increase due to advection alone was calculated to be 12.9 mgPO_4^{3-}P/L-hr using the monthly average PO_4^{3-}P from the upstream tank (AO1) and the total flowrate (i.e., influent and RAS flowrates). Because the observed P increase during the air-off period was greater than the predicted P increase due to advection, the results provide evidence that cyclic P release and uptake is occurring during the air-on/off cycles of intermittent aeration.

These results do not provide any evidence of denitrification being associated with phosphorus uptake, as would be expected if denitrifying PAO activity was taking place [23]. Instead, the data support the hypothesis that under the rapid air-on/off cycles that are established with intermittent aeration, PAOs may quickly shift to P release during air-off periods. The ability of PAOs to use nitrite or nitrate as the electron acceptor (i.e., denitrifying PAO, DPAO) has been investigated [24-26] and existing literature suggests that some PAO strains are able to use one or both of these nitrogen species as electron acceptors, while other strains lack specific enzymes to perform full denitrification. In an intermittently aerated sequencing batch reactor (SBR) with aerobic/anoxic interval lengths of 10 – 20 minutes, Roots et al [20] reported that DPAO activity was insignificant due to a combination of low nitrite concentrations and DO inhibition. However, with longer anoxic intervals, such as those seen in this study (~ 61 min), others have reported DPAO activity [27]. In the absence of a P sensor, our discrete measurements of P fluctuations

during intermittent aeration in the AOia pilot were not supportive of DPAO activity in the AOia pilot plant. Further analysis of P cycling will be necessary to ascertain any potential role of DPAO activity in the AOia process.

2.6.3 Oxygen and ammonium dynamics during continuous aeration

Online ammonium, NH_4^+, and DO sensors were used to carry out continuous ABAC aeration in the UCTca pilot. Sensor data trends are shown in **Figure 2-6** for day 273 thru day 279, which is the same period shown in **Figure 2-5** for the AOia plant and typical of daily trends after the flow rate was switched to mimic flow changes in the full-scale plant. Ammonium in the UCT4 tank (**Figure 2-6**), where the sensor was located, fluctuated around the set point of 5.0 mgN/L and was generally stable regardless of the diurnal flow variations (**Figure 2-5A**). In this control system, a DO set point was not selected *a priori* for tanks UCT3 and UCT4. Rather, DO was allowed to fluctuate in the tanks between 0.1 and 0.6 mg/L, in response to the deviation between measured NH_4^+ concentration and the NH_4^+ setpoint. In general, during the entire operation DO concentrations in tank UCT3 and UCT4 averaged 0.38 mg/L and 0.35 mg/L, respectively. The DO concentration in tank UCT5, independently controlled to a setpoint of 0.6 mg/L (day 0-217) and 1.0mg/L (day 218 – 483), exhibited average DO concentrations of 0.73 mg/L throughout the entire operation. Under the average volume-weighted DO concentration experienced in the UCTca pilot of 0.5 mg/L, a 16% in energy savings may be realized when compared with a DO concentration of 2.0 mg/L under continuously aerated conditions.

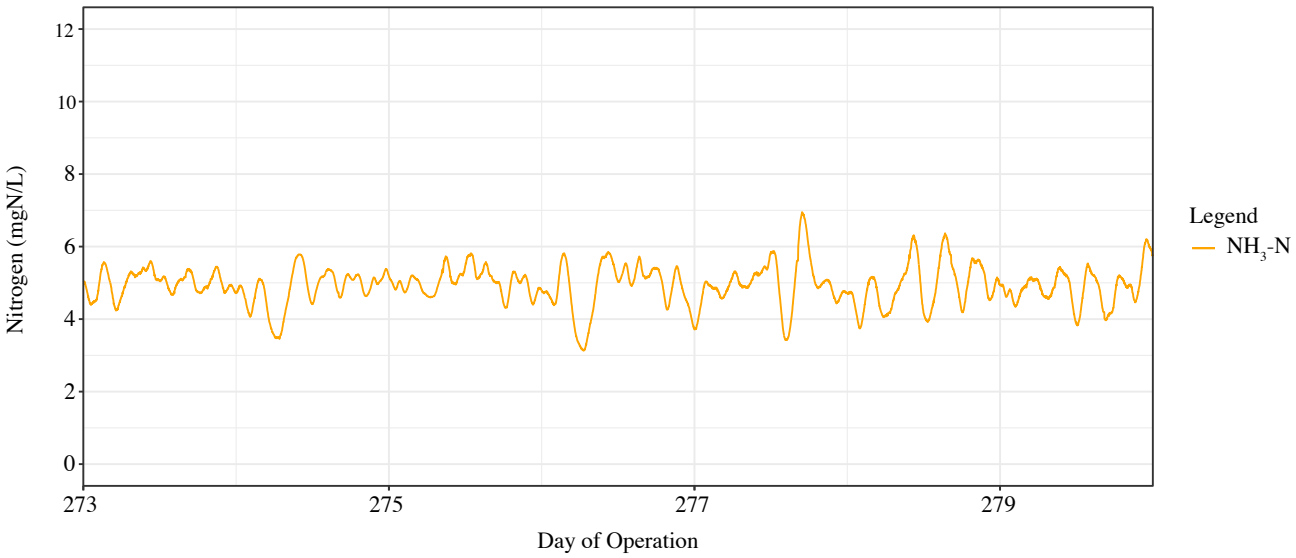

Figure 2-6 Sensor NH4+ recordings on days 273-279 in tank UCT4 of the UCTca pilot plant. Sensor NH_4^+ recordings on days 273-279 in tank UCT4 of the UCTca pilot plant show that NH_4^+ was maintained close to the 5 mg/L setpoint.

Sludge settling characteristics

Our prior observations from the UCTca pilot plant operating at low-DO conditions showed that efficient TKN removal is difficult to achieve when the temperature decreases during the winter and the SRT is not preemptively increased (**Supplementary Figure 2-3**), whereas nitrification in the full-scale treatment plant is not affected during winter [14], likely because it operates with higher DO concentrations. One option that we explored to maintain TKN removal during low temperature conditions was to preemptively increase the SRT to accumulate more nitrifying biomass (Supplementary document). The stepwise SRT changes influenced both the suspended solids concentration and the solids volume index (SVI) (**Figure 2-7**). Although the SRT increase was indeed effective at maintaining nitrification efficiency throughout the winter (**Figure 2-3B**), the SVI in both plants increased at similar rates reaching nearly 300 mL/g in the UCTca pilot and above 400 mL/g in the AOia pilot, exceeding the desired full-scale SVI values of less than 120 mL/g [28]. This degradation in sludge settling capacity necessitated an increase in

RAS flow rates to much higher values than recommended for activated sludge operation [29] in both pilot plants to prevent biomass loss in the effluent. Foaming on the clarifiers also became a recurrent problem with the high SRT operation. Although, the solids concentrations decreased during the stepwise SRT decrease after the winter period (**Figure 2-7A**), a recovery in SVI was not observed in either plant until the end of the study period, and sludge settleability was worse in the AOia than in the UCTca plant. This limits the applicability of full-scale implementation of the tested stepwise SRT increase, which brought up the SRT to a value as high as 16 days and resulted in total suspended solids concentrations as high as 5,000 mg/L, which are too high for conventional activated sludge processes.

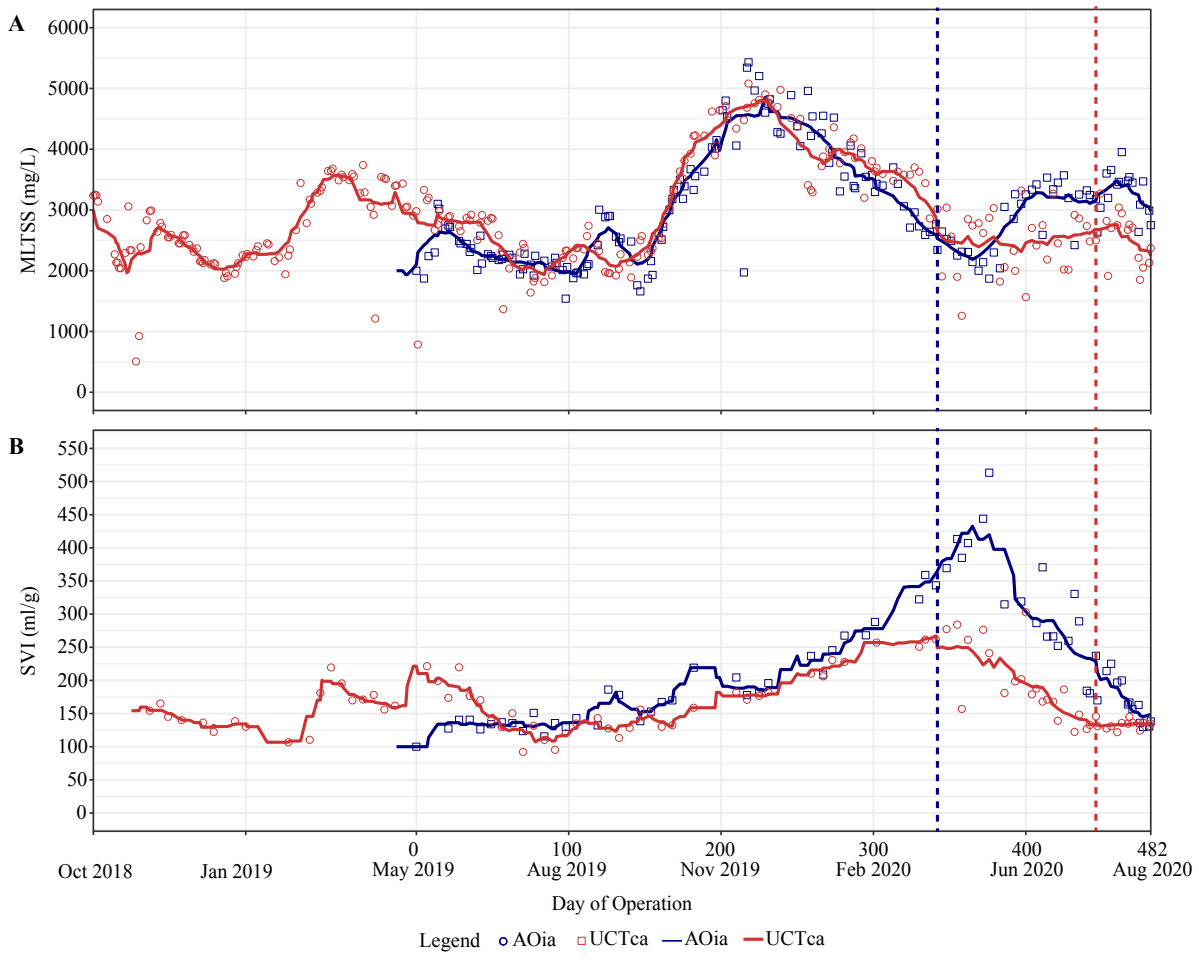

Figure 2-7 Effect of stepwise SRT changes on (A) mixed liquor total suspended solids (MLTSS) concentrations and (B) sludge volume index. Effect of stepwise SRT changes on

(A) mixed liquor total suspended solids (MLTSS) concentrations measured in the last aerated tank in both plants, and (B) sludge volume index (SVI) measured with suspended solids collected from the last aerated tank in both plants. Measurements for the UCTca system are shown since the start of reactor operation in October 2018. The vertical, dotted blue and red lines correspond to configuration changes in the AOia and UCTca systems, respectively.

The challenge of increased SVI has been recognized for operating activated sludge processes under low-DO conditions, which results in SVIs that are generally higher than those in conventional BNR processes [30]. For instance, Han et al. [31] reported SVIs between 120 and 220 mL/g at DO between 0.15 and 0.65 mg/L and Martins et al. [32] reported SVIs over 250 mL/g at DO < 1.1 mg/L. The main problem with increased SVI is the requirement for additional surface area of clarifiers, which in practice will require the construction of additional clarifiers when retrofitting a high-DO process into a low-DO process. Alternatively, should SVI levels reach such high values during full-scale operation, other corrective actions may need to be implemented, such as polymer dosing, RAS chlorination, tertiary filtration or selective sludge wasting, that will increase operational costs. Thus, methods to improve sludge settleability through selective sludge wasting [33-35], selector zone design [36], or other factors that may influence dense floc formation and retention during low-DO BNR operation remains an issue that requires further investigation.

2.7 CONCLUSIONS

- Pilot-scale treatment trains operated using intermittent and continuous ABAC were both effective at ammonia oxidation, total nitrogen removal, and phosphorus removal.
- A statistically significant difference in the nitrification and denitrification performance was observed when comparing both pilot plants, with the AOia plant performing better than the UCTca plant. The location where denitrification occurred was different, with

most denitrification occurring in AOia in the intermittently aerated zones and in UCTca in the unaerated zone.

- Intermittent and continuous ABAC were effective at controlling aeration and maintaining the operation of the pilot scale reactors at low-DO conditions and efficient nutrient removal.
- Stepwise increases to SRT proved effective at sustaining nitrification throughout the winter, although the increase led to increased SVI.
- EBPR was not inhibited by continuous or intermittent aeration at low-DO. There was no evidence of DPAO activity under intermittent aeration in the AOia pilot plant.

2.8 SUPPLEMENTARY MATERIAL

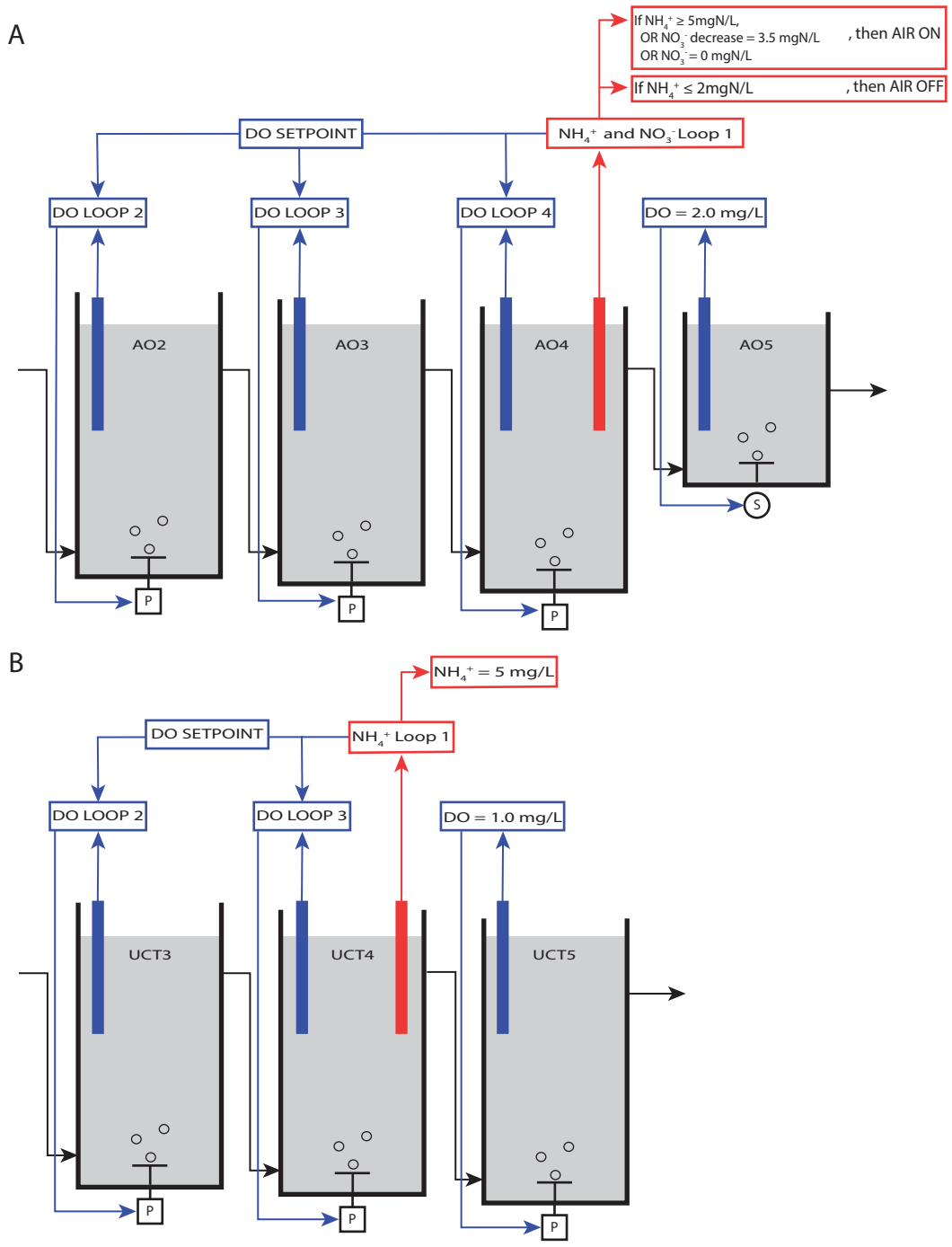

Supplementary Figure 2-1Aeration control cascading loops in the AOia and UCTca pilot-scale treatment trains. (A) Intermittent aeration control loops within the AOia pilot-plant. Ammonium (NH4+) and nitrate (NO3-) sensors were mounted in tank AO4. DO sensors (DO) were mounted in tank AO4. DO sensors (DO) were mounted in tanks AO2, AO3, AO4, and AO5. Tanks AO2, AO3, and AO4 were equipped proportional air valves (P), while air delivery

in AO5 was through an on/off solenoid valve (S). (B) Continuous aeration control lools in the UCTca pilot-scale treatment train. Ammonium (NH_4^+) sensors were mounted in tank UCT4. DO sensors (DO) were mounted in tanks UCT3, UCT4, and UCT5. All aerated tanks were equipped with proportional air valves (P).

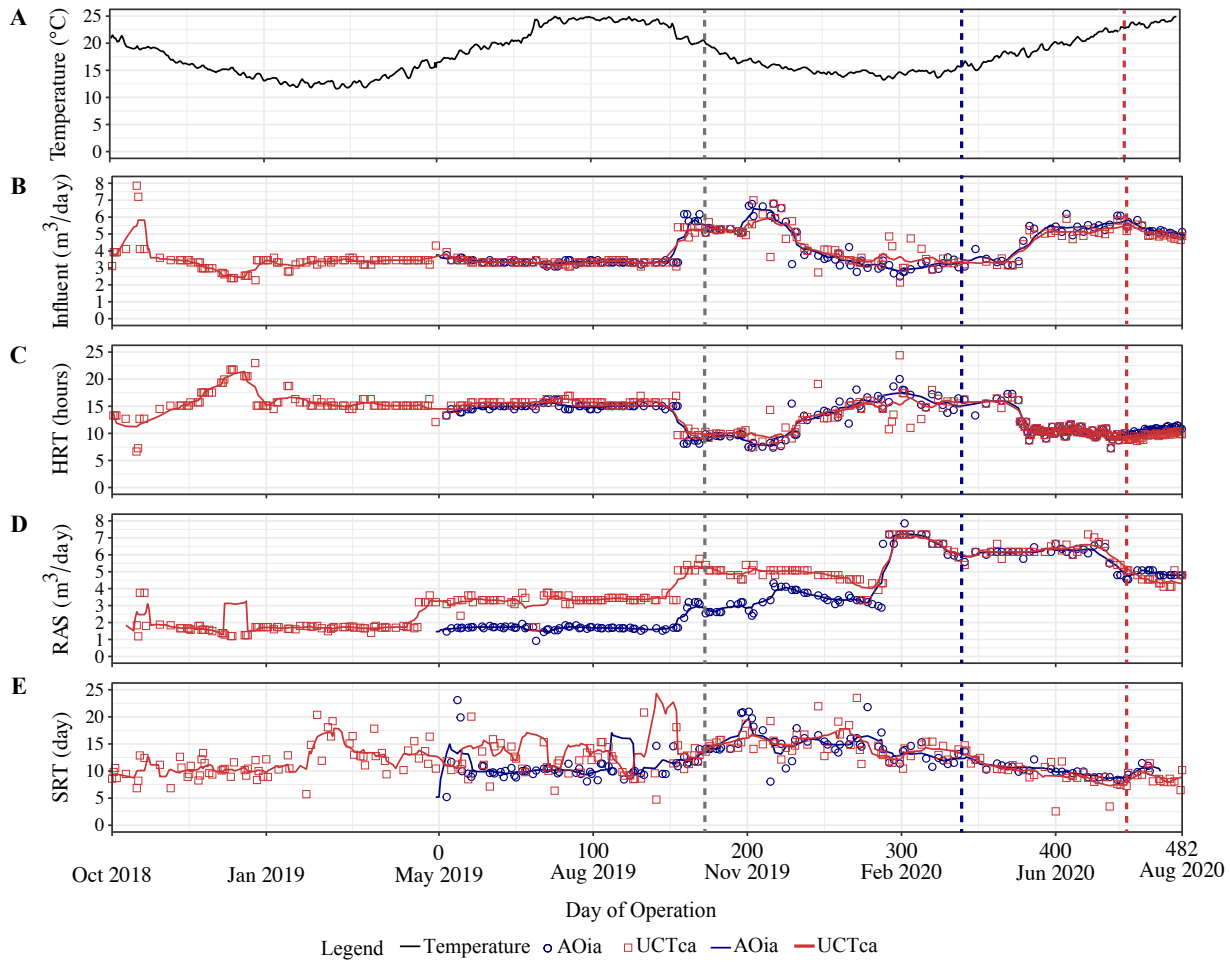

Supplementary Figure 2-2 Biosolids and HRT management in pilot-scale plants. Data from UCTca operation starting in October 2018 and AOia operation starting in May 2019 are shown. The vertical dotted lines indicate when pumps were installed allowing influent flowrates to mimic full-scale flow (grey) and when the reactor configurations were changed in the AOia (blue line) and the UCTca (red line) plants. (A) Water temperature, (B) Influent flowrate, (C) HRT, (D) RAS flowrate, (E) SRT.

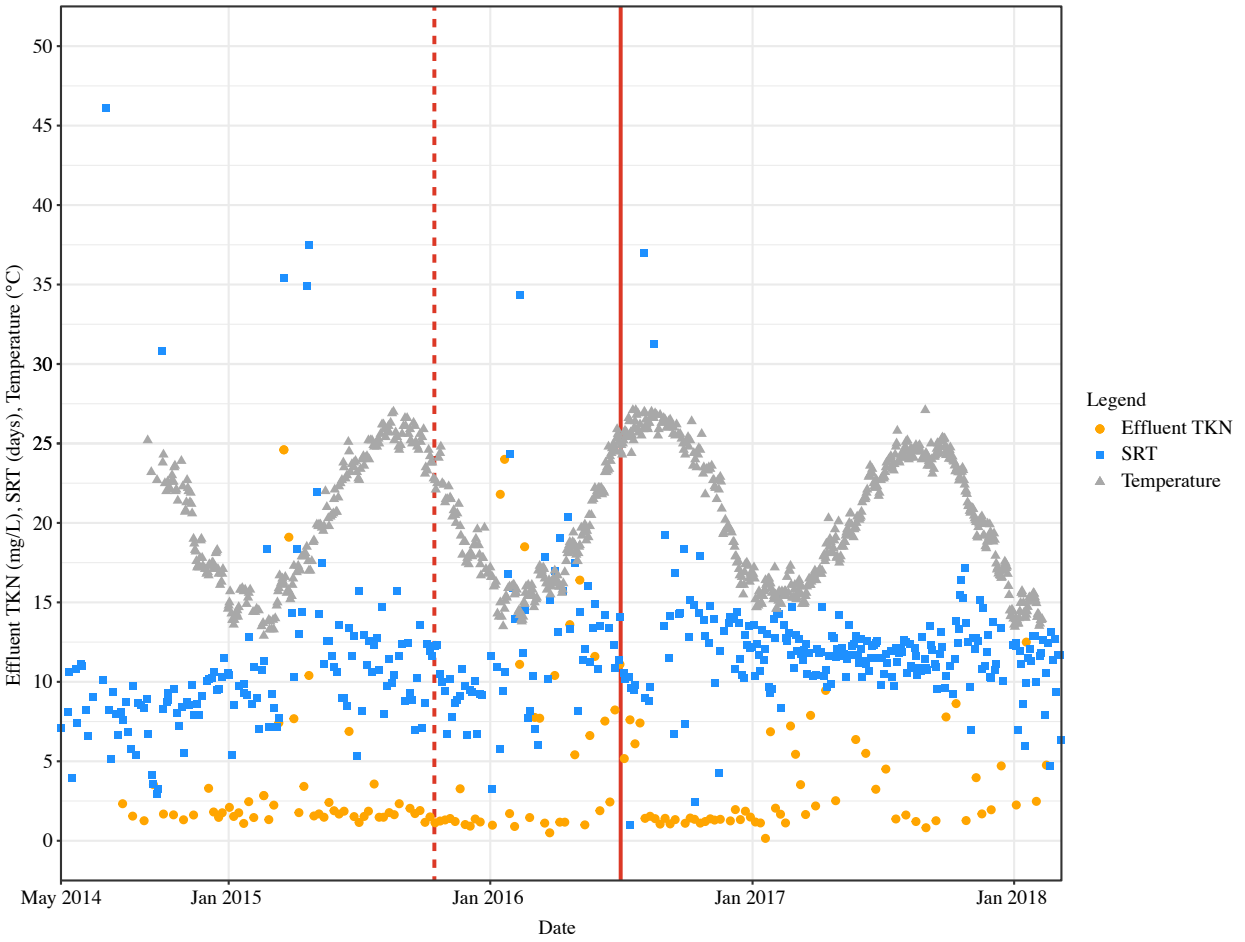

Supplementary Figure 2-3 Historical effluent TKN, SRT, and temperature of previous pilot plant operations at Nine Springs WWTP (Madison, WI) before the reconstruction of the two pilot plants described in this study. Data presented before the dotted red line was collected while the pilot was configured as a modified UCT process without an internal nitrate recycle. This operational period is described in detail in Keene et al., 2017. Data presented between the dotted and solid red lines was collected while the pilot was configured as a Johannesburg process. Data presented after the solid red line was collected when the pilot was reconfigured back into a modified UCT process.

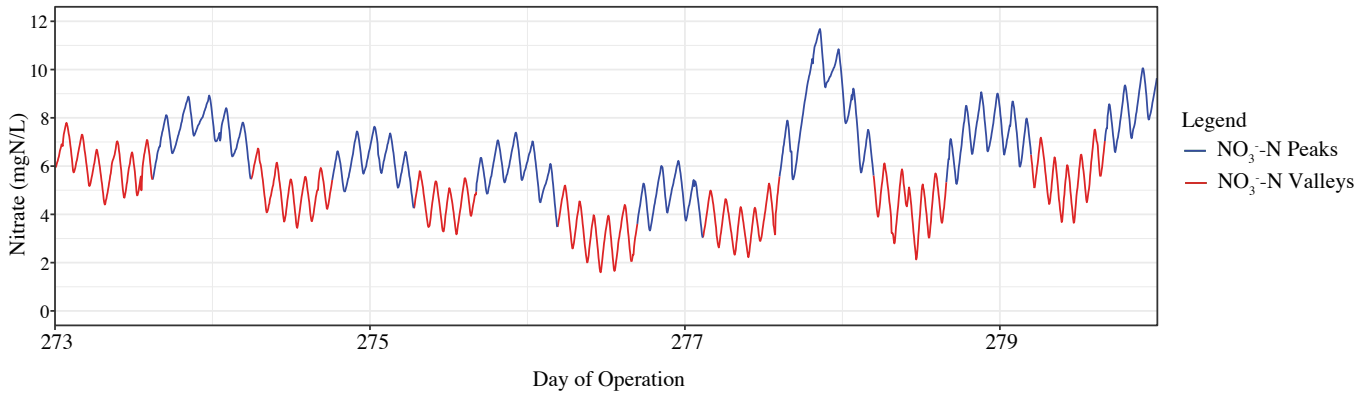

Supplementary Figure 2-4 Nitrate sensor recordings from days 273-279, with nitrate peaks and valleys defined and color coded (nitrate peaks in blue and nitrate valleys in red). During air-off periods nitrate concentrations decrease; during air-on periods nitrate concentrations increase.

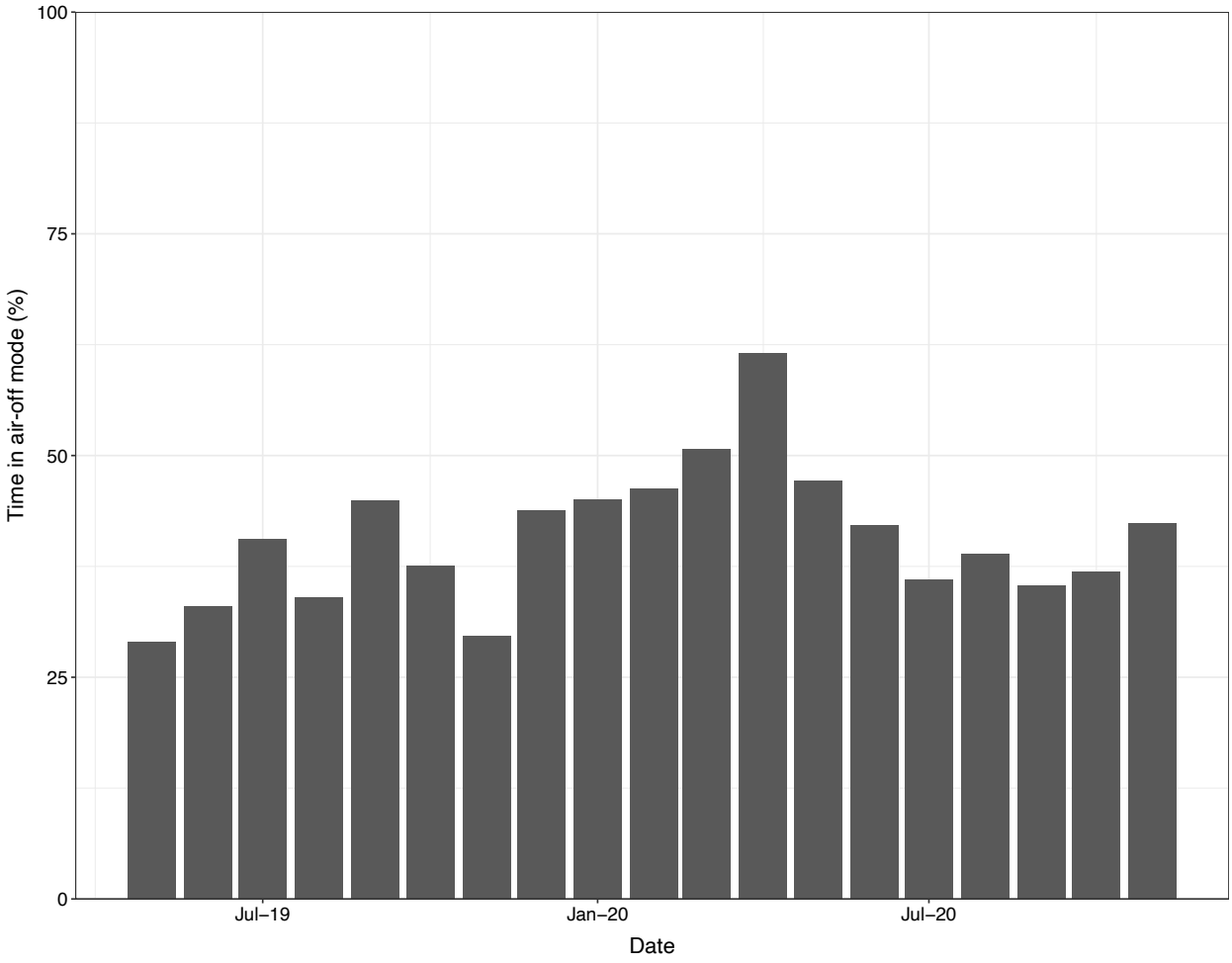

Supplementary Figure 2-5 Monthly average of the percent of time the intermittently aerated zones of the AOia pilot system spent in air-off mode. Monthly averages were calculated from datasets at 5-minute intervals.

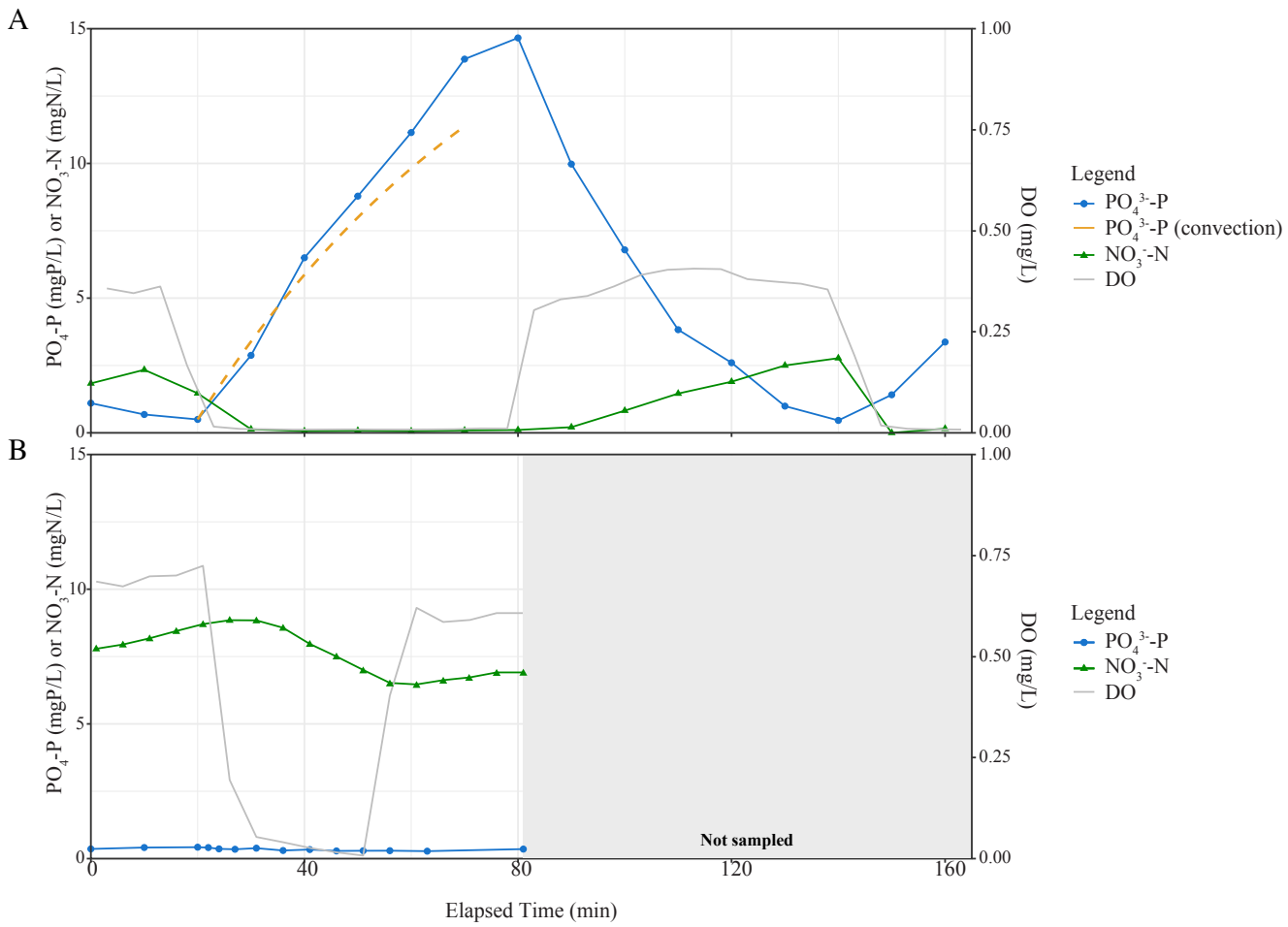

Supplementary Figure 2-6 In-situ chemical profiles in the AOia pilot during one air-on/air-off cycle. (A) Concentrations of PO_4^{3-}, DO, and NO_3^- during one air-on/air-off cycle in tank AO2 of the AOia pilot plant. During the air-off period, PO_4^{3-} increases and NO_3^- decreases. The dotted orange line represents the expected PO_4^{3-} increase during the air-off period due to convection alone. During the air-on period, PO_4^{3-} decreases and NO_3^- increases. (B) Concentrations of PO_4^{3-}, DO, and NO_3^- during one air-on/air-off cycle in tank AO4 of the AOia pilot plant. Due to the low concentrations of PO_4^{3-} towards the end of the treatment train, patterns of increase and decrease are not significantly observed.

Supplementary Table 1 Pairwise comparison of TKN, TP, and TN removal efficiency before and after the installation of the variable spped influent pump on day 175.

	AOia			UCTca		
	Before	After	p-value	Before	After	p-value
TKN	94%	95%	0.0038	91%	94%	5.5e-07
TP	87%	91%	0.0015	92%	90%	0.72
TN	60%	72%	1.6e-05	56%	67%	4.4e-06

2.9 ACKNOWLEDGMENTS

This work was partially supported by funding from the Madison Metropolitan Sewerage District, the National Science Foundation (CBET-1803055 and HRD-1810916), and the Graduate Engineering Research Scholars (GERS) program of the College of Engineering at UW-Madison. We thank Jackie Bastyr-Cooper for her assistance in the lab with training, protocols, and equipment. We also thank Morgan Keck, Trenton Weiss, James Alvin, and Michael Liu for support with laboratory analysis and operation of the pilot plants. Finally, we thank the lab staff and other district personnel at Nine Springs Wastewater Treatment Plant for their support of this research.

2.10 REFERENCES

1. Metcalf and Eddy, *Wastewater Engineering Treatment and Reuse.* New York: McGraw-Hill, 2003.
2. Barnard, J.L., *Biological nutrient removal without the addition of chemicals.* Water Research, 1975. **9**(5): p. 485-490.
3. Keene, N.A., et al., *Pilot plant demonstration of stable and efficient high rate biological nutrient removal with low dissolved oxygen conditions.* Water Res, 2017. **121**: p. 72-85.
4. Zheng, X., et al., *The investigation of effect of organic carbon sources addition in anaerobic-aerobic (low dissolved oxygen) sequencing batch reactor for nutrients removal from wastewaters.* Bioresour Technol, 2009. **100**(9): p. 2515-20.
5. Gao, H., Y.D. Scherson, and G.F. Wells, *Towards energy neutral wastewater treatment: methodology and state of the art.* Environ Sci Process Impacts, 2014. **16**(6): p. 1223-46.
6. Åmand, L. and B. Carlsson, *Optimal aeration control in a nitrifying activated sludge process.* Water Research, 2012. **46**(7): p. 2101-2110.
7. Åmand, L., G. Olsson, and B. Carlsson, *Aeration control – a review.* Water Science and Technology, 2013. **67**(11): p. 2374-2398.
8. Rieger, L., et al., *Ammonia-based feedforward and feedback aeration control in activated sludge processes.* Water Environ Res, 2014. **86**(1): p. 63-73.
9. Regmi, P., et al., *Ammonia-based intermittent aeration control optimized for efficient nitrogen removal.* Biotechnol Bioeng, 2015. **112**(10): p. 2060-7.
10. Regmi, P., et al., *Control of aeration, aerobic SRT and COD input for mainstream nitritation/denitritation.* Water Research, 2014. **57**: p. 162-171.
11. Klaus, S. and C.B. Bott, *Comparison of sensor driven aeration control strategies for improved understanding of simultaneous nitrification/denitrification.* Water Environment Research, 2020. **92**(11): p. 1999-2014.

12. Roots, P., et al., *Comammox Nitrospira are the dominant ammonia oxidizers in a mainstream low dissolved oxygen nitrification reactor.* Water Research, 2019. **157**: p. 396-405.
13. Bayer, N., *A Modeling Approach to Analyze Performance of a Minimal Aeration Biological Nutrient Removal (BNR) Pilot-Scale Plant* in *Department of Civil and Environmental Engineering*. 2018, University of Wisconsin-Madison: Madison, WI.
14. Park, H.D., et al., *Taking advantage of aerated-anoxic operation in a full-scale University of Cape Town process.* Water Environment Research, 2006. **78**(6): p. 637-642.
15. APHA, AWWA, and WEF, *Standard Methods for the Examination of Water and Wastewater*. 21st ed, ed. L.S.C. A. D. Eaton, E. W. Rice, and A. E. Greenberg. 2005, Washington D.C.: APHA.
16. R Core Team, *R: A language and environment for statistical computing*. 2016, R Foundation for Statistical Computing: Vienna, Austria.
17. Kang, D.W. and D.R. Noguera, *Pilot-Scale Investigation to Achieve Very Low Nitrogen and Phosphorus Effluents by Retrofitting a University of Cape Town (UCT) Process*, in *80th Annual Conference of the Water Environment Federation*, W.E. Federation, Editor. 2007, Water Environment Federation: San Diego, CA. p. 7396 - 7411.
18. Park, H.D. and D.R. Noguera, *Evaluating the effect of dissolved oxygen on ammonia-oxidizing bacterial communities in activated sludge.* Water Res, 2004. **38**(14-15): p. 3275-86.
19. Medinilla, V.R., et al., *Impact of Ammonia-Based Aeration Control (ABAC) on Energy Consumption.* Applied Sciences, 2020. **10**(15).
20. Roots, P., et al., *Integrated shortcut nitrogen and biological phosphorus removal from mainstream wastewater: process operation and modeling.* Environmental Science: Water Research & Technology, 2020. **6**(3): p. 566-580.
21. Garcia Martin, H., et al., *Metagenomic analysis of two enhanced biological phosphorus removal (EBPR) sludge communities.* Nat Biotechnol, 2006. **24**(10): p. 1263-9.
22. Sanitaire, *Diffused aeration design guide.*
23. Zeng, R.J., et al., *Identification and comparison of aerobic and denitrifying polyphosphate-accumulating organisms.* Biotechnology and bioengineering, 2003. **83**(2): p. 140-148.
24. Gao, H., et al., *Genome-centric metagenomics resolves microbial diversity and prevalent truncated denitrification pathways in a denitrifying PAO-enriched bioprocess.* Water Research, 2019. **155**: p. 275-287.
25. Camejo, P.Y., et al., *Candidatus Accumulibacter phosphatis clades enriched under cyclic anaerobic and microaerobic conditions simultaneously use different electron acceptors.* Water Res, 2016. **102**: p. 125-137.
26. Zeng, R.J., et al., *Simultaneous nitrification, denitrification, and phosphorus removal in a lab-scale sequencing batch reactor.* Biotechnology and Bioengineering, 2003. **84**(2): p. 170-178.
27. Lee, D.S., C.O. Jeon, and J.M. Park, *Biological nitrogen removal with enhanced phosphate uptake in a sequencing batch reactor using single sludge system.* Water Research, 2001. **35**(16): p. 3968-3976.
28. Martins, A.M.P., et al., *Filamentous bulking sludge—a critical review.* Water Research, 2004. **38**(4): p. 793-817.
29. Metcalf, amp, and Eddy, *Wastewater engineering : treatment and resource recovery*. 2014: Fifth edition / revised by George Tchobanoglous, H. David Stensel, Ryujiro Tsuchihashi,

Franklin Burton ; contributing authors, Mohammad Abu-Orf, Gregory Bowden, William Pfrang. New York, NY : McGraw-Hill Education, [2014] ©2014.

30. Huang, L. and L.-K. Ju, *Sludge settling and online NAD(P)H fluorescence profiles in wastewater treatment bioreactors operated at low dissolved oxygen concentrations.* Water Research, 2007. **41**(9): p. 1877-1884.
31. Han, W., et al., *Control of sludge settleability based on organic load and ammonia nitrogen load under low dissolved oxygen.* Water Science and Technology, 2018. **78**(10): p. 2113-2118.
32. Martins, A.M.P., J.J. Heijnen, and M.C.M. van Loosdrecht, *Effect of dissolved oxygen concentration on sludge settleability.* Applied Microbiology and Biotechnology, 2003. **62**(5-6): p. 586-593.
33. Liu, Y., et al., *Selection pressure-driven aerobic granulation in a sequencing batch reactor.* Appl Microbiol Biotechnol, 2005. **67**(1): p. 26-32.
34. Sun, Y., B. Angelotti, and Z.W. Wang, *Continuous-flow aerobic granulation in plug-flow bioreactors fed with real domestic wastewater.* Sci Total Environ, 2019. **688**: p. 762-770.
35. Liu, H., et al., *Stable aerobic granules in continuous-flow bioreactor with self-forming dynamic membrane.* Bioresource technology, 2012. **121**: p. 111-118.
36. Daigger, G.T., E. Redmond, and L. Downing, *Enhanced settling in activated sludge: design and operation considerations.* Water Sci Technol, 2018. **78**(1-2): p. 247-258.

3 Nitrous oxide (N_2O) measurements in pilot-scale plants operated under low dissolved oxygen conditions

This chapter has been submitted to the Madison Metropolitan Sewerage District (MMSD) as apart of the UW-Madison – MMSD cooperative agreement with the following authors:

Rachel D. Stewart, Carly Amstadt, Lillian Glackin, Daniel R. Noguera

Author Contributions:

RDS and DRN developed the research plan. RDS, CA, and LG operated the pilot-scale plants and collected samples. RDS performed data analyses. RDS and DRN wrote the manuscript.

Submitted December 2022

3.1 INTRODUCTION

Nitrous oxide (N_2O) is a potent greenhouse gas (GHG) that can be emitted from wastewater treatment plants (WWTPs) during biological nitrogen (N) removal. According to the US EPA, N_2O emissions from WWTPs account for 6% of total N_2O emissions that are due to human activity [1]. N_2O is ~300 times more potent as a GHG than CO_2, and according to some estimates, N_2O emissions can account for up to 83% of the entire carbon footprint of a WWTP [2, 3]. As WWTPs strive to meet stricter treatment standards and at the same time decrease energy consumption and carbon footprint, strategies to understand and mitigate N_2O emissions during the biological nutrient removal process at WWTPs are gaining worldwide attention.

Most N_2O is generated through the biologically mediated nitrification and denitrification steps of N removal (**Figure 3-1**). Autotrophic ammonia oxidizing bacteria (AOB), which carry out the first step of nitrification (the oxidation of ammonia, NH_3, to nitrite, NO_2^-) can generate N_2O through the incomplete oxidation of hydroxylamine (NH_2OH), an obligatory intermediate. AOBs can also sequentially reduce NO_2^- to nitric oxide (NO) and finally to N_2O, a process that has been termed nitrifier denitrification. Similarly, N_2O is an intermediate of heterotrophic denitrification which is the sequential reduction of nitrate (NO_3^-) or NO_2^- to nitrogen gas (N_2). Each of these three N_2O generation pathways and emissions are affected by a number of operational and environmental conditions that can act simultaneously in a system.

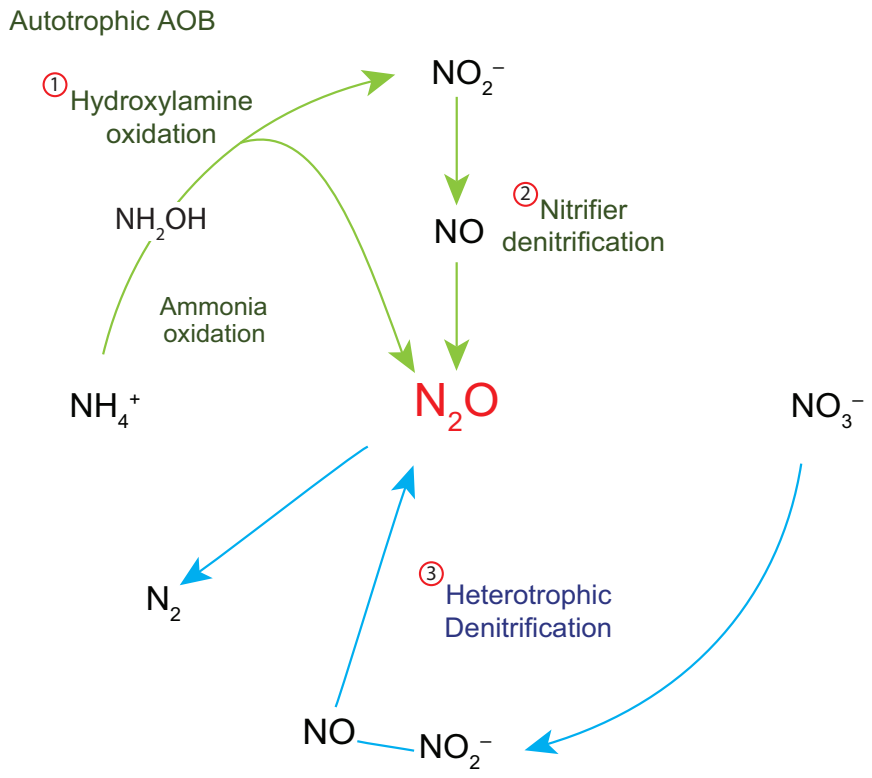

Figure 3-1 Biologically mediated nitrous oxide (N2O) production pathways Biologically mediated nitrous oxide (N_2O) production pathways via (1) Incomplete oxidation of hydroxylamine (NH_2OH) and (2) nitrifier denitrification by autotrophic ammonia oxidizing bacteria (AOB) or (3) heterotrophic denitrification.

Dissolved oxygen (DO) is an important operational parameter as it affects facility costs, nitrification efficiency, and N_2O emissions. In the UW-Madison – MMSD collaboration, the use of low-DO in aerated sections of the treatment train has been studied at pilot scale [4-10]. When DO is limited, AOBs may produce N_2O through the nitrifier denitrification pathway where NO_2^- and NO are reduced by electrons generated from NH_3 oxidation [11-13]. Conversely, high DO conditions can promote N_2O production through the hydroxylamine oxidation pathway as increased ammonia oxidation rates cause hydroxylamine accumulation and incomplete oxidation [11, 14, 15]. While N_2O production is obligatory through heterotrophic denitrification, accumulation of N_2O is experienced through incomplete denitrification which can be induced under low carbon to N conditions or oxygen inhibition [16-18]. On the other hand, if undisturbed, heterotrophic denitrification serves as

a means for N_2O consumption. Most studies on the effect of DO on N_2O emissions have been carried out for short periods of time (e.g., batch experiments or 1-day sampling campaigns), measuring short-term response to variations in DO [11, 19-22].

The N_2O emission factor (EF) is defined as the amount of N_2O emitted relative to the N-load entering the treatment plant. The EF in a WWTP is typically less than 2%, but EFs as high as 25% have been reported [19, 22-24]. It is suggested that the wide range of reported EFs is due to variations in DO, NH_3, and NO_2^- concentrations, as well as reactor configuration, operational conditions, and sampling methods [25, 26]. As WWTPs seek to implement energy-efficient treatment methods, such as low-DO operation, an understanding of immediate and long-term N_2O formation and emission throughout varying environmental and operational conditions is necessary. Given the potential connection between N_2O emissions and low-DO operation, we evaluated N_2O emissions in two pilot-scale plant operations. Here we report the experiments conducted and the methods used to calculate N_2O emissions based on measured N_2O concentrations.

3.2 METHODS

3.2.1 Pilot-scale plant operations

Two pilot-scale treatment trains were operated in parallel at the Nine Springs WWTP (Madison, WI). The pilot plants were configured as anoxic-oxic (AO) processes simulating the plug flow conditions of the full-scale plant (**Figures 3-2 and 3-3**). Each pilot plant consisted of three 140-L unaerated tanks that simulated the anoxic zone, three 473-L aerated tanks that simulated the oxic zone, and a final 95-L polishing tank operated with high DO. The total volume of the activated sludge process was 1,934-L. A secondary clarifier followed the final aerated tank and separated the microbial culture from the treated water. The two pilots differed in 3 important ways: (i) the secondary clarifier volumes (ii) the inclusion of a return activated sludge (RAS)

fermentation zone in one of the systems, and (iii) the method of activated sludge wasting. The final two differentiations led to the naming designation of the two pilots: AO-G, for wasting by gravity separation, and AO-FF, for wasting through floc filtering and presence of a fermentation zone. The AO-G (**Figure 3-2**) was equipped with a 1,210-L secondary clarifier, whereas the AO-FF (**Figure 3-3**) was equipped with a 1,010-L clarifier. Both plants were seeded with activated sludge from the full-scale plant in June 2021. Both plants received primary effluent from the full-scale plant as the influent stream. The influent flow was automatically controlled via a variable speed pump to mimic real-time changes in influent flow experienced at full-scale. During the entire operation, average daily influent flow rates ranged from 2.8 to 4.2 m^3/day corresponding to an average hydraulic retention time (HRT) of 12.9 ± 1 hours. In the AO-G pilot, 100% of RAS flow was returned to the first unaerated tank at an average of 2.2 m^3/day. In the AO-FF, 90% of RAS was returned to the first unaerated tank at an average of 2.2 m^3/day and 10% was sent to a 140-L fermentation reactor, at an average flow rate of 0.22 m^3/day (**Figure 3-3**). The effluent from the fermentation reactor was sent to the first unaerated tank. Additional details of the operation and performance of these pilot plants were reported elsewhere [4].

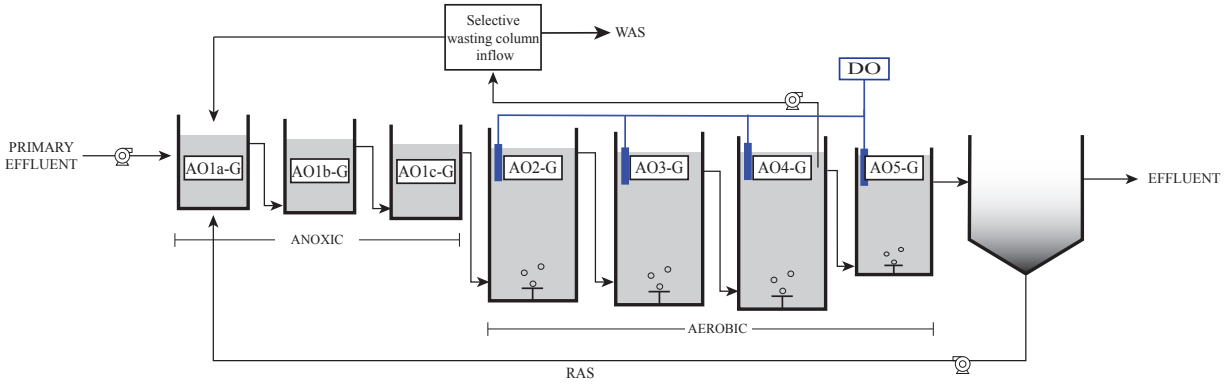

Figure 3-2 AO-G pilot-scale treatment train configuration. The AO-G pilot-scale treatment train configuration showing unaerated tanks (AO1a-G, AO1b-G, AO1c-G), aerated tanks (AO2-G, AO3-G, AO4-G, AO5-G), and the clarifier. Return activated sludge (RAS) was pumped from the bottom of the clarifier into the first unaerated tank. Selective activated sludge wasting was

implemented using a gravity-based floc density separator. Waste activated sludge (WAS) was pumped from the selector. Stepwise reductions in DO were made in tanks AO2-G, AO3-G, and AO4-G, while tank AO5-G was operated as a high-DO polishing tank. DO sensors were installed in each of the aerated tanks.

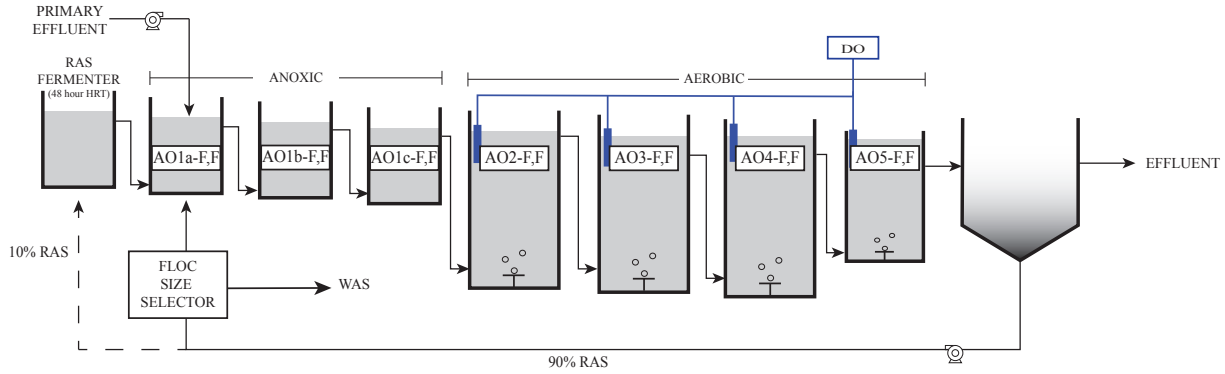

Figure 3-3 AO-FF pilot-scale treatment train configuration. The AO-FF pilot-scale treatment train configuration showing the return activated sludge fermentation tank (RAS Fermenter), unaerated tanks (AO1a-FF, AO1b-FF, AO1c-FF), aerated tanks (AO2-FF, AO3-FF, AO4-FF, AO5-FF), and the clarifier. RAS was pumped from the bottom of the clarifier into the floc size selector. Waste activated sludge (WAS) was pumped from the size selector. 90% of RAS flow from the size selector was pumped into the first unaerated tank, and 10% of RAS flow was pumped into the RAS fermenter. DO sensors were installed in only the first three aerated tanks which were subjected to the stepwise reductions in DO. AO5-G was operated as a high-polishing DO tank. DO sensors were installed in each of the aerated tanks.

3.2.2 Solids retention time (SRT) control

The pilot plants were operated with target SRTs between 9 and 10 days. The SRT management plan throughout the operation is listed in Table 3-1. Activated sludge was wasted in the AO-G pilot via a gravity-based selective wasting column, where dense flocs were separated from light flocs. Mixed liquor from tank AO4-G (**Figure 3-2**) was pumped directly to the selective wasting column. This column was operated as a sequencing batch reactor (SBR) with a 4.4-L working volume. The operational sequence was as follows: 3-min fill phase of mixed liquor from tank AO4-G, 2-min settle phase, 1-min decant phase, and 4-min return phase. During the decant phase the top volume of the SBR, including mixed liquor that did not settle fast, was wasted from the system. SRT was controlled by determining the volume that needed to be wasted in this phase, based on measured mixed liquor solids concentrations in the pilot plant tanks, in the decanted

mixed liquor, and in the effluent of the pilot plant [4]. This wasted volume fluctuated between 0 and 2 L/cycle. During the return phase, the mixed liquor remaining in the SBR was returned to the first unaerated tank (**Figure 3-2**).

Table 3-1 SRT management throughout operation of both pilot-scale plants.

Dates	Target SRT (days)	Average Measured SRT (days)	
		AO-G	AO-FF
5/24/21 – 6/9/21	10	10.9	9.9
6/10/21 – 1/9/22	9	9.2	11.4
1/10/22 – 3/27/22	10	9.5	12.1
3/28/22 – 4/3/22	9.5	13.0	8.7
4/4/22 – 10/10/22	9	8.3	10.7

An in-line RAS filtering apparatus was used in the AO-FF pilot to facilitate wastage of small, activated sludge flocs from the RAS stream. Flocs passing through a 50 mesh (297-μm) filter were pumped from the apparatus and removed from the system, whereas the larger flocs were returned to the first unaerated tank (**Figure 3-3**). SRT was controlled by adjusting the flow rate of the sludge wasted out of this size selector apparatus based on measured mixed liquor solids concentrations in the pilot plant tanks, in the waste stream, and in the pilot plant effluent [4].

3.2.3 DO control

During this phase of pilot-scale testing, the team was evaluating the effect of selective wasting and DO decreases on mixed liquor settleability [4]. Accordingly, stepwise decreases in DO were carried out as listed in Table 3-2. Adjustments to DO were only implemented in the middle three aerated tanks of each pilot plant. DO setpoints were maintained using DO sensors and proportional-integral (PI) control systems using control systems reported elsewhere (Stewart et al., 2021). Airflow to each of these tanks was supplied through a motorized proportional air valve that adjusted position according to the PI control. All tanks in the AO-G pilot plant, and only tank

AO4-FF in the AO-FF pilot plant, were equipped with rotameters to measure the instantaneous airflow rate. Aeration to the polishing tank in each pilot was controlled through an on/off air solenoid valve set to maintain at least a DO concentration of 3 mg/L.

Table 3-2 DO control phases throughout operation of both pilot-scale plants.

DO operational phase	Dates	DO setpoint (mg/L)		
		AO2	AO3	AO4
Phase 1 (Full-scale conditions)	5/21/21 – 8/31/21	0.4	0.8	3.5
Phase 2	9/1/21 – 10/5/21	0.4	0.8	2.0
Phase 3	10/6/21 – 11/28/21	0.4	0.8	1.5
Phase 4	11/29/21 – 4/11/22	0.4	0.8	1.0
Phase 5	4/12/22 – 6/9/22	0.3	0.6	0.8
Phase 6	6/10/22 – 10/10/22	0.2	0.3	0.5

3.2.4 Analytical Methods

TKN, NO_3^-, and NO_2^-: Filtered influent, effluent, and RAS grab samples were collected and analyzed for total Kjeldahl nitrogen (TKN) using Standard Methods. These samples were also analyzed for NO_3^- and NO_2^- using HACH test kits. TKN measurements were performed by the MMSD laboratory, whereas NO_3^- and NO_2^- measurements were done on site by UW-Madison personnel.

N_2O: Instantaneous in-situ measurements of dissolved N_2O were taken primarily in the aerated tanks using a Unisense N_2O Clark-type microsensor (N_2O-R, Unisense A/S, Denmark). The same sensor was used to estimate gaseous N_2O concentrations by measuring N_2O concentrations in liquid set to reach equilibrium with the off-gas coming out of the aerated tanks and using Henry's Law (0.025 mol/L-bar at 20 °C). The setup consisted of an inverted funnel that was placed on the water surface of each tank, making a seal so that only off-gas was entering the funnel **(Figure 3-4**). Off-gas trapped in the inverted funnel was pumped, using a peristaltic pump,

into a diffuser stone placed in a graduated cylinder containing 200 mL of water. The N_2O sensor was placed in this water and a dissolved N_2O measurement was recorded.

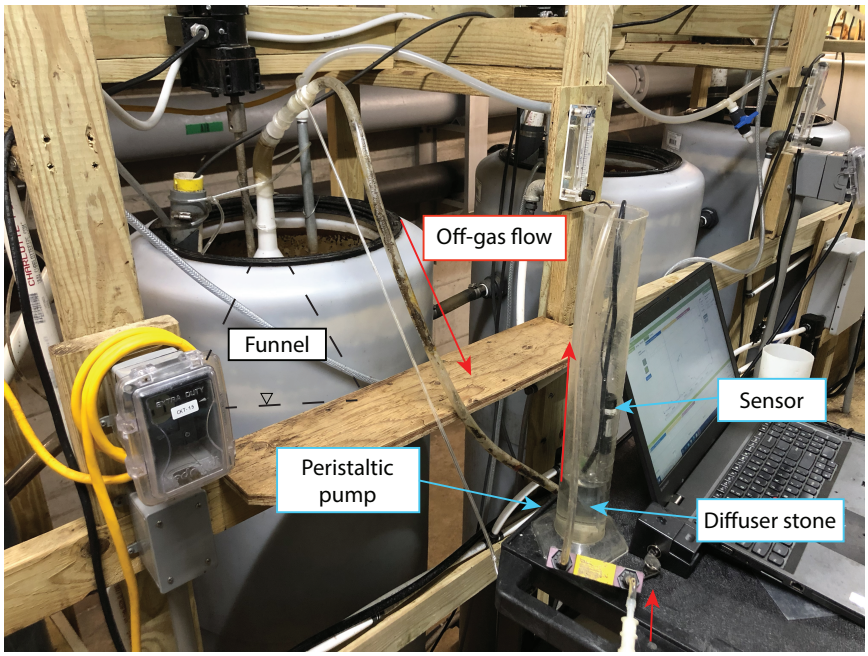

Figure 3-4 Air pumping set up for measurement of N_2O gaseous emissions measurements.

$$P_{N_2O} = \left(\frac{C_{N_2O}}{K_{N_2O}}\right) * 0.987 \frac{atm}{bar}$$

P_{N2O}: partial pressure N_2O (atm)
C_{N2O}: concentration N_2O (M)
K_{N2O}: Henry's law constant for solubility in water at 298.15 K (0.025 mol L^{-1} bar^{-1}) [27]

Eqn 1

$$[N_2O] = \frac{P_{N_2O}}{R * T}$$

$[N_2O]$: molar gas concentration of N_2O (M)
R: Ideal gas constant (0.08205 L atm mol^{-1} K^{-1})
T: temperature 298.15 K

Eqn 2

$$ER = [N_2O] * LPD * (2 \frac{mol\ N}{mol\ N_2}) * MW_N$$

ER: emission rate (gN_2O-N/day)
LPD: airflow rate (L/d)
MW_N: Molecular weight if N (14 g/mol)

Eqn 3

$$TN = (TKN)_{inf} * Q_{inf}$$

TN: total N load (gN/day)
TKN_{inf}: influent TKN (g/L)
Q_{inf}: influent flowrate (L/day)

Eqn 4

$$EF = \frac{ER}{TN} * 100$$

EF: emission factor (%)

Eqn 5

Using Henry's Law, the partial pressure of N_2O in the off-gas was calculated using Eqn 1. The partial pressure was then converted to a molar concentration using the Ideal Gas Law, according to Eqn 2. The airflow rate into each tank was used to calculate the N_2O mass emitted per day, according to Eqn 3. The airflow rate into the third aerated tank, AO4, of each pilot was recorded from a rotameter at the time of the N_2O measurement. Since some of the tanks did not have rotameters installed, a 2-hr average airflow rate into the first two tanks of each pilot, AO2 and AO3, was estimated based on the proportional air valve position at the time of the measurements. For this, a regression analysis of proportional air valve positions to measured airflow rates was performed. Finally, an EF could be calculated according to Eqn 5 using the total N load (Eqn 4) to the first unaerated tank in each pilot.

3.3 RESULTS

3.3.1 Nitrification performance

It has been previously demonstrated that biological N removal systems could be successfully transitioned to low-DO treatment using a stepwise DO reduction strategy [7]. This observation was reproduced in the pilot plant operations used in this research [4]. Additionally, we have shown that an appropriate SRT management plan to account for varying water temperatures aides in complete nitrification at low-DO[10]. In this iteration of pilot-scale operations influent filtered TKN was 46 ± 6.6 mgN/L. The AO-G and AO-FF pilots achieved an average effluent TKN of 2.6 ± 3.6 and 4.2 ± 6.6 mgN/L, respectively. The TKN removal performance during each DO phase is shown in Table 3-3. While brief upsets in performance were experienced at the start of new DO phases, lasting at longest 6 weeks, stable nitrification was regained over time.

Effluent NO_3^- throughout the entire operation in the AO-G and AO-FF pilots was 15.9 ± 4.1 and 14.8 ± 5.8 mgN/L, respectively. While complete nitrification was experienced for most of

the operation for both pilots, NO_2^- did accumulate at the start of DO phases 5 and 6 (**Figure 3-5 and Figure 3-6**). NO_2^- accumulation was also experienced for 5 weeks during an infestation of bristle worms in both pilots (**Figure 3-7**). This period of infestation was more prevalent in the AO-G pilot and lasted for about 2 months. Coincidentally, the NO_2^- accumulation was more severe in the AO-G pilot. Larvicide (AQUABACxt, Aquafix, Madison, WI) was added to the mixed liquor of both pilots to control the bristle worm infestation.

Table 3-3 Average nitrification performance in each pilot throughout each DO operational phase.

DO Phase (DO concentration range; mg/L)	Average Effluent TKN (mgN/L)	
	AO-G	AO-FF
1 (0.4 – 3.5)	1.46	1.54
2 (0.4 – 2.0)	1.73	1.51
3 (0.4 – 1.5)	1.39	1.31
4 (0.4 – 1.0)	2.10	1.65
5 (0.3 – 0.8)	6.54	3.94
6 (0.2 – 0.5)	2.84	13.25

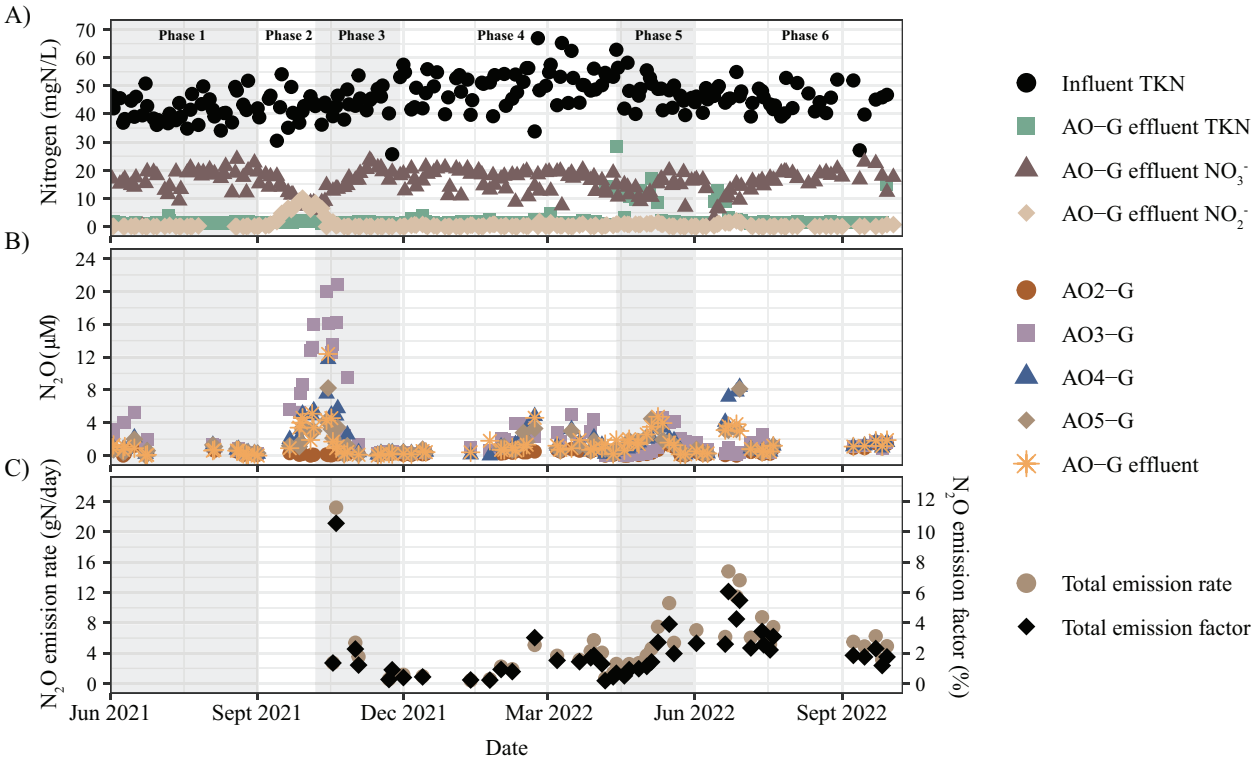

Figure 3-5 Nitrogen removal in the AO-G pilot.(A) nitrification performance (B) dissolved N_2O (B) N_2O emissions. DO phases are noted in panel

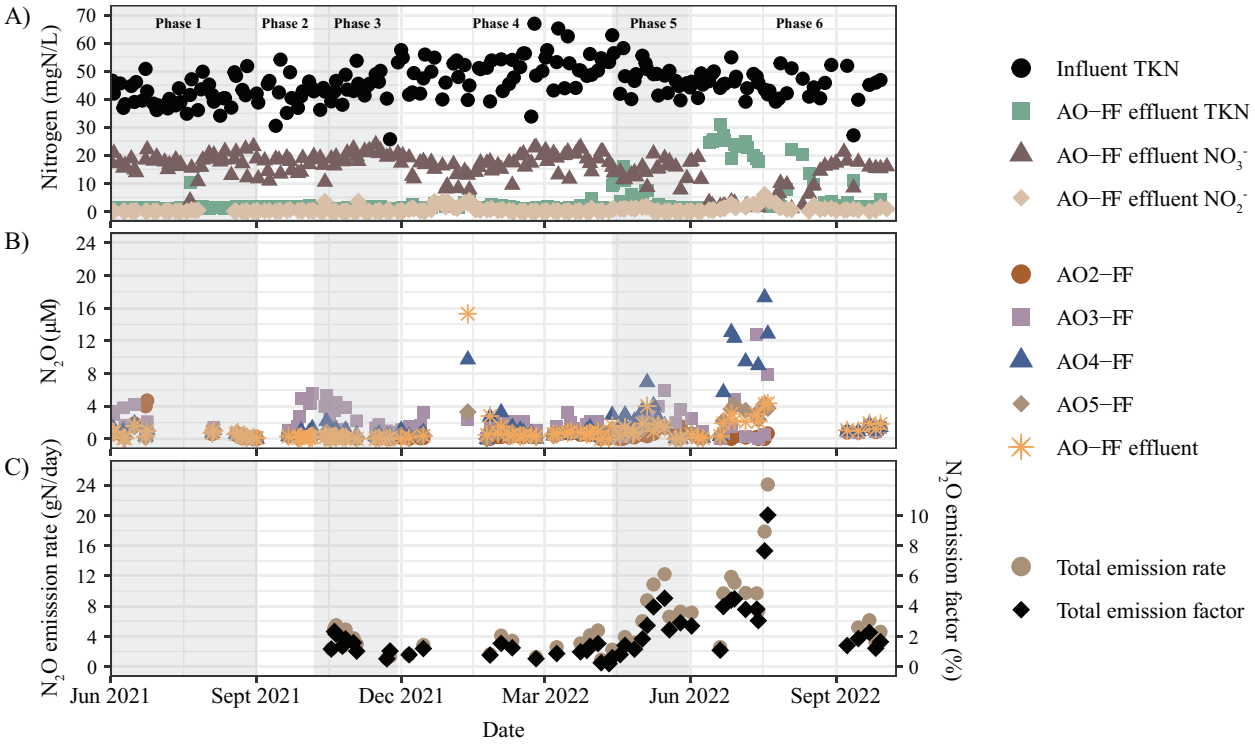

Figure 3-6 Nitrogen removal in the AO-FF pilot. (A) nitrification performance (B) dissolved N_2O (C) N_2O emissions. DO phases are noted in panel.

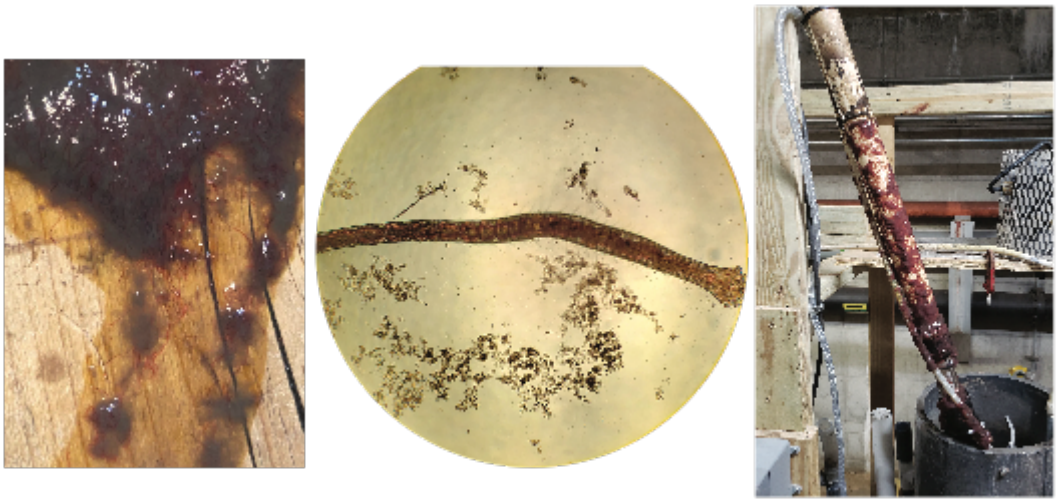

Figure 3-7 Bristle worms that were found in the mixed liquor and attached to reactor surfaces. During the bristle worm infestation in the mixed liquor , nitrite accumulation and an increase in N_2O production was also observed.

3.3.2 Total nitrogen removal and SND

Using a mass balance approach, we estimated the extent of SND by calculating the difference between total nitrogen in the final unaerated tank and the total nitrogen in the effluent. The extent of SND during each DO phase is shown in Table 3-4. Total nitrogen removal efficiency was similar between both pilots throughout the operation, at 58 ± 9% and 57 ± 11% in the AO-G and AO-FF pilot, respectively (**Figure 3-8**).

Table 3-4 Extent of SND in each pilot during each DO phase.

DO Phase	AO-G		AO-FF	
	SND (gN/day)	%SND	SND (gN/day)	%SND
1	72	52	80	55
2	69	50	93	60
3	70	52	82	53
4	86	57	96	60
5	94	55	109	59
6	92	59	115	61

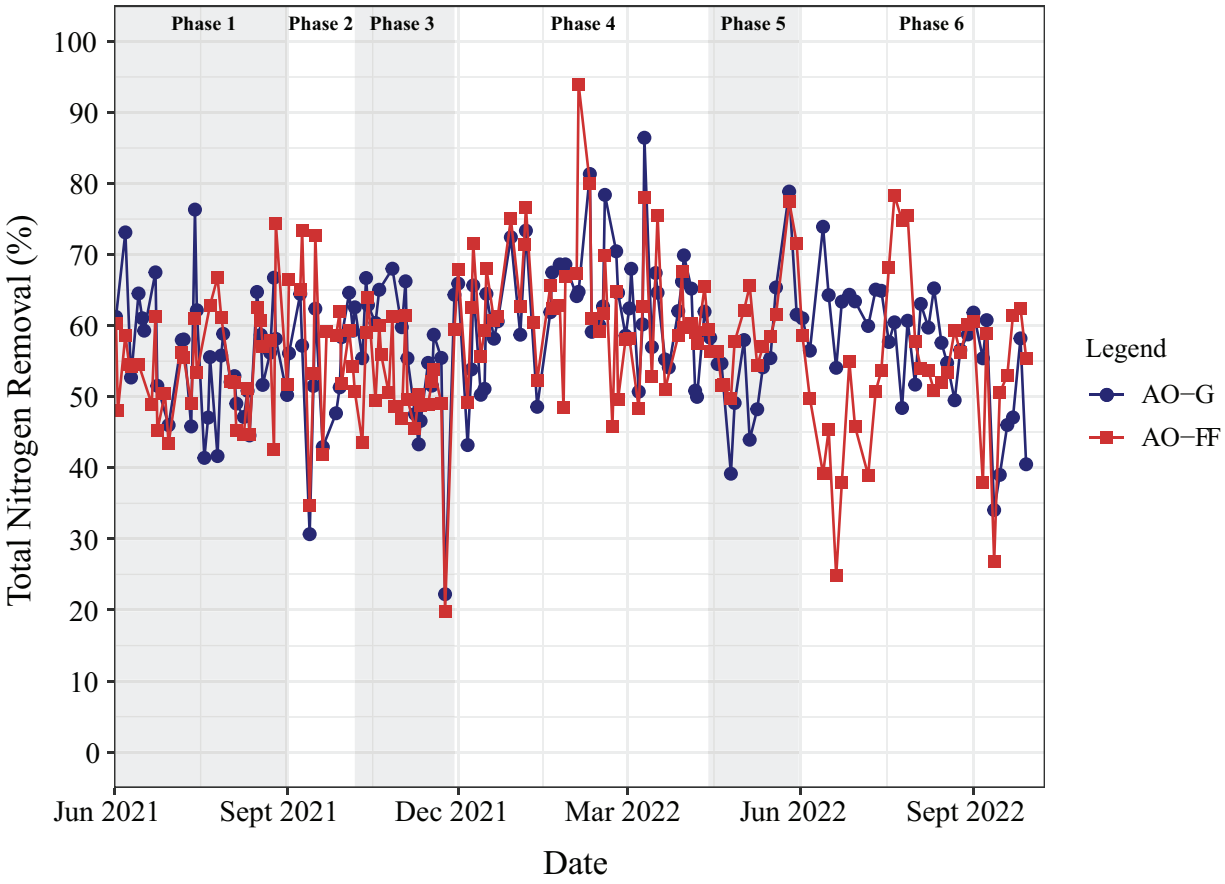

Figure 3-8 Total nitrogen removal of both pilot plants throughout the entire operation.

3.3.3 N_2O production and emissions

Dissolved N_2O and gaseous emissions are shown in Figures 3-5 and 3-6, and individual tank measurements are summarized in Table 3-5. The averages of dissolved N_2O concentrations in tanks AO2-G, AO3-G, AO4-G, AO5-G and the effluent were 0.4, 3.7, 2.0, 1.5, and 1.5 µM respectively throughout the entire operation. These measurements were 0.48, 2.2, 2.0, 0.88, and 1.0 µM in the AO-FF pilot, respectively. Average gaseous emissions rates throughout the operation from the three middle aerated tanks in the AO-G pilot were 0.66, 1.87, and 1.50 gN_2O-N/day, respectively, whereas those of the AO-FF pilot were 0.62, 2.39, and 2.84 gN_2O-N/day, respectively.

Since the three aerated tanks in each of the pilot plants had different aeration rates, we evaluated whether the dissolved N_2O concentrations in these tanks were correlated with N_2O emission rates. A correlation was indeed found, with excursions in the N_2O concentrations generally corresponding to higher emission rates (**Figure 3-9**).

Table 3-5 Average dissolved concentrations and emission rates of N_2O in the individual tanks of each pilot plant throughout operation.

Tank	AO-G		AO-FF	
	Dissolved N_2O^+	Emission Rate*	Dissolved N_2O^+	Emission Rate*
AO2	0.39 ± 0.38	0.69 ± 0.44	0.51 ± 0.72	0.62 ± 0.44
AO3	3.25 ± 4.69	1.87 ± 2.34	2.10 ± 1.94	2.39 ± 1.97
AO4	1.93 ± 2.21	1.50 ± 1.44	1.97 ± 3.19	2.84 ± 2.98
AO5	1.49 ± 1.52	-	0.87 ± 0.98	-

+: Dissolved N_2O concentration (μM)
*: N_2O emission rate (gN_2O-N/day)

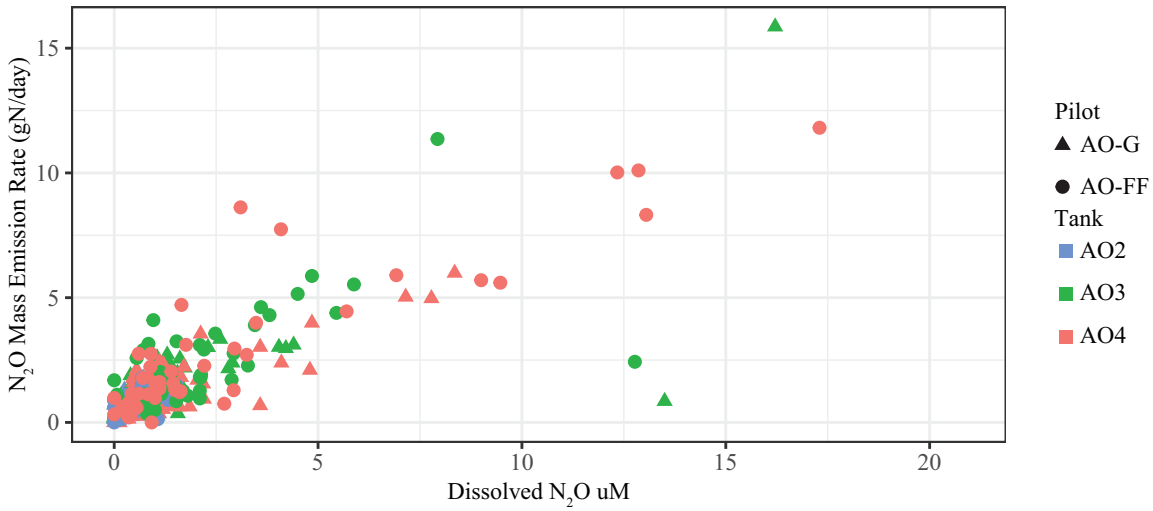

Figure 3-9 Dissolved N_2O versus the N_2O emission rate in each aerated tank of both pilot plants.

Combining the emission rates estimated for each aerated tank we estimated an overall EF for each pilot plant (Eqn 4). The average EF throughout the operation were 2.55 ± 2.37% and 3.54 ± 2.88% in the AO-G and AO-FF pilot plants, respectively. The average EF in either pilot during each DO phase is shown in Table 3-6. The largest production and emission of N_2O in the AO-G

pilot was during the period of high NO_2^- accumulation and bristle worm infestation. This period corresponded to a N_2O emission rate as high as 20.37 gN_2O-N/day and EF of 14.57%. The spike in N_2O, although to a much lesser extent, was also observed in the AO-FF pilot during the same time period, corresponding to a N_2O emission rate as high as 7.24 gN_2O-N/L and an EF of 4.44%. Following the disappearance of the bristle worms and decrease in NO_2^-, dissolved and emitted N_2O decreased. The highest emissions observed in the AO-FF pilot was during the beginning of DO phase 6, at 10.62% and 16.37 gN_2O-N/day when nitrification performance was negatively impacted due to the implemented DO reduction, as discussed below.

Table 3-6 Average emission factor from each pilot during each DO phase.

DO Phase (DO concentration range; mg/L)	Average Emission Factor (%N-load)	
	AO-G	AO-FF
1 (0.4 – 3.5)	-	-
2 (0.4 – 2.0)	-	-
3 (0.4 – 1.5)	3.92 ± 5.33 (n = 6)	2.65 ± 0.59 (n = 9)
4 (0.4 – 1.0)	1.59 ± 2.37 (n = 14)	1.72 ± 0.44 (n = 13)
5 (0.3 – 0.8)	1.82 ± 1.30 (n = 10)	3.53 ± 1.26 (n = 11)
6 (0.2 – 0.5)	3.45 ± 1.19 (n = 14)	5.81 ± 2.56 (n = 14)

Increases in N_2O were observed following reductions in DO setpoints, particularly during DO phases 5 and 6. During DO phase 5 in the AO-G pilot an increase in dissolved N_2O concentrations and in gaseous emissions was experienced as early as 8 days after the DO reduction. During this phase, dissolved N_2O concentrations in each tank increased moving along the treatment train and peaked in the pilot plant effluent, which reached N_2O concentrations as high as 4.73 μM during the N_2O spike. However, as the dissolved N_2O concentrations began to decrease, the concentration gradient nearly flipped and was highest in AO3-G, measuring at 0.69 μM at the end of phase 5. Dissolved N_2O concentrations decreased in all tanks and in the effluent to less than 1 μM just before the start of DO phase 6. The N_2O emissions followed a similar trend, with the emission rate and EF peaking at 7.80 gN_2O-N/day and 4.53% during DO phase 5. A return

to steady state was not observed in these two parameters before the next DO phase. During DO phase 5, the AO-FF pilot experienced an increase in N_2O production as well. Dissolved concentrations were highest in AO4-FF during the increasing period, while concentrations were highest in AO3-FF during the decreasing period. A return to a steady state concentration of less than 1 μM was only observed in all sampling locations before the start of DO phase 6. Emissions in the AO-FF pilot increased to 11.37 gN_2O-N/day and EF of 6.60%. Following the switch to DO phase 6, N_2O formation and emissions again increased in both pilots. Dissolved N_2O was highest in the second aerated tank of both pilots, reaching 8.4 and 17.3 μM in tanks AO4-G and AO4-F,F, respectively. The emission rate and EF in the AO-G pilot reached 9.10 gN_2O-N/day and 5.86%, respectively. One month after the switch to DO Phase 6, the highest N_2O emissions were observed in the AO-FF, as mentioned previously. Dissolved N_2O began to decrease in all measured locations after 4 weeks in the AO-G pilot, while a consistent decrease was observed 3 months after the start of DO phase 6 in the AO-FF pilot. In the final month of DO phase 6, the average EF from the AO-G and AO-FF pilots were 2.50 ± 0.59% and 2.72 ± 0.77%, respectively.

3.4 DISCUSSION

Energy optimization during the biological wastewater treatment process is necessary in achieving energy neutral and even energy positive facilities. Reducing the DO is seen as a primary solution to reducing the energy consumption at a WWTP. However, the trade-off between aeration reductions and N_2O emissions must be minimized to realize energy efficient and sustainable treatment. In this study we aimed to understand how lowering the DO during biological nutrient removal would impact N_2O production and emission immediately following a DO reduction, as well as its long-term significance.

3.4.1 N_2O emissions immediately following DO reductions and during performance upsets

DO is often recognized as an important parameter affecting N_2O production, particularly in AOB. For instance, a microbial community performing ammonia oxidation and enriched under high DO conditions has been shown to increase N_2O emissions through the nitrifier denitrification pathway upon exposure to low-DO[28]. Significant reductions in ammonia oxidation and increases in N_2O emissions following DO reductions were not observed in either pilot, until DO phases 5 and 6. During these periods, nitrification performance was poor and accumulation of NO_2^- was observed. Nitrite accumulation reached as high as 6.0 mgNO_2^-N/L in either pilot following the switch to DO phases 5 and 6. Under limiting oxygen conditions AOBs can reduce NO_2^- to NO and NO to N_2O. Effluent NO_2^- concentrations greater than 0.5 mgN/L correlated significantly with increases in EF (**Figure 3-9**), which is in agreement with a previous study that examined the combined effect of low-DO and increasing NO_2^- concentrations [20]. Nitrifier denitrification is suspected to be the dominant pathway leading to N_2O production under high NO_2^- conditions as ammonia oxidizers use NO_2^- as an electron acceptor from ammonia oxidation.

At effluent NO_2^- concentrations less than 0.5mgN/L there was a wide variation in the EF across different DO phases (**Figure 3-10**). At the start of DO phase 3, the bristle worms were beginning to disappear and NO_2^- was decreasing, however, dissolved N_2O and presumably emissions were still increasing. It is likely we captured the N_2O emission peak during the bristle worm infestation in both pilots as measurements were collected when the dissolved N_2O concentrations were at a peak. It is unclear whether nitrifier denitrification is the dominant source of N_2O formation during this time. Another possible explanation for this result is either a delayed decrease in N_2O production after NO_2^- decreases or that another metabolic pathway leads to N_2O

emissions at low NO_2^-concentrations. This same delay in decreasing N_2O emissions following decreased NO_2^- was experienced in a full-scale A^2O process [29]. Here, the authors hypothesize other complex factors may influence microbial physiological properties such as cell membrane permeability and subsequent release of N_2O across the cell.

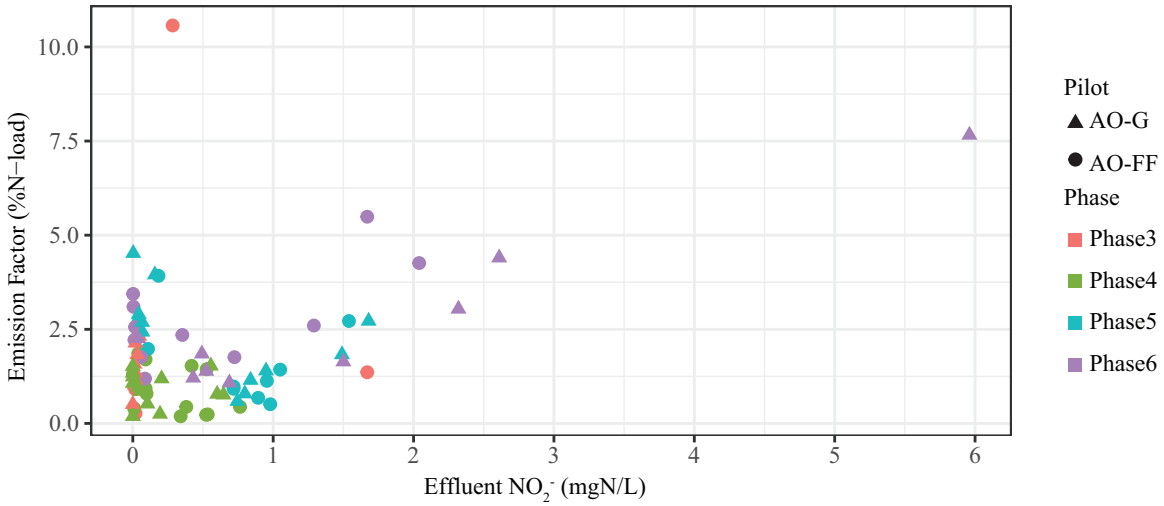

Figure 3-10 Effluent NO2- versus the emission factor (EF) in each of the pilot plants across DO phases 3-6 shows NO_2^- accumulation may correlate with increased EF. However, at very low NO_2^- concentrations other factors are responsible for increased emissions.

While we were unable to collect dissolved and gaseous emissions during the end of December and most of January, a minimal upset in nitrification was observed in the AO-FF pilot where effluent TKN increased to 3.32 mgN/L and NO_2^- increased to 3.5 mgN/L. This period was observed about one month after the switch to DO phase 4 and when water temperatures are nearing the coldest of the year. It is likely during this time N_2O emissions were increased due to the increased effluent NO_2^- (**Figure 3-10**).

3.4.2 Long-term impact of low-DO on N_2O emissions

An increase in N_2O production and emission is expected under dramatic shifts in operating conditions, particularly reductions in DO. However, a microbial adaptation or a shift in the microbial community members may result in decreased N_2O emissions after prolonged exposure to low-DO [28, 30].

Recently, Vasilaki et al. (2019) conducted a review on N_2O monitoring campaigns from full-scale WWTPs and other mainstream processes. The review included a wide range of reactor configurations and operation, including AO, A^2O, conventional activated sludge, modified Ludzack-Ettinger, oxidation ditch, sequencing batch reactor, partial nitritation/partial nitritiation-annamox, and other full-scale processes. We used this database as a benchmark to compare our results with full-scale N_2O emissions. The review reports that generally, full-scale EFs range between 0.01 and 2% of the incoming nitrogen load for most treatment configurations. Significant deviations from this are partial nitritation/partial nitritation-anammox and sequencing batch reactor systems. In this study only during DO phase 4 for both pilots and phase 5 for the AO-G pilot, does the average EF fall within what has been reported for various processes. The increased EF in both pilots outside of these phases are likely due to schedule reductions in DO and uncontrollable process upsets (i.e., the bristle worm infestation). An improved N_2O monitoring campaign (e.g., sampling frequency) and longer DO phases may be needed to better capture the dynamics of N_2O emissions in response to stepwise DO decreases, as well as the apparent return to lower emissions upon long-term stable operation at low-DO. For instance, while the average EF for the entirety of phase 6 in the AO-FF pilot is relatively increased, during the final month of operation in this phase the average EF is lower than the average EF during the entirety of DO phases 5 and 6, suggesting an acclimation of the microbial community to low-DO conditions.

3.5 CONCLUSIONS

- Stepwise reductions in DO result in immediate increases in N_2O production and emissions.
- N_2O emissions decrease after long-term operation at low-DO.

- Periods with NO_2^- accumulation result in greater N_2O emissions.
- A comparison of N_2O emissions estimated from the pilot plants to N_2O emissions observed in the full-scale treatment process at the Nine Springs facility is recommended.

3.6 ACKNOWLEDGMENTS

This work was partially supported by funding from the Madison Metropolitan Sewerage District, the National Science Foundation (CBET-1803055), and the Graduate Engineering Research Scholars (GERS) program of the College of Engineering at UW-Madison. We thank Jackie Bastyr-Cooper for her assistance in the lab with training, protocols, and equipment. We also thank Brennan Ellis and Anthony Radicia for support with laboratory analysis and operation of the pilot plants. Finally, we thank the lab staff and other district personnel at the Nine Springs Wastewater Treatment Plant for their support of this research.

3.7 REFERENCES

1. EPA, U.S. *Overview of Greenhouse Gases*. 2022 September 26, 2022]; Available from: https://www.epa.gov/ghgemissions/overview-greenhouse-gases.
2. Daelman, M.R., et al., *Methane and nitrous oxide emissions from municipal wastewater treatment - results from a long-term study.* Water Sci Technol, 2013. **67**(10): p. 2350-5.
3. Desloover, J., et al., *Floc-based sequential partial nitritation and anammox at full scale with contrasting N2O emissions.* Water Res, 2011. **45**(9): p. 2811-21.
4. Amstadt, C., *Assessing the effect of selective wasting and fermentation on slduge settleability and biological nutrient removal in two anoxic-oxic pilot-scale treatment plants*, in *Department of Civil and Environmental Engineering*. 2022, University of Wisconsin-Madison: Madison, WI.
5. Chambers, E.D., *A Pilot Scale Study of Low Dissolved Oxygen Nutrient Removal Supplemented with Ammonia-Based Aeration Controls*. 2018, University of Wisconsin-Madison: Madison, WI.
6. Martirano, J.M., *Evaluating biological nutrient removal processes in a pilot-scale sequencing batch reactor using low dissolved oxygen aeration*, in *Department of Civil and Environmental Engineering*. 2015, University of Wisconsin-Madison: Madison, WI.
7. Keene, N.A., et al., *Pilot plant demonstration of stable and efficient high rate biological nutrient removal with low dissolved oxygen conditions.* Water Res, 2017. **121**: p. 72-85.

8. Bayer, N., *A Modeling Approach to Analyze Performance of a Minimal Aeration Biological Nutrient Removal (BNR) Pilot-Scale Plant*, in *Department of Civil and Environmental Engineering*. 2018, University of Wisconsin-Madison: Madison, WI.
9. Uribe Santos, G.A., *A Pilot Scale-Study at the Nine Springs Wastewater Treatment Plant: Seasonal Cod and F/M Ratio Trends and Their Application To Modeling Treatment Processes*, in *Department of Civil and Envirnomental Engineering*. 2021, University of Wisconsin-Madison: Madison, WI.
10. Stewart, R.D., et al., *Pilot-scale comparison of biological nutrient removal (BNR) using intermittent and continuous ammonia-based low dissolved oxygen aeration control systems.* Water Science and Technology, 2021. **85**(2): p. 578-590.
11. Peng, L., et al., *The effect of dissolved oxygen on N2O production by ammonia-oxidizing bacteria in an enriched nitrifying sludge.* Water Res, 2014. **66**: p. 12-21.
12. Kampschreur, M.J., et al., *Dynamics of nitric oxide and nitrous oxide emission during full-scale reject water treatment.* Water Res, 2008. **42**(3): p. 812-26.
13. Young, M.N., et al., *Thermodynamic Analysis of Intermediary Metabolic Steps and Nitrous Oxide Production by Ammonium-Oxidizing Bacteria.* Environ Sci Technol, 2022. **56**(17): p. 12532-12541.
14. Law, Y., et al., *N2O production rate of an enriched ammonia-oxidising bacteria culture exponentially correlates to its ammonia oxidation rate.* Water Res, 2012. **46**(10): p. 3409-19.
15. Ribera-Guardia, A. and M. Pijuan, *Distinctive NO and N 2 O emission patterns in ammonia oxidizing bacteria: Effect of ammonia oxidation rate, DO and pH.* Chemical Engineering Journal, 2017. **321**: p. 358-365.
16. Tallec, G., et al., *Nitrous oxide emissions from denitrifying activated sludge of urban wastewater treatment plants, under anoxia and low oxygenation.* Bioresour Technol, 2008. **99**(7): p. 2200-9.
17. Schulthess, R.v., D. Wild, and W. Gujer, *Nitric and nitrous oxides from denitrifying activated sludge at low oxygen concentration.* Water Science and Technology, 1994. **30**(6): p. 123-132.
18. Guo, G., et al., *Enzymatic nitrous oxide emissions from wastewater treatment.* Frontiers of Environmental Science & Engineering, 2017. **12**(1).
19. Foley, J., et al., *Nitrous oxide generation in full-scale biological nutrient removal wastewater treatment plants.* Water Res, 2010. **44**(3): p. 831-44.
20. Peng, L., et al., *The combined effect of dissolved oxygen and nitrite on N2O production by ammonia oxidizing bacteria in an enriched nitrifying sludge.* Water Res, 2015. **73**: p. 29-36.
21. Stenstrom, F., K. Tjus, and J. la Cour Jansen, *Oxygen-induced dynamics of nitrous oxide in water and off-gas during the treatment of digester supernatant.* Water Sci Technol, 2014. **69**(1): p. 84-91.
22. Ahn, J.H., et al., *N2O Emissions from Activated Sludge Processes, 2008−2009: Results of a National Monitoring Survey in the United States.* Environmental Science & Technology, 2010. **44**(12): p. 4505-4511.
23. Law, Y., et al., *Nitrous oxide emissions from wastewater treatment processes.* Philos Trans R Soc Lond B Biol Sci, 2012. **367**(1593): p. 1265-77.
24. Kampschreur, M.J., et al., *Nitrous oxide emission during wastewater treatment.* Water Res, 2009. **43**(17): p. 4093-103.

25. Massara, T.M., et al., *A review on nitrous oxide (N2O) emissions during biological nutrient removal from municipal wastewater and sludge reject water.* Sci Total Environ, 2017. **596-597**: p. 106-123.
26. Vasilaki, V., et al., *A decade of nitrous oxide (N2O) monitoring in full-scale wastewater treatment processes: A critical review.* Water Res, 2019. **161**: p. 392-412.
27. Sander, R., *Henry's Law Constants*, in *NIST Chemistry WebBook, NIST Standard Reference Database Number 69*, P.J. Linstrom and W.G. Mallard, Editors. 2022, National Institute of Standards and Technology: Gaithersburg, MD.
28. Liu, G., et al., *Long-Term Low Dissolved Oxygen Operation Decreases N2O Emissions in the Activated Sludge Process.* Environ Sci Technol, 2021. **55**(10): p. 6975-6983.
29. Wang, Y., et al., *Nitric oxide and nitrous oxide emissions from a full-scale activated sludge anaerobic/anoxic/oxic process.* Chemical Engineering Journal, 2016. **289**: p. 330-340.
30. Ahn, J.H., T. Kwan, and K. Chandran, *Comparison of partial and full nitrification processes applied for treating high-strength nitrogen wastewaters: microbial ecology through nitrous oxide production.* Environ Sci Technol, 2011. **45**(7): p. 2734-40.

4 Metagenomic Analysis of the *Candidatus* Accumulibacter Genus in Biological Nutrient Removal (BNR) Pilot-Scale Plants Operated with Minimal Aeration

This chapter has been formatted for submission to the American Society of Microbiology with the following authors:

Rachel D. Stewart, Kevin Myers, Matt Seib, Katherine D. McMahon, Daniel R. Noguera

Author Contributions:

RDS, KDM, and DRN developed the research plan. RDS collected samples for sequencing. RDS and KM performed sequencing analyses. RDS, KDM, DRN contributed to data analyses and wrote the manuscript with input from all authors.

4.1 ABSTRACT

Increasingly more wastewater treatment facilities are considering reduced aeration as a means to decrease operational costs and energy consumption. While successful biological nutrient removal (BNR) has been demonstrated in systems with minimal aeration, an understanding of the microbial community dynamics under these conditions, particularly outside of lab-scale reactors, is needed. *Candidatus* Accumulibacter is widely studied as a polyphosphate accumulating organism (PAO) in wastewater treatment facilities performing enhanced biological phosphorus removal (EBPR). Accumulibacter abundance and activity have been demonstrated in low dissolved oxygen (DO) systems, and it has been suggested that ecological niche-differentiating features or adaptations may explain the coexistence of particular species. Here, we investigate the Accumulibacter community diversity and dynamics in pilot-scale treatment trains performing BNR under low-DO conditions using genome-resolved metagenomics and metatranscriptomics. We assembled two improved Accumulibacter species representative genomes and five potentially novel Accumulibacter species representative genomes, one of which we identify as a novel Accumulibacter clade (IIJ). Using the Accumulibacter genomes assembled in this study and previously published genomes, we show that the Accumulibacter community is highly heterogeneous and dynamic within the low-DO systems supporting evidence that most members of this lineage have a high affinity for oxygen. An examination of the denitrification potential within the Accumulibacter lineage revealed differing nitrogenous reduction capabilities suggesting that the coexistence of several species is due to niche differentiating roles which overall contribute to BNR.

4.2 IMPORTANCE

Candidatus Accumulibacter is often found in conventional full-scale wastewater treatment facilities contributing to phosphorus removal. It is often proposed that environmental conditions, such as dissolved oxygen, contribute to the Accumulibacter population structure. Similarly, the ability to perform various steps within the denitrification pathway are species dependent and may influence the Accumulibacter species present in low dissolved oxygen biological nutrient removal systems where nitrate/nitrite may serve as an alternative electron acceptor as opposed to oxygen. Using genome-resolved metagenomics and metatranscriptomics, we show that multiple species with varying capacities to denitrify exist within pilot-scale nutrient removal systems operating under low dissolved oxygen. Our results add to existing knowledge of the intra-population diversity of these organisms in minimally aerated systems, particularly outside of highly controlled lab-scale reactors.

4.3 KEY WORDS

Accumulibacter, enhanced biological phosphorus removal, low dissolved oxygen, denitrification, metagenomics, metatranscriptomics

4.4 INTRODUCTION

Enhanced biological phosphorus removal (EBPR) is a critical process for excess phosphorus (P) removal from wastewater and helps prevent eutrophication of water bodies receiving the treated effluent [1]. EBPR is achieved through organisms known as polyphosphate accumulating organisms (PAOs) that can intracellularly store polyphosphate. "*Candidatus* Accumulibacter", commonly referred to as Accumulibacter, affiliated with the *Rhodocyclaceae* family in *Proteobacteria* has been identified as a PAO commonly found in EBPR systems [2]. Accumulibacter possesses the ability to anaerobically generate internal energy and reducing equivalents through use of intracellularly stored polyphosphate and glycogen. This energy is used to take up volatile fatty acids (VFAs) and convert them to internally stored polyhydroxyalkanoate (PHA). Aerobically, Accumulibacter uses the stored PHA as an energy source for growth and to replenish the intracellularly stored polyphosphate and glycogen [3]. Under these cyclic anaerobic-aerobic conditions, net P removal from the bulk liquid is achieved [4].

A key aspect in the design of biological nutrient removal (BNR) treatment plants is the optimization of the anaerobic and aerobic environments that favor Accumulibacter activity [5]. However, as BNR treatment plant designs expand towards more energy efficient alternatives, such as operation with minimal or no aeration [6-8], the cycles of anaerobic and aerobic conditions often deviate from those initially considered optimal for Accumulibacter. Some members of the Accumulibacter lineage have been shown to thrive on anaerobic and aerobic cycles in which the dissolved oxygen (DO) is severely limited [9]. Others thrive under conditions in which the aerobic zone is replaced by an anoxic zone where oxidized nitrogen species serve as the electron acceptor [10, 11]. PAOs exhibiting P uptake under anoxic conditions have been termed denitrifying PAOs

(DPAOs). The adaptation of Accumulibacter species to these different environments illustrates the diversity of the lineage, with respect to both phylogeny and function [12, 13].

The Accumulibacter lineage has been traditionally subdivided, using the polyphosphate kinase (*ppk1*) gene as a phylogenetic marker, into two types (I and II) and several clades (IA-IH and IIA-III) [9, 14-16]. A recent metagenome-based evaluation of the Accumulibacter lineage confirmed the *ppk1*-based classification as a good choice to resolve Accumulibacter phylogeny, as it mirrors genome-based phylogeny [12]. However, the *ppk1* sequence differences do not necessarily reflect phenotypic and ecological variations amongst the clades or sub-clades [12, 17]. Particularly, the expected ability to couple P uptake to denitrification is not resolved by *ppk1* differences. Although it was initially suggested that nitrogen metabolism was a key ecological differentiator of Accumulibacter types and clades [18, 19], inspection of Accumulibacter metagenome assembled genomes (MAGs) has shown an inconsistent distribution of genes involved in the denitrification process [12]. In general, four steps are involved in the reduction of nitrate (NO_3^-) to nitrogen gas (N_2), with nitrate reductase (*narGHI* or *napAB*) reducing NO_3^- to nitrite (NO_2^-), nitrite reductase (*nirS* or *nirK*) reducing NO_2^- to nitric oxide (NO), nitric oxide reductase (*norBC* or *norZ*) reducing NO to nitrous oxide (N_2O), and nitrous oxide reductase (*nosZ*) reducing N_2O to N_2 [20]. Genes within the denitrification pathway have been identified as core genes in several genomes within the Accumulibacter lineage. For example, the *nir*S gene has been identified as a core Accumulibacter gene in the entire Accumulibacter genus, whereas *napAB* and *nosZ* have been identified as core genes to Type I Accumulibacter [21]. Yet, the presence or absence of other genes in the denitrification pathway is not uniform in all genomes of a particular clade [12], negating the use of the *ppk1*-based taxonomic classification as predictors of DPAO capability. The importance of DPAO activity and correctly identifying PAOs that can denitrify becomes important

in activated sludge systems operated with aerated zones having low-DO concentrations, where P removal can be accomplished by either PAOs with high affinity for oxygen [22] or by DPAOs that could also contribute to N removal from the wastewater [23-25].

We are interested in elucidating the role that different members of the Accumulibacter lineage play in P removal in BNR processes operated with minimal aeration, and here we describe a metagenome-based analysis of the Accumulibacter populations in pilot-scale systems treating primary effluent and subjected to the typical variations in water temperature, flow rates, and loadings that are experienced at full-scale. Accumulibacter MAGs obtained from samples collected during four separate long-term pilot plant experiments were used in combination with the growing list of publicly available and nearly complete, high-quality Accumulibacter MAGs [12] to assess their relative abundance during different stages of pilot plant operation. A recent metagenome-based analysis of the Accumulibacter lineage proposed the subdivision of the *Candidatus* Accumulibacter genus into several new species that mirrors the *ppk1*-based classification system [12]. Here we adopt the new species designations to refer to the distinct members of the Accumulibacter lineage, while retaining useful features of the *ppk1*-based classification.

4.5 METHODS

4.5.1 Operation of pilot-scale plants

Samples from four instances of pilot-scale plant experiments were used in this study (**Figure 4-1**). In all four experiments, the objective was to evaluate BNR performance when oxygen availability was reduced, compared to aeration conditions used in typical full-scale operation. In all cases, treatment trains were operated at the Nine Springs WWTP (Madison, WI)

and mimicked flow rate variations experienced in the full-scale process. Water temperature was not controlled and followed the same trends experienced in the full-scale process. All pilot plants treated primary effluent produced by the full-scale operation. In one set of experiments, two pilot plants were operated for 731 days. In a second set of experiments, two pilot plants were operated for 505 days.

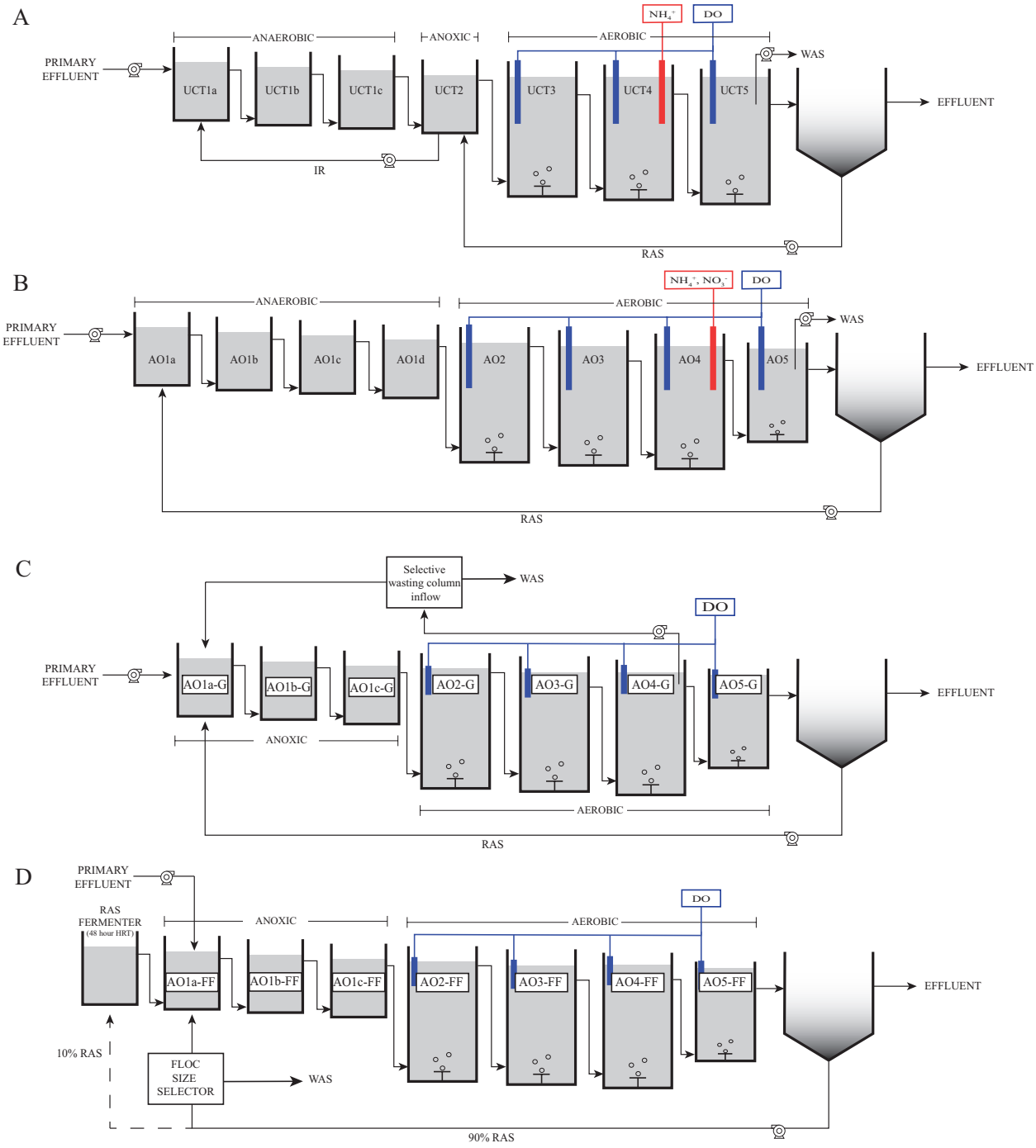

Figure 4-1 UCTca, AOia, AO-G, and AO-FF pilot-scale treatment train configurations

A detailed explanation of the first 483 days of operation of the first set of experiments was described in Stewart, Bashar [26]. Briefly, one pilot-scale system was configured as an anoxic-oxic (AO) process with intermittent aeration in the aerated zone (AOia), and the other was

configured as a University of Cape Town-type (UCT) process without internal sludge recycle and with continuous low-oxygen aeration in the aerated zones (UCTca). Aeration in each pilot-scale plant was controlled via ammonia-based aeration control (ABAC). Intermittent aeration in the AOia pilot reactor was designed to maintain an ammonium (NH_4^+) concentration between 2 and 5 mgNH_4^+-N/L at the mid-point of the aerated section. Air-on mode was initiated once the NH_4^+ concentration reached the high setpoint of 5 mgNH_4^+-N/L. Conversely, once the low setpoint of 2 mgNH_4^+-N/L was reached air-off mode began. During air-on mode the DO was maintained at or below 0.7 mg/L. Continuous aeration in the UCTca pilot reactor was controlled to maintain an ammonium concentration of 5 mgNH_4^+-N/L at the mid-point of the aerated section in the treatment train. In this setting, the aeration rate was adjusted as necessary to reach the NH_4^+ setpoint, but with the aeration rate also constrained to maintain DO between 0.1 and 0.6 mg/L. The solids retention time (SRT) of both plants was increased to overcome lower nitrification rates during the winter season when water temperatures reach as low as 12°C.

In the second set of pilot-plant experiments, the pilot plants were configured as AO processes and operated to evaluate the effect of selective wasting on activated sludge settleability while transitioning a BNR system from conventional high-DO to low-DO treatment. A detailed explanation of the operation of these pilot-scale systems can be found in Amstadt [27]. One pilot was equipped with a gravity-based selective wasting device, and therefore designated as the AO-G pilot-scale plant. Selective wasting in the other pilot was implemented through a floc filtering device, and therefore designated as the AO-FF. Return activated sludge (RAS) fermentation was also implemented in the AO-FF pilot-scale plant by deviating 10% of the RAS to a fermentation tank. Stepwise reductions in DO were carried out in phases throughout the operation of these two pilot-scale plants.

4.5.2 Metagenomic sequencing

Sequencing of DNA extracted from mixed liquor samples was carried out with either short-read Illumina NovaSeq (Illumina, Inc. San Diego, CA) or long-read PacBio Sequel IIe (Pacific Biosciences, Inc., Menlo Park, CA, USA) technology. Table 4-1 summarizes the days mixed liquor samples were collected and used for either short- or long-read metagenomic sequencing.

Table 4-1 Summary of DNA and RNA sampling.

Pilot ID	Days sampled for Illumina metagenomes	Days Sampled for PacBio 6-10kb library metagenomes	Days Sampled for PacBio 3kb library metagenomes	Days sampled for metatranscriptomics
UCTca	36, 190, 253, 373	288, 429, 631	441,638	
AOia	36, 190, 253, 301,373,440	162, 176, 288, 429, 631, 638	155,281	
AO-G	324, 382	39, 88, 95, 150	35	326, 327, 385
AO-FF		32, 135	42,91	

For short-read sequencing, samples were stored at -80°C until DNA extraction was performed. DNA was extracted using a DNeasy PowerSoil Kit (Qiagen), quantified using a Qubit fluorometer (ThermoFisher Scientific), and stored at -20°C until shipment to the sequencing facility. Samples were submitted to one of three sequencing facilities: Vincent J. Coates Genomics Sequencing Lab (QB3 Genomics; UC Berkeley; Berkeley, CA), the Joint Genome Institute (JGI; Berkeley, CA), or SeqCenter (Pittsburg, PA). Library preparation at QB3 Genomics was performed with a Kapa Biosystem Library Prep kit, targeting inserts 2x600 bp in length (Roche Sequencing and Life Science, Kapa Biosystems, Wilmington, MA). At the JGI, genomic DNA was sheared to 300bp using the Covaris LE220 instrument and size selected with SPRI using TotalPure NGS beads (Omega Bio-tek). Library prep included fragment end treatment, A-tailing, and ligation of Illumina-compatible adapters (IDT, Inc.) using the Kapa-HyperPrep kit (Kapa Biosystems). DNA was then sequenced 2 x 150bp on the Illumina NovaSeq 6000 platform using

S4 flow cells. At SeqCenter, sample libraries were prepared using the Illumina DNA Prep kit and IDT 10bp UDI indices, and sequenced on an Illumina NextSeq 2000, producing 2x151 bp reads.

For long read sequencing, DNA was extracted using two methods: 1) DNeasy PowerSoil Kit (Qiagen) without bead-beating and vortexing steps and 2) a modified published phenol-chloroform method [28, 29]. DNA was quantified using a Qubit fluorometer (ThermoFisher Scientific), and quality was assessed using a Nanodrop 2000 spectrophotometer (ThermoFisher Scientific). DNA samples extracted using the kit were submitted to the University of Wisconsin Biotechnology Center DNA Sequencing Facility (Madison, WI) for additional quantity control analyses including quantification using Qubit fluorometer (ThermoFisher Scientific), sizing using the FemtoPulse system (Agilent), and quality using NanoDrop One (ThermoFisher Scientific). Extracted DNA was sequenced from both methods, however, adequate DNA size, quantity and quality was more reliably obtained using the commercially available kit with modifications for a gentler extraction, as described in the manufacturer's protocol. Sequencing at the Joint Genome Institute (JGI) was performed on a PacBio Sequel IIe platform (Pacific Biosciences, Inc., Menlo Park, CA, USA). A PacBio HiFi library was prepared by shearing genomic DNA to either 3 kb or 6 to 10 kb depending on the quality of extracted DNA and performing ligation using the SMRTbell Express template prep kit (Pacific Biosciences). Size selection was performed with BluePippin (Sage Sciences). Library quality was assessed using the FemptoPulse system and quantified using the Qubit. Finally, the library was sequenced on a Sequel IIe using Sequel Polymerase Binding Kit 2.2 at the JGI.

4.5.3 Metatranscriptomic sequencing

In order to evaluate whether metatranscriptomic sequencing could help in the analysis of the Accumulibacter activity in the pilot plants, mixed liquor samples were collected from the AO-G reactor on days 324, 325, and 383 and used for RNA extraction. The samples at days 324 and 325 corresponded to immediately before and immediately after a reduction in DO setpoints (from 0.4, 0.8, and 1.0 to 0.3, 0.6, and 0.8 mg/L in AO2, AO3, and AO4, respectively) and the 383 day sample was two months after this DO setpoint change. Samples were centrifuged at 10000 rpm at room temperature for 2 min then immediately flash frozen in liquid nitrogen. Samples were stored at -80°C until extraction. RNA was extraction performed using a TRIzol-based (Invitrogen) method followed by phenol-chloroform separation and RNA precipitation. Sterile ceramic beads from PowerBead Tubes (Qiagen) and 1-mL of TRIzol were added to each of tubes containing the frozen pellets. The pellets were subjected to 2-3 minutes of beadbeating so that the pellets were fully homogenized. Next, successive phase separation was performed using mixtures of phenol, chloroform, and isoamyl-alcohol and chloroform to separate nucleic acids from other cell material. RNA was further purified using RNEasy (Qiagen). RNA was quantified using a Qubit fluormeter (ThermoFisher Scientific). At the SeqCenter sequencing facility, the RNA was further treated with DNAse (Invitrogen). Library preparation was performed using Illumina's Stranded Total RNA Prep Ligation with Ribo-Zero Plus kit and 10bp IDT for Illumina indices. Sequencing was done on a NextSeq2000 giving 2x51bp reads. Demultiplexing, quality control, and adapter trimming was performed with bcl-convert (Illumina).

4.5.4 Metagenome assembly, binning, and annotation

Raw short-reads that were sequenced at either QB3 Genomics or SeqCenter were quality filtered and trimmed using fastp [30]. Cleaned reads were individually assembled with metaSPAdes [31] with a range of k-mer values (21, 33, 55, 77, 99, 127). Each of the assemblies were binned using metaWRAP [32], which maximizes the strengths of three binning tools: metaBAT2 [33], CONCOCT [34], and MaxBin2 [35]. The resulting bins were further consolidated using the bin refinement module included in metaWRAP's software. DNA sequenced for short-reads at JGI were also processed by JGI using their Metagenome Workflow [36]. Briefly, raw reads were quality filtered, all metagenome samples were individually assembled using metaSPAdes [31], and binned using metaBAT2 [33].

Raw long-reads were filtered using BBTools (https://jgi.doe.gov/data-and-tools/bbtools/), and CCS reads were assembled using metaFlye [37]. Cleaned reads were then mapped on to the assemblies using minimap2[38]. Finally, the assemblies were polished using Racon [39]. The assemblies were binned using two approaches: with metaBAT2 (performed by JGI) and with metaWRAP (as described above).

All resulting MAGs from short- and long-reads were further quality controlled by identifying contaminated contigs for each bin using ProDeGe (v2.3 with default parameters) [40] and custom tetranucleotide frequency analysis scripts (run.GC.sh and Calculating_TF_Correlations.R; https://github.com/GLBRC/metagenome_analysis). Contigs identified as contaminated by both methods were removed from the MAGs to improve the overall quality. All MAGs were quality-checked using CheckM [41] before further analysis. Functional annotations for each MAG were assigned with Prokka [42] and anvi'o [43],which predicts metabolic capability using those defined by KEGG Orthologs [44].

4.5.5 Phylogenetic analysis and relative abundance

Assembled MAGs were classified using GTDB-Tk "classify_wf" [45]. MAGs belonging to the Accumulibacter lineage were combined with a total of 36 additional high-quality (HQ) MAGs compiled from the phylogenetic analysis by Petriglieri, Singleton [12]. A genome-based phylogenetic tree was constructed using 120 single-copy marker gene protein sequences identified with GTDB-Tk (**Supplementary Figure 4-1**). A maximum likelihood tree was created using the alignment with RAxML-NG [46] and visualized in iTOL [47]. Pairwise genome-wide ANI calculations between the MAGs recovered in this study and the 36 HQ genomes were made with FastANI [48] (**Supplementary Figure 4-2**).

To eliminate redundancy in the set of Accumulibacter genomes used for further analyses, we dereplicated 18 MAGs that were designated as species representatives by Petriglieri, Singleton [12] and the assembled MAGs from this study passing an >80% completeness and <5% contamination threshold at 98% ANI using dRep [49]. This non-redundant species set was used for metagenome read mapping. Filtered PacBio long-reads of both 3kb and 6-10kb libraries were divided into smaller 500bp long sequences using BBMap/shred.sh with no overlap between successive reads [50]. The shortened PacBio reads and the cleaned short-reads from Illumina sequenced metagenomes were competitively mapped (i.e. reads were mapped onto multiple genomes simultaneously) onto the non-redundant Accumulibacter MAG set using Bowtie2 with the default "--end-to-end" and "--fast" options [51]. We used coverM (https://github.com/wwood/CoverM) to obtain the relative abundance and percent of bases covered by at least one read of each MAG.

4.5.6 *ppk1* gene phylogenetic analysis

A phylogenetic analysis of the *ppk1* gene was conducted using a database of reference and clone sequences compiled by McDaniel, Moya-Flores [17], supplemented with sequences from Petriglieri, Singleton [12], and Accumulibacter MAGs assembled in this study. Duplicate *ppk1* sequences were removed using seqkit [52], and the resulting non-redundant sequences were aligned using MAFFT [53]. A maximum-likelihood phylogenetic tree of the aligned *ppk1* sequences was constructed with RAxML-NG with 100x bootstraps [46] and visualized in iTOL [47].

4.5.7 Tetrasphaera relative abundance analysis

Tetrasphaera relative abundance was estimated in all metagenome samples by, again, using read mapping. Cleaned short- and long-reads were competitively mapped onto a collection of Tetrasphaera genomes compiled by Singleton, Petriglieri [54] using Bowtie2 with the default "--end-to-end" and "--fast" options [51]. Relative abundance metrics were obtained using coverM (https://github.com/wwood/CoverM).

4.5.8 Metatranscriptomic data analysis

RNA reads were quality filtered using fastp [30], and rRNA reads were removed using SortMeRNA [55]. The protein-coding genes of all non-redundant Accumulibacter species representatives were predicted using Prodigal [56], annotated using Prokka [42], and concatenated together. Metatranscriptomic non-rRNA reads were pseudoaligned to the mapping index, and read counts were quantified using kallisto [57].

4.6 RESULTS AND DISCUSSION

4.6.1 Pilot-scale EBPR performance

Four pilot-scale plant experiments were conducted to evaluate BNR performance when aerobic sections of the treatment train are operated with lower DO concentrations than is typical in conventional BNR operations (**Figure 4-1**). To control aeration, two pilot-scale experiments used ammonia-based aeration control [26] and two experiments used stepwise reduction based on target DO concentrations [27]. In one instance (UCTca pilot plant; **Figure 4-1A**), the first 2 out of 3 aerated tanks (UCT3 and UCT4) maintained average continuous DO concentration less than 0.38 mgDO/L by controlling aeration to achieve an ammonium setpoint of 5 mgN/L in tank UCT4. The last aerated tank (UCT5) was operated to maintain a DO concentration of 1.0 mgDO/L [26]. In a second treatment train (AOia; **Figure 4-1B**), we implemented an intermittent aeration scheme in the aerated zone, with aeration in the first 3 tanks (tanks AO2, AO3, and AO4) controlled by allowing cyclic accumulation and consumption of ammonium. Aeration to the first 3 aerated tanks (AO2, AO3, AO4) was turned on when the ammonium concentration in tank AO4 reached 5 mgN/L and turned off when the ammonium in the same tank reached 2 mgN/L. During the aerated periods, DO was not allowed to accumulate above 0.7 mgDO/L. In the last aerated tank of this treatment train (AO5) the DO was constantly maintained at 2.0 mgDO/L. This ammonia-controlled aeration scheme resulted in aeration being off 42% of the time [26]. In the third and fourth pilot-scale experiments (AO-G, **Figure 4-1C**, and AO-FF, **Figure 4-1D**) aeration was controlled by setting different DO setpoints in the first three aerated tanks and using the last aerated tank as a high-DO polishing step. The first aerated tank in each treatment train was started with a setpoint of 0.4 mgDO/L and was gradually reduced to 0.2 mgDO/L, the second aerated tank started with a setpoint of 0.8 mgDO/L and had stepwise reductions to 0.3 mgDO/L, the third aerated tank was

initiated with a setpoint of 3.5 mgDO/L and gradually reduced to 0.5 mgDO/L. The last aerated tank was maintained at 3.5 mgDO/L [27].

All treatment trains demonstrated efficient P removal regardless of the aeration mode used. Influent filtered total P (TP) to the first set of pilot-scale experiments (UCTca and AOia) and the second set of pilots was 4.3 ± 1.9 and 5.5 ± 1.4 mgP/L, respectively. Average effluent filtered TP concentration in the treatment trains ranged from 0.29 mgP/L to 0.38 mgP/L (**Table 4-2**). Stable and complete nitrification was exhibited in all pilot-scale systems throughout the operation. Average filtered influent total Kjheldal nitrogen (TKN) was 38.6 ± 8.0 and 46.2 ± 6.3 mgTKN/L to the first and second set of pilot plant experiments, respectively, and effluent filtered TKN averaged between 1.83 and 4.43 mgTKN/L in the four pilot plants (**Table 4-2**). No substantial nitrite (NO_2^-) accumulation was observed in the effluent of any of the treatment trains (<1.0 mgNO_2^--N/L). Effluent nitrate (NO_3^-) ranged from 11.2 to 15.8 mgNO_3^--N/L.

Table 4-2 Pilot-scale reactor BNR performance summary

Pilot	Average Influent		Average Effluent			
	TP (mgP/L)	TKN (mgN/L)	TP (mgP/L)	TKN (mgN/L)	NO_3^- (mgN/L)	NO_2^- (mgN/L)
UCTca	4.3 ± 1.9	38.6 ± 8.03	0.38 ± 0.61	2.13 ± 1.03	13.0 ± 3.91	0.26 ± 0.25
AOia			0.33 ± 0.39	1.83 ± 1.06	11.2 ± 3.16	0.20 ± 0.16
AO-G	5.5 ± 1.4	46.2 ± 6.3	0.40 ± 0.66	2.42 ± 2.98	15.8 ± 4.07	0.84 ± 1.89
AO-FF			0.29 ± 0.59	4.43 ± 6.94	14.5 ± 6.05	0.67 ± 1.01

4.6.2 Assembly of Ca. Accumulibacter draft genomes

To analyze the microbial communities in the pilot-scale reactors we extracted DNA at different times during pilot plant operations (**Table 4-1**). In total, we obtained individual metagenomes from 12 Illumina libraries, 15 PacBio 6-10kb libraries, and 7 PacBio 3kb libraries (**Table 4-1**). Among all the assembled MAGs, 25 MAGs that were >50% complete and <10% contaminated (i.e.

medium quality based on MIMAG standards [58]) were classified as belonging to the Accumulibacter lineage (**Table 4-3**).

Table 4-3 Assembled Accumulibacter MAG statistics. MAGs are ordered to resemble phylogenetic clusters in Supplementary Figure 1. Bolded MAGs represent the best-quality Accumulibacter MAGs from each species assembled in this study.

Accumulibacter species	Pilot-scale plant	MAG ID – Strain name[a]	dRep score	Sequencing Platform	Completeness (%)	Contamination (%)	Size (bp)	Contigs	GC (%)	16S rRNA copies[b]
Ca. Accumulibacter regalis	-	*UW3	102.0		99.94	0.03	4329894	6	63.9	0
Ca. Accumulibacter appositus	-	*BA-92	88.3	Illumina	93.33	1.49	4947936	583	62.9	0
Ca. Accumulibacter adiacens	-	*HKU1	79.0	Illumina	90.06	2.54	3625256	824	63.9	0
Ca. Accumulibacter meliphilus	-	*UW-LDO	93.8	Nanopore and Illumina	95.24	0.7	4701482	187	62.5	0
Ca. Accumulibacter UW14	AOia	**3300056759_486 UW14**	79.7	PacBio (6-10kb)	95.24	4.02	5539002	26	62.5	2
Ca. Accumulibacter delftensis	-	*Ca. Accumulibacter delftensis	102.1		100	0.03	5278942	-	-	1[+]
	UCTca	**sample_331044_bin_402 UW15**	94.1	PacBio (6-10kb)	97.15	1.27	4895943	12	62.3	3
	UCTca	3300056625_186	-	PacBio (6-10kb)	96.44	5.27	5074113	15	62.4	3
	AOia	AO_20190605_bin_77	-	Illumina	50.86	1.72	1885282	69	63.0	0
Ca. Accumulibacter aalborgensis	-	*Ca. Accumulibacter aalborgensis	100.7	-	99.52	0.06	4325360	181	62.3	1
Ca. Accumulibacter phosphatis	-	*UW1	101.0	-	99.84	0.24	5306133	4	64.0	2
Ca. Accumulibacter UW22	AOia	**3300056831_295 UW22**	-	PacBio (6-10kb)	50.86	8.62	2847345	43	61.7	4
Ca. Accumulibacter propinquus	UCTca	**sample_331040_bin_374 UW16**	97.2	PacBio (6-10kb)	97.7	0.77	5010931	2	62.3	2
	UCTca	3300056624_334	97.1	PacBio (6-10kb)	97.62	0.77	5011213	2	62.3	2
	-	*OdNE_BAT3C.415	93.2	Nanopore and Illumina	95.26	0.98	4325360	62	63	2
	AO-G	sample_331047_bin_197	73.6	PacBio (6-10kb)	89.11	4.31	5490626	34	62.2	2
	AO-G	3300056599_153	-	PacBio (6-10kb)	92.45	9.57	5504906	39	62.4	2
Ca. Accumulibacter contiguus	UCTca	**sample_331044_bin_501 UW17**	96.6	PacBio (6-10kb)	98.81	1.22	5612843	4	61.6	2

	-	*SBR_L	95.2	IonTorrent	96.85	0.98	5024437	167	61.7	0
	UCTca	3300056625_204	95.0	PacBio (6-10kb)	97.29	1.22	5500985	3	61.6	2
	AOia	AO_20200108_bin_22	86.5	Illumina	85.24	0.21	3744202	133	61.7	0
Ca. Accumulibacter UW18	AOia	**3300055001_362 UW18**	89.5	Illumina	95.74	1.59	4577441	125	62	0
Ca. Accumulibacter vicinus		*UBA5574	93.8	Illumina	93.65	0.24	4283242	326	62.0	1^{+}
Ca. Accumulibacter cognatus	-	*SSA1	95.9	Nanopore	99.05	1.11	5169514	3	61.4	2
Ca. Accumulibacter affinis	-	*Fred_BAT3C.720	91.3	Nanopore and Illumina	93.81	0.98	5041483	13	62.3	1
Ca. Accumulibacter proximus	-	*EsbW_BATAC.285	82.1	Nanopore and Illumina	96.67	3.63	5402764	40	62.7	1
Ca. Accumulibacter necessarius	-	*UW12-POB	94.9	Illumina	98.1	0.98	4564207	91	62.7	0
Ca. Accumulibacter UW19	AOia	3300056623_77 **UW19**	78.4	PacBio (6-10kb)	80	0.98	4180114	5	62.1	2
	AOia	AO_20200108_bin_11	72.9	Illumina	82.97	2.76	3990905	393	62.8	0
	UCTca	3300056624_146	-	PacBio (6-10kb)	95.24	9.31	5512878	20	62.6	2
Ca. Accumulibacter UW20	AO-G	**sample_310334_bin_400 UW20**	99.3	PacBio (6-10kb)	99.05	0.57	4280132	5	63.6	2
	AO-G	3300056999_154	98.9	PacBio (6-10kb)	99.05	0.64	4517007	6	63.6	2
	AOia	3300056827_258	95.6	PacBio (6-10kb)	97.25	1.05	4226414	3	63.4	2
	AOia	sample_331041_bin_88	97.1	PacBio (6-10kb)	94.29	0.1	4028608	2	63.4	2
	AOia	3300055001_270	89.9	Illumina	90.03	0.54	3630092	47	64.3	0
	UCTca	LD_20200507_bin_113	87.3	Illumina	85.24	0.1	3206672	44	64.1	0
	AOia	3300057002_150	-	Illumina	67.42	0.06	2310040	98	64.7	0
Ca. Accumulibacter iunctus	-	*UBA2327	92.3	Illumina	92.43	0.29	4431027	325	65.2	1
Ca. Accumulibacter adjunctus	-	*SK-12	93.9	Illumina	92.6	0.05	4412715	331	65.8	0
Ca Accumulibacter UW21	AO-FF	3300056999_35	100.3	PacBio (6-10kb)	98.1	0.03	5194397	1	65.8	2

Ca Accumulibacter UW23	AO-G	3300056626_235 UW23	-	PacBio (6-10kb)	72.99	1.72	4288616	14	65.5	1
Ca. Accumulibacter similis	-	*SSB1	101.3	Oxford Nanopore	99.05	0.03	5039009	-	66	2
Ca. Accumulibacter conexus	-	*UW7	85.2	Illumina	98.97	3.04	4870756	102	66.3	1[+]

[a] Asterisks (*) denotes the representative MAGs used by Petriglieri et al. (2022) to define the candidatus species.
[b] Plus sign (+) denotes partial 16S rRNA gene sequence

4.6.3 Phylogeny of recovered Accumulibacter MAGs

We performed a genome-based phylogenetic analysis using the 25 Accumulibacter MAGs recovered in this study and the set of 36 HQ Accumulibacter MAGs compiled by Petriglieri, Singleton [12]. Based on the genome phylogeny, each of the 25 MAGs falls within the expected Accumulibacter lineage and Type (I or II) classifications (**Supplementary Figure 4-1**). Of the total 25 Accumulibacter MAGs assembled from the pilot reactors, 21 were Type II Accumulibacter. We also conducted pairwise genome-wide ANI comparisons to assess sequence similarities between the recovered MAGs in this study and HQ publicly available Accumulibacter genomes (**Supplementary Figure 4-2**).

To refine the collection of 25 new Accumulibacter MAGs and the 18 HQ Accumulibacter MAGs designated as species representatives by Petriglieri, Singleton [12], we dereplicated all 43 MAGs at 98% ANI and ensured the MAGs were at least 80% complete and <5% contaminated (**Table 4-3**). Of the 25 MAGs we assembled, 10 MAGs shared >98% ANI with 3 previously defined Accumulibacter species (Ca. Accumulibacter delftensis, Ca. Accummulibacter propinquus, Ca. Accumulibacter contiguus; **Table 4-3**), indicating they represent the same species. The other 15 MAGs clustered into 7 different groups in the dereplication analysis (**Table 4-3**). We identify the best Accumulibacter assemblies for each group, that were obtained in this study, with UW## identifiers, building upon the UW collection of Accumulibacter MAGs that have been assembled from activated sludge originally collected from the Madison Metropolitan Sewerage District wastewater treatment plant [17, 28, 59-61].

For the candidatus species Ca. Accumulibacter propinquus and Ca. Accumulibacter contiguus, one of the MAGs assembled in this study was of better quality than the representative MAGs used by Petriglieri, Singleton [12] to define the proposed species (i.e.,

sample_331040_bin_374 UW16 and sample_331044_bin_501 UW17 are of better quality than Accumulibacter propinquus OdNE_BAT3C.415 and Ca. Accumulibacter contiguus SBR_L, respectively), and thus, we propose that these new MAGs be considered as the best available species representatives for these candidatus species. Notably, Ca. Accumulibacter contiguus UW17 possess two full-length copies of the 16S rRNA gene, whereas Ca. Accumulibacter contiguus SBR_L does not contain 16S rRNA genes in its assembly.

Three MAGs assembled in this study clustered within the Ca. Accumulibacter delftensis species (**Table 4-3).** In this case, with 100% completeness and 0.03% contamination, the MAG already used to define the species by Petriglieri, Singleton [12] was found to be of higher quality than the 3 Ca. Accumulibacter delftensis MAGs assembled in this study. However, the assembly of the species representative did not include copies of the 16S rRNA gene, whereas two of the 3 MAGs assembled in this study contained 3 copies of the 16S rRNA gene in their assemblies. The best assembly from this study was designated as UW15 (**Table 4-3**).

A total of 15 MAGs shared no more than 96% ANI with any of the proposed candidatus species, and formed 7 different clusters (Ca. Accumulibacter UW14, UW22, UW18, UW19, UW20, UW 21, and UW 23 in **Table 4-3**). Out of these, 7 MAGs originating from 3 different pilot-plant operations clustered together, forming the Ca. Accumulibacter UW20 cluster which shared no more than 82% ANI with previously identified Accumulibacter species. Each of the other 8 MAGs shared less than 96% ANI with previously assigned species representatives and formed their own clusters in the dereplication analysis. Based on the *ppk1* gene phylogeny, for which Accumulibacter Type and Clade designations are assigned, we identified Ca. Accumulibacter UW14, Ca. Accumulibacter UW18, Ca. Accumulibacter UW19, and Ca. Accumulibacter UW21 as belonging to Clades IC, IIC, IID, and IIF (**Supplementary Figure 4-**

4). We propose Clade IIJ, a novel clade for the Ca. Accumulibacter UW20 cluster. We acknowledge that additional experiments are required to confirm the activities of these new clades as PAOs using FISH and a method such as Raman microspectroscopy to detect the presence of storage polymers, as described in Petriglieri, Singleton [12].

Two of the MAGs that formed separate clusters, 3300056831_295 (UW22 in **Table 4-3**) and 3300056626_235 (UW 23), had low completeness (<75%) and shared <98% ANI with any of the other genomes (**Supplementary Figure 4-2**). In the genome tree, 3300056831_295 is clustered nearest with members of the Ca. Accumulibacter propinquus species, however, shares at most 89.9% ANI with a member of this species. Further, MASH ANI analysis carried out by dRep [49], clusters 3300056831_295 with Clade IID members (**Supplementary Figure 4-3**). In fact, 3300056831_295 shares the highest ANI (94.4%) with members from Clade IID, and three of its four 16S rRNA gene copies cluster with those of Ca. Accumulibacter UW19, while one copy clusters with members of Ca. Accumulibacter propinquus likely indicating contamination (**Supplementary Figure 4-5**). This evidence led us to confidently remove this MAG from further analyses without concern of unaccounting for a previously identified Accumulibacter species. Likewise, we opted to remove 3300056626_235 from further analysis as this MAG shared 97.8% ANI with Ca. Accumulibacter UW21. We will henceforth refer to the dereplicated MAG set consisting of 16 previously defined species representatives, 2 improved species representatives, and 5 representatives of potentially novel species as the “non-redundant Accumulibacter species set”. A genome-wide maximum-likelihood phylogenetic tree of the non-redundant Accumulibacter species set is shown in Figure 4-2.

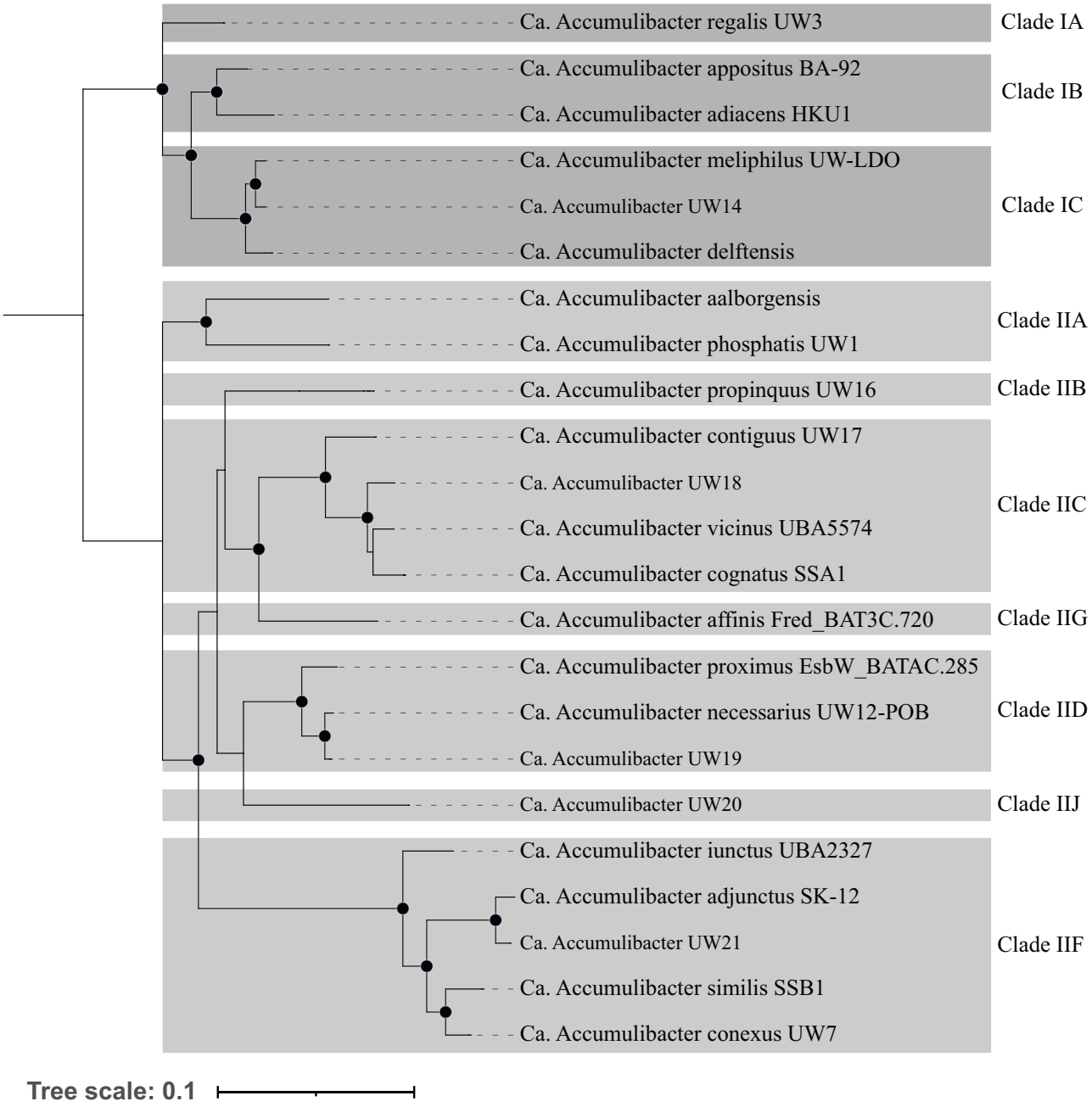

Figure 4-2 Maximum-likelihood genome tree of the non-redundant Accumulibacter species set created from the concatenated alignment of 120 single-copy marker genes using GTDBTk and 200x bootstraps. Bootstrap values >70% are denoted with filled black dot in the tree. The tree was visualized in iTOL.

4.6.4 Accumulibacter diversity and dynamics

Accumulibacter diversity within EBPR systems has typically been described using the *ppk1*-based phylogeny, which subdivides the lineage into two Types and several phylogenetically coherent Clades. Because Accumulibacter has not been isolated in pure culture, cultivation-independent methods, such as sequencing and quantification of the *ppk1* gene, have been applied to study Accumulibacter clade diversity. While the *ppk1*-based and genome-based phylogenies resemble each other, *ppk1* clade definitions do not capture the full extent of intra-clade genetic diversity.

To examine Accumulibacter diversity in the unconventionally aerated pilot-scale systems at low-DO, we used metagenome read mapping against the non-redundant Accumulibacter species set as a proxy for relative abundance of each species. Overall, the Accumulibacter community was more diverse than observed in lab-scale reactors, consisting of several species at any particular time, with rather even distribution of relative abundance which has been observed in previous lab-, pilot-, and full-scale reactors [9, 62]. Of the non-redundant Accumulibacter species set, Ca. Accumulibacter propinquus UW16, Ca. Accumulibacter necessarius UW12-POB, and Ca. Accumulibacter UW19 – classified as Type II Accumulibacter species – were abundant in at least 67% of the metagenomes analyzed from each of the four pilot-scale experiments (**Figure 4-3 and 4-4**). These three species on average made up between 48 and 75% of the total Accumulibacter population in all four pilot-scale treatment trains (**Figure 4-5**). At the beginning of operation in the AOia reactor, total Accumulibacter abundance was at its highest and consisted of the most diverse Accumulibacter community of all four pilot-scale systems. Ca. Accumulibacter regalis UW3, Ca. Accumulibacter appositus BA-92, Ca. Accumulibacter meliphilus UW-LDO, Ca. Accumulibacter UW14, and Ca. Accumulibacter delftensis – all Type I Accumulibacter species – were all notably more abundant at the start of operation in the AOia pilot reactor. After ~5 months

of AOia pilot operation, Ca. Accumulibacter UW20 appeared more frequently in the metagenomes and made up 7% of the Accumulibacter population, on average. Total Accumulibacter abundance in the UCTca pilot-scale plant was a third of that in the AOia pilot pilot-scale plant and less diverse at the start of the operation. After six months of operation, the total Accumulibacter abundance doubled and remained fairly consistent in the next 5 metagenome samples spanning 6 months. Following this period, the Accumulibacter abundance decreased significantly. Ca. Accumulibacter affinis Fred_BAT3C.720 was uniquely abundant in only the UCTca reactor during the first year of operation making up 5% of total Accumulibacter. In both the AOia and UCTca pilot-scale plant, Ca. Accumulibacter contiguus UW17 (Type II) appeared more frequently after ~5 months of operation, particularly in the AOia reactor. It is important to note that each pilot reactor had been seeded with activated sludge from the Nine Springs WWTP and operated for 7-months under different conditions prior to the operation and sampling described here, thus the initial Accumulibacter population differed between the two pilot-scale plants and did not reflect the diversity in the full-scale WWTP.

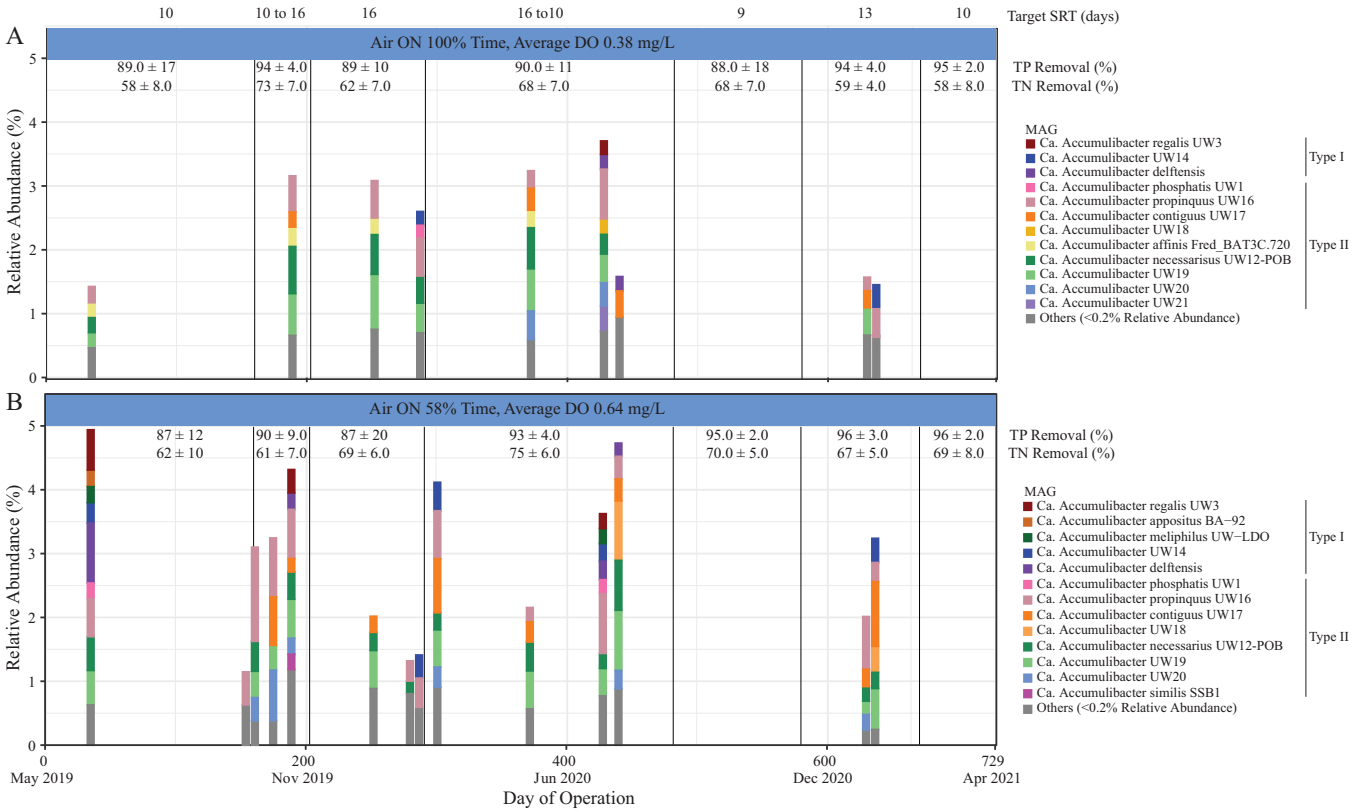

Figure 4-3 Accumulibacter relative abundance throughout the operation of the (A) UCTca and (B) AOia pilot-scale systems. The non-redundant MAGs that were >0.2% relative abundance at the time of the respective metagenome sample are plotted in each bar. The relative abundance of non-redundant species <0.2% relative abundance are plotted as “Others”. The average ± standard deviation total phosphorus (TP) and total nitrogen (TN) removal are noted for each solids retention time (SRT) setpoint throughout operation.

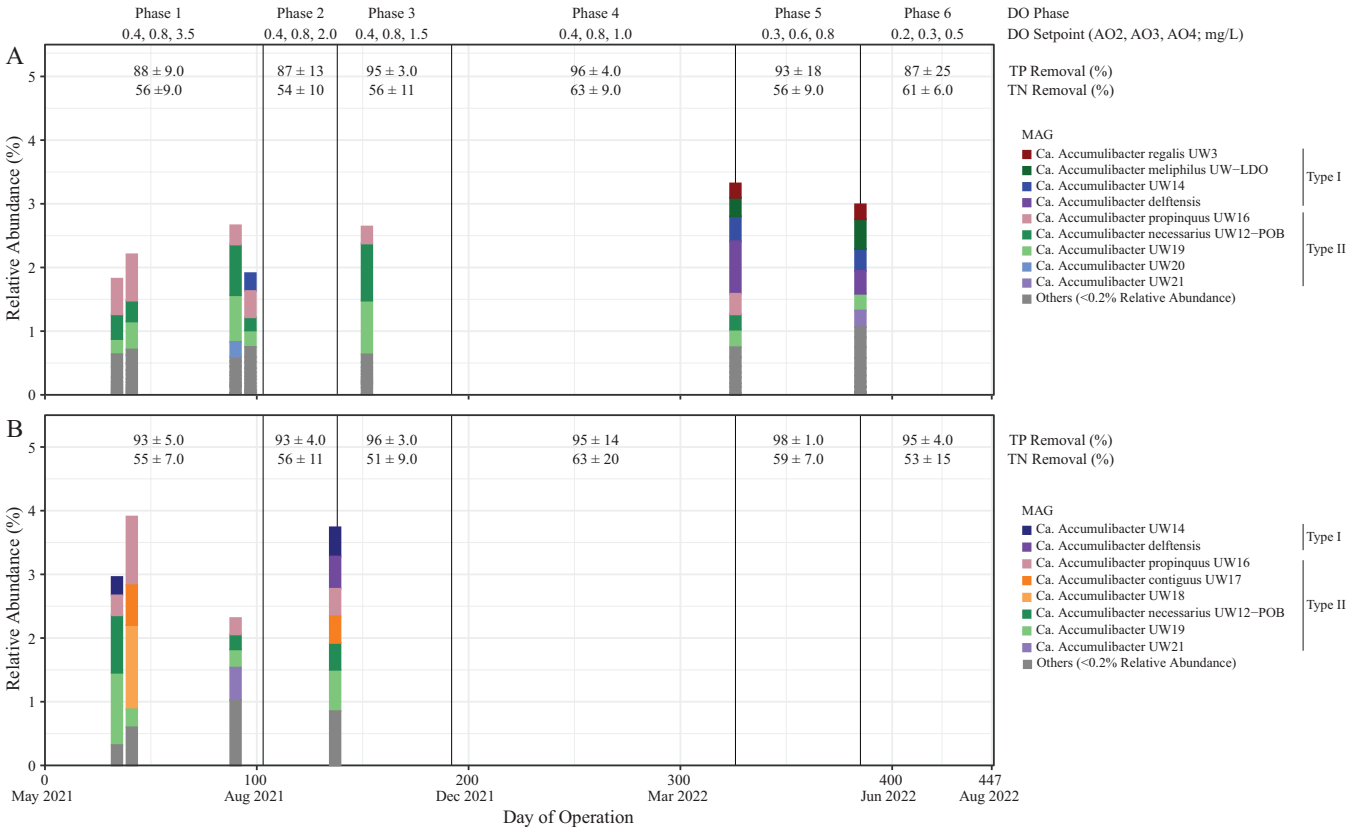

Figure 4-4 Accumulibacter relative abundance throughout operation of the (A) AO-G and (B) AO-FF pilots The non-redundant MAGs that were >0.2% relative abundance at the time of the respective metagenome sample are plotted in each bar. The relative abundance of MQ non-redundant species <0.2% relative abundance are plotted as "Others". The average ± standard deviation total phosphorus (TP) and total nitrogen (TN) removal are noted for each solids retention time (SRT) setpoint throughout operation.

At the start of the AO-G and AO-FF experiments, both pilots were reseeded with activated sludge from the full-scale WWTP. As stated previously, Ca. Accumulibacter propinquus UW16, Ca. Accumulibacter necessarius UW12-POB, and Ca. Accumulibacter UW19 were abundant in metagenomes from both pilots spanning the first 5 months of operation. In the AO-G reactor, these three species represented up to 80% of the Accumulibacter population in the initial operation. While Type II species were the dominant Accumulibacter present, Ca. Accumulibacter UW14 – Clade IC Accumulibacter – was abundant in one metagenome from the AO-G pilot and two metagenomes from the AO-FF pilot. Ca. Accumulibacter delftensis (Clade IC) was also abundant

after 5 months of operation in the AO-FF pilot. Notably, at the end of DO phase 4 and DO phase 5, sequentially lower in DO, Clade IA Accumulibacter species Ca. Accumulibacter regalis UW3, Ca. Accumulibacter meliphilus UW-LDO, Ca. Accumulibacter UW14, and Ca. Accumulibacter delftensis consisted of about half of the Accumulibacter population present in the AO-G pilot.

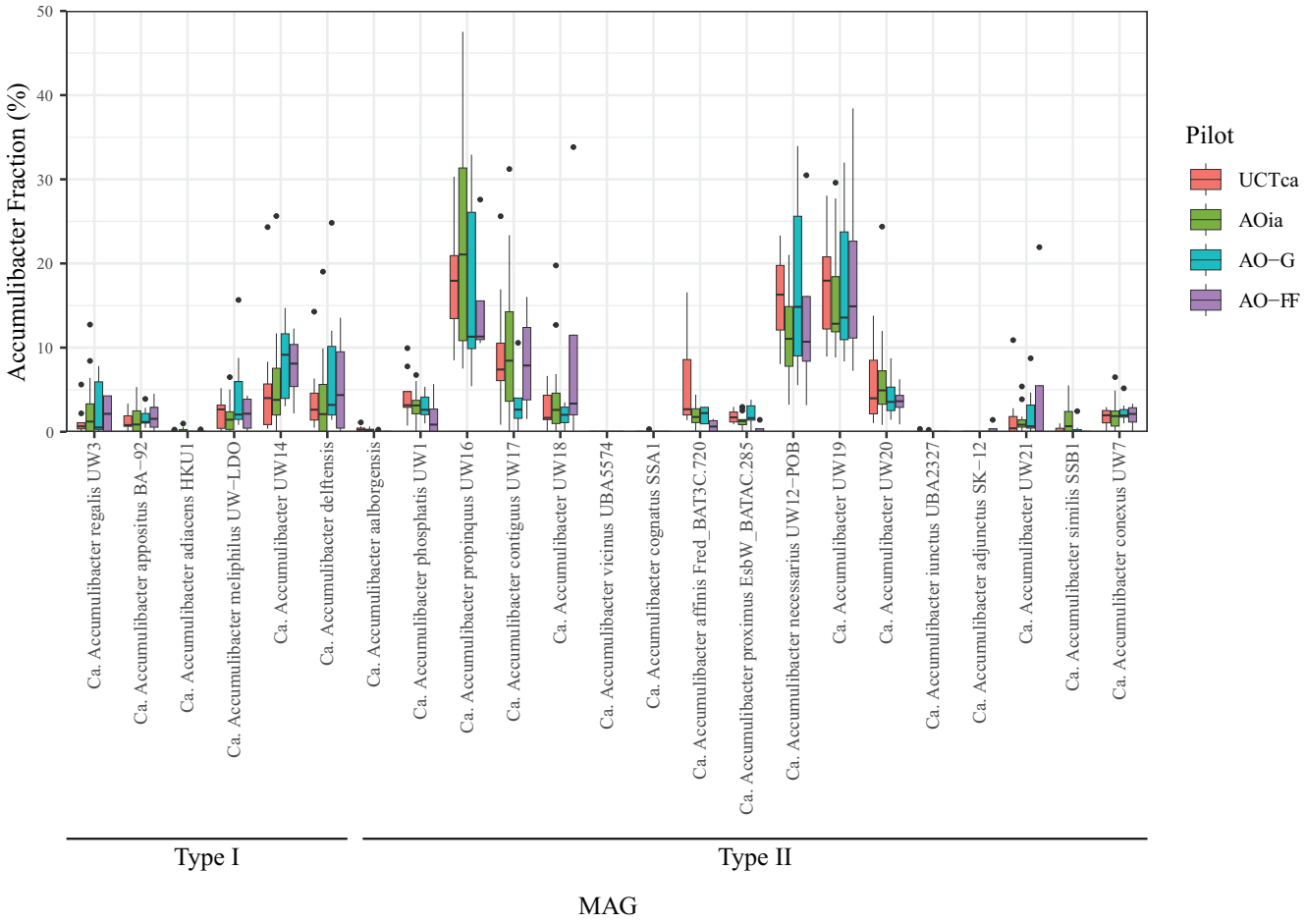

Figure 4-5 Average abundance of MAGs in the non-redundant Accumulibacter species set relative to the total Accumulibacter population.

Previous studies of Accumulibacter in low-DO and anoxic systems, has focused primarily on Type I, as this lineage has been the dominant Accumulibacter species present in these reactors [15, 21, 61, 63, 64]. However, Type II occurrence in low-DO systems is much less documented. The dominance of Type II Accumulibacter has been demonstrated in a previous pilot-scale study in

which an SBR was seeded and operated at the Nine Springs WWTP under low-DO conditions (between 0.2 and 0.7 mg/L) [9]. In that reactor Accumulibacter Clades IIA-IID were quantified using qPCR and were found to comprise 70-90% of the Accumulibacter abundance throughout operation. While the newly-defined species that were present within these clades were not measured, the dominant species in the pilot reactors of the current study (Ca. Accumulibacter propinquus UW16, Ca. Accumulibacter UW19, Ca. Accumulibacter necessarius UW12-POB, and Ca. Accumulibacter contiguus UW17), belong to clades IIB-IID. Ca. Accumulibacter necessarius UW12-POB was recovered from a photosynthetic bioreactor in which measured DO was <0.05 mg/L 70% of the time [60, 65]. Clade IID also dominated a lab-scale SBR under cyclic anaerobic and micro-aerobic conditions, however, a shift in dominance to a Clade IC strain (later identified as Ca. Accumulibacter meliphilus UW-LDO) was observed possibly due to reactor perturbation [61]. Despite the occurrence of Type II Accumulibacter in the pilot reactors of this study, there is no clear evidence of the dominance of one or a select few species of Accumulibacter under low-DO conditions. Rather, the heterogenous makeup of the Accumulibacter population suggests that the majority of members in the lineage have a high affinity for oxygen, and other environmental or operational factors contributed to the diversity of species present.

4.6.5 Tetrasphaera abundance and diversity

While Accumulibacter has been considered the key PAO in EBPR systems, the prevalence of the genus Tetrasphaera has gained attention as its abundance has been shown to outnumber that of Accumulibacter in many full-scale systems [54, 66]. In order to estimate the abundance of Tetrasphaera in the pilots we again used read mapping onto a HQ publicly available set of Tetrasphaera genomes compiled by Singleton, Petriglieri [54] (**Figures 4-6 and 4-7).** Abundant

species throughout the operation of both pilots were members of Clade 3 Tetrasphaera – Pbr2_Ega_b001, Pbr2_AalE_b188, and Pbr1_EsbW_b295. The two former species were recently given a proposed species name of *Ca.* Phosphoribacter hodrii, while the later species was named *Ca.* Phosphoribacter baldrii. The combined abundance of Accumulibacter and Tetrasphaera species is comparable to that observed of the PAO communities in full-scale BNR facilities [16, 67].

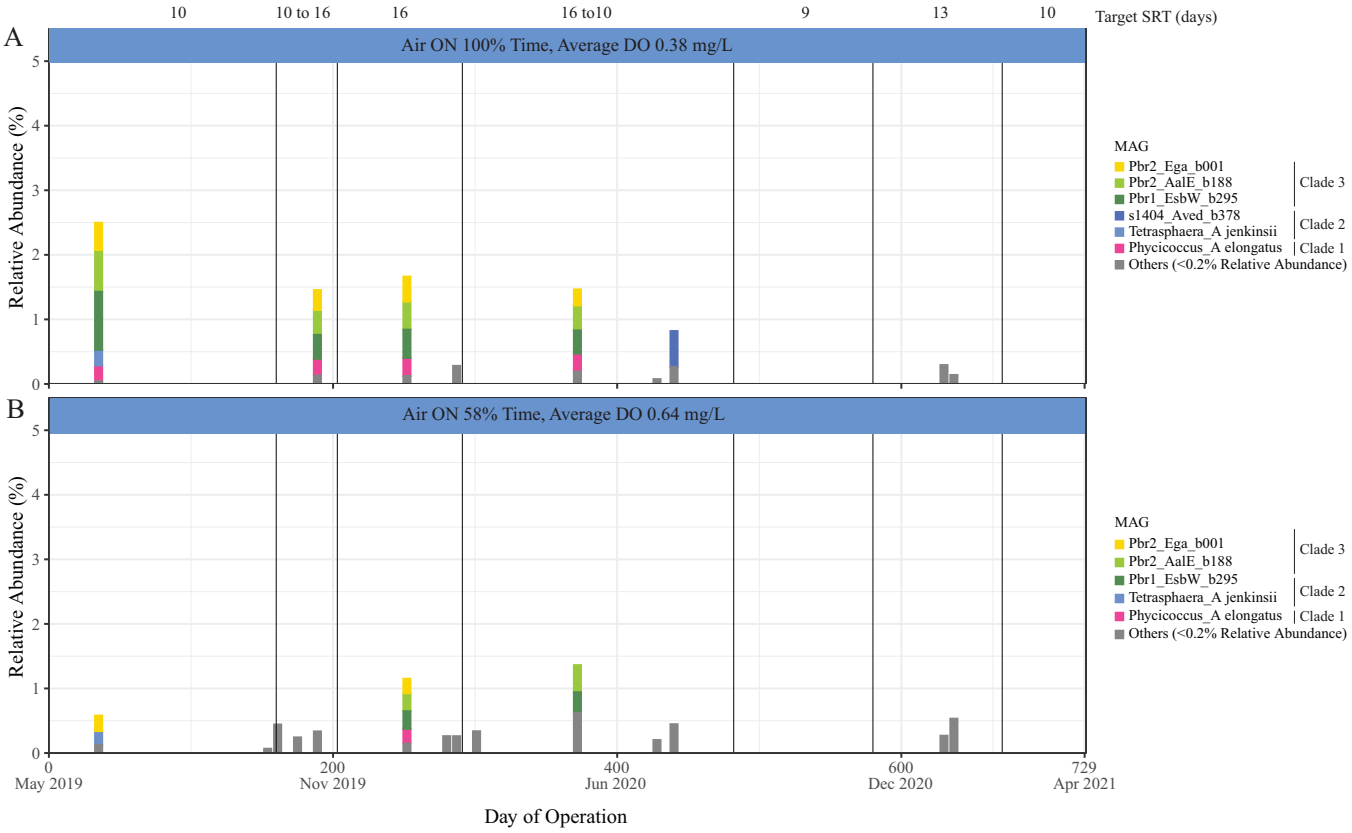

Figure 4-6 Tetrasphaera relative abundance in the (A) UCTca and (B) AOia pilots.

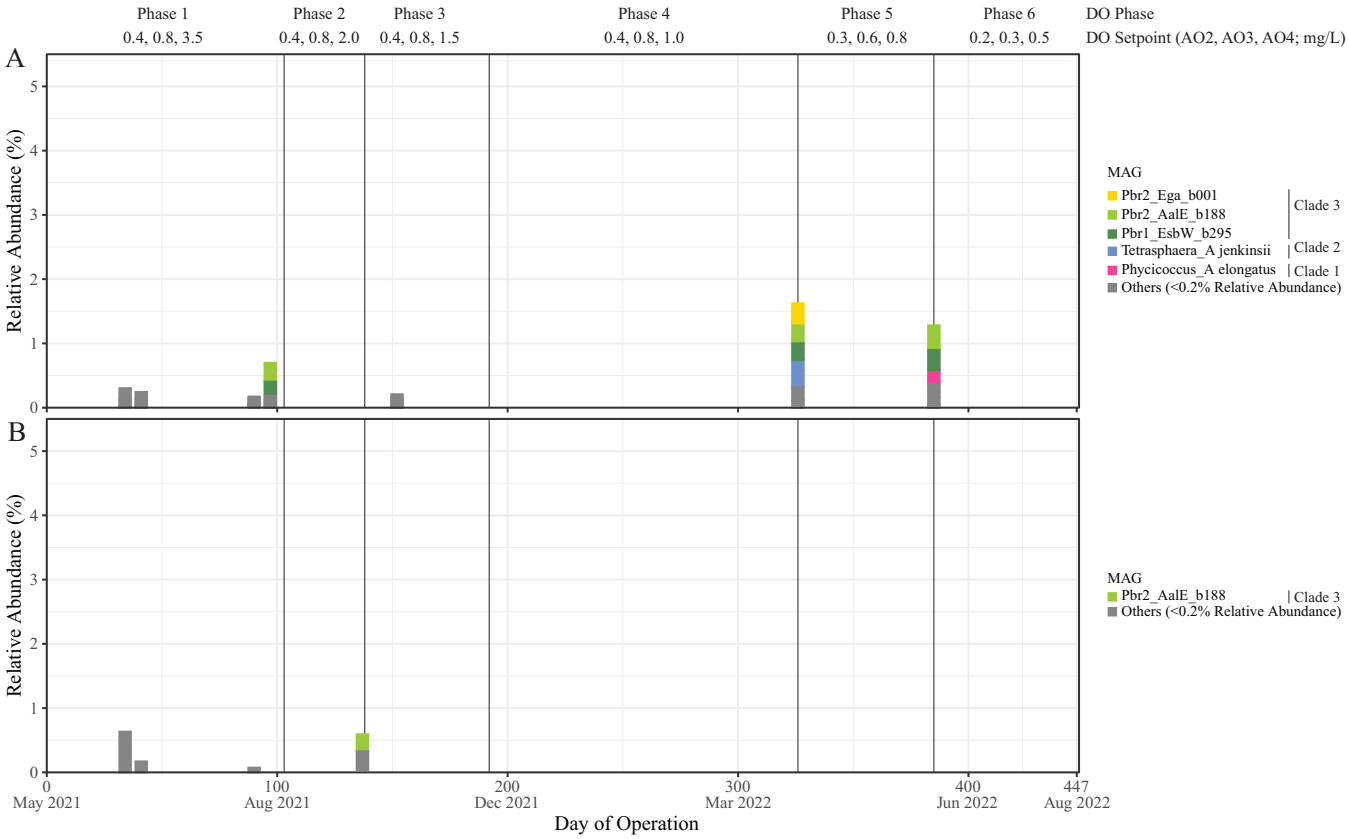

Figure 4-7 Tetrasphaera relative abundance in the (A) AO-G and (B) AO-FF pilots.

4.6.6 Denitrification and aerobic respiration potential of the Accumulibacter population

We hypothesized that Accumulibacter strains with some denitrification capability would become enriched in the pilot-scale reactors and would contribute to simultaneous denitrification and phosphorus removal during aerated periods. We also predicted that in the AOia pilot, Accumulibacter strains adapted to the intermittent anoxic periods would become enriched. To evaluate these predictions, we compared the denitrification machinery within the non-redundant Accumulibacter species set (**Table 4-4**). A summary of denitrification machinery in the 36 previously published HQ Accumulibacter MAGs can be found be found in Petriglieri, Singleton [12].

Table 4-4 Presence/absence of denitrification and aerobic respiration genes in MAGs assembled in this study. Determined using annotations from anvi'o which uses the KEGG database.

MAG ID	Completeness (%)	Contamination (%)	Species Rep.
Ca. Accumulibacter UW14	95.2	4.02	UW14
sample_331044_bin.402	97.2	1.27	UW14
AO_20190605_bin_77	50.8	1.72	delftensis
3300056625_186	96.4	5.27	delftensis
3300056831_295	50.9	8.62	NA
Ca. Accumulibacter propinquus UW16	97.7	0.77	UW16
3300056624_334	97.6	0.77	UW16
sample_331047_bin.197	89.1	4.31	UW16
3300056599_153	92.5	9.57	UW16
Ca. Accumulibacter contiguus UW17	98.8	1.22	UW17
3300056625_204	97.4	1.22	UW17
AO_20200108_bin_22	85.7	2.22	UW17
Ca. Accumulibacter UW18	95.7	1.59	UW18
Ca. Accumulibacter UW19	80.0	0.98	UW19
AO_20200108_bin_11	83.0	2.76	UW19
3300056624_146	95.2	9.31	UW19
Ca. Accumulibacter UW20	99.1	0.57	UW20
3300056999_154	99.1	0.64	UW20
3300055001_270	90.0	0.54	UW20
LD_20200507_bin_113	85.2	0.89	UW20
3300057002_150	67.4	0.06	UW20
sample_331041_bin_88	94.3	0.1	UW20
3300056827_258	97.3	1.05	UW20
Ca. Accumulibacter UW21	98.1	0.03	UW21
3300056626_235	73.0	1.72	UW21

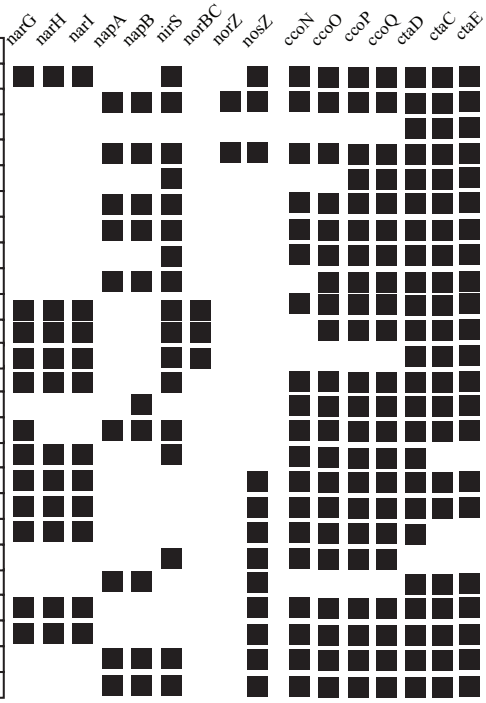

All species harboring the membrane-bound nitrate reductase (Nar), necessary for anoxic phosphorus uptake coupled with nitrate respiration, belong to Type II except for Ca. Accumulibacter meliphilus UW-LDO and Ca. Accumulibacter UW14 recovered in this study (**Table 4-4**). Ca. Accumulibacter necessarius UW12-POB (Clade IID), which was abundant in at least 75% of the metagenomes from the AOia, AO-G, and AO-FF pilots, contained the necessary machinery to carry out nitrate respiration (*narGHI*). A complete set of nitrate reductase genes was also present in Ca. Accumulibacter contiguus UW17 (Clade IIC), which was dominant in the AOia pilot, and Ca. Accumulibacter affinis (Clade IIG) which was uniquely dominant in the UCTca pilot. Notably, Ca. Accumulibacter UW19 (Clade IID), only contained the periplasmic nitrate reductase (*napB*) gene. Yet, MAG 3300056624_146, assembled in this study, shared >98% ANI with Ca. Accumulibacter UW19 and contained *narGHI* and *nirS* genes. MAG

AO_20200108_bin_11 also shared >98% ANI with Ca. Accumulibacter UW19 and contained *narG, napAB,* and *nirS* genes. Ca. Accumulibacter necessarius UW12-POB and Ca. Accumulibacter contiguus UW17 both carry two copies of the nitrite reductase (*nirS*) gene, with one copy downstream of the NAR operon (**Figure 4-8**). While Ca. Accumulibacter affinis Fred_BAT3C.720 also harbors two copies of the *nirS* gene, neither are positioned next to the *nar* operon. Periplasmic nitrate reductase, *nap*, does not translocate protons, thus it ultimately does not contribute to energy generation via proton motive force. Through gene-flux analysis, it has been suggested that the *nap* system is core amongst all Type I Accumulibacter [21], however its presence is also widespread amongst Type II Accumulibacter genomes [12, 13]. In this study, *nap* was encoded primarily by the Type I Accumulibacter species that were most abundant at the start of the operation in the AOia pilot reactor and in the final two metagenomes collected from the AO-G pilot. These species included Ca. Accumulibacter delftensis, Ca. Accumulibacter regalis UW3, and Ca. Accumulibacter appositus BA-92. NAP was also found in Clade IIB member Ca. Accumulibacter propinquus UW16 which made up a significant portion of the Accumulibacter population in all four pilots. The nitrite reductase gene, *nirS,* has been identified as a core, ancestral gene to the entire Accumulibacter lineage [21] and was present in the entire non-redundant Accumulibacter species set except Type II strains Ca. Accumulibacter cognatus SSA1 (Clade IIC), Ca. Accumulibacter UW19 (Clade IID) and Ca. Accumulibacter UW20 (proposed Clade IIJ).

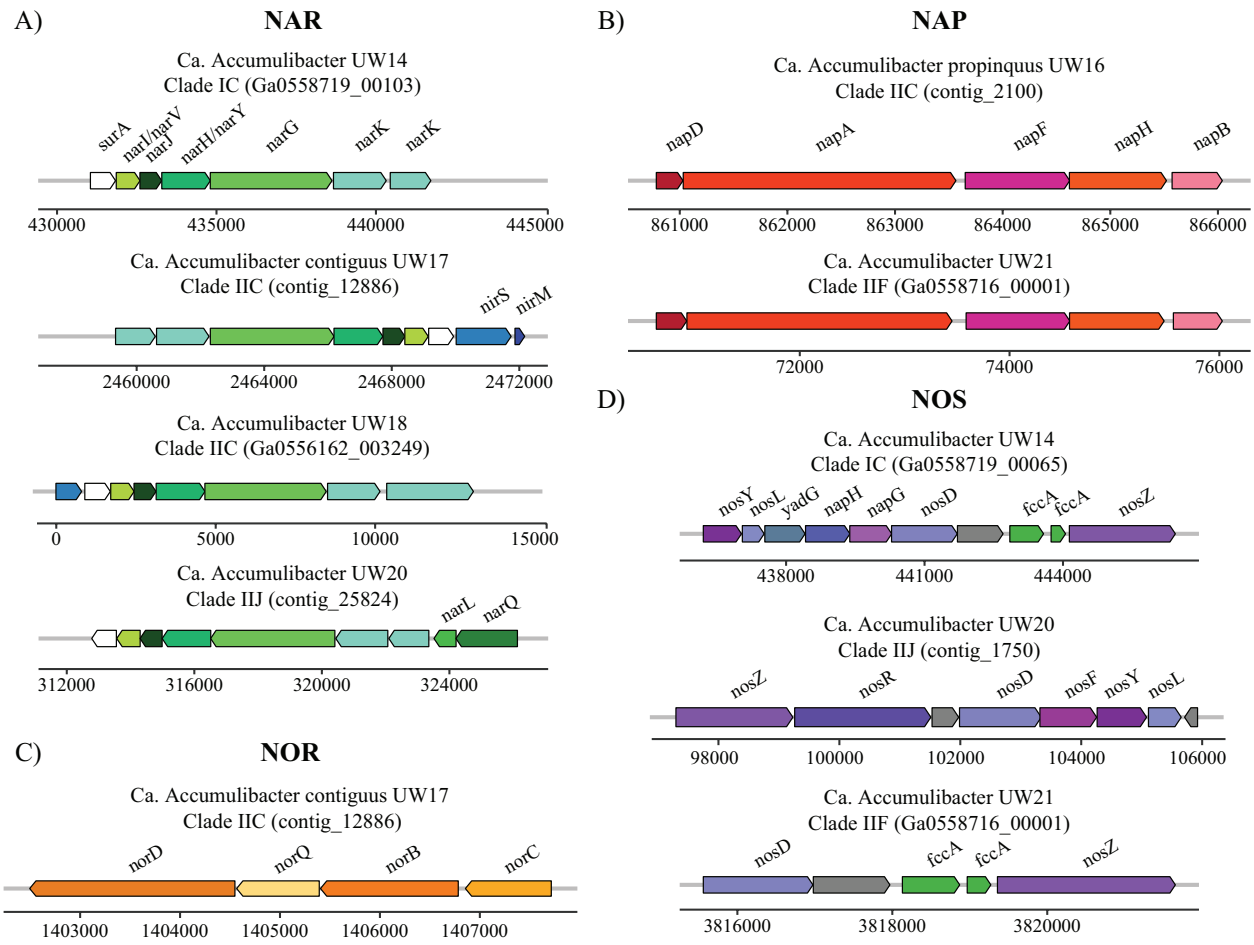

Figure 4-8 Denitrification gene neighborhoods of Accumulibacter MAGs assembled in this study. A) respiratory nitrate reductase (NAR) B) periplasmic nitrate reductase (NAP) C) nitric oxide reductase (NOR) and D) nitrous oxide reductase (NOS). Proteins with unknown function are colored in grey. Contig IDs from which the genes were recovered are shown in parenthesis for each MAG.

The final two steps in the denitrification pathway, nitric oxide and nitrous oxide reduction, are important because nitrous oxide production and consumption have implications for the emission of nitrous oxide, a potent greenhouse gas, from the wastewater treatment process. Nitric oxide reductase (NOR) can be classified into two types: cNor or qNor. The cNor form is encoded by *norB* and *norC* and genes while the alternate form qNor is encoded by the *norZ* gene. Of the non-redundant Accumulibacter species set, *norZ* is only found in Type I Accumulibacter species and Ca. Accumulibacter phosphatis UW1 (Clade IIA), while *norBC* was only found in Ca.

Accumulibacter contiguus UW17 (Clade IIC). Downstream of the *norBC* genes in this MAG were *norQ* and *norD* genes. Nitrous oxide reduction capability, the last reaction in the denitrification pathway encoded by the *nosZ* gene, was primarily found in the Type I Accumulibacter species that were most abundant in the AOia pilot during the start of the operation. Ca. Accumulibacter phosphatis and Ca. Accumulibacter UW20 were the only Type II species relevant to the Accumulibacter population in the pilots that harbored the *nosZ* gene.

To date, a full respiratory denitrification pathway has only been identified in Type I Ca. Accumulibacter meliphilus UW-LDO, consisting of *narGHI*, *nirS*, *norZ*, and *nosZ* genes. This species was only of significance in the AOia and AO-G pilots. However, Ca. Accumulibacter UW15, which clusters with Ca. Accumulibacter meliphilus UW-LDO, was abundant in some metagenomes from all pilots and lacks *norBC/Z* genes. Clade IID Accumulibacter species with respiratory nitrate reduction potential, namely Ca. Accumulibacter necessarius UW12-POB and 3300056624_146, a member of the Ca. Accumulibacter UW19 species cluster, were dominant in the majority of metagenomes from all pilots. Clade IID dominance has also been reported in a study aimed at achieving nitritiation [68]. This clade was associated with good denitrifying P removal under high NO_2^- concentrations and poor EBPR performance under NO_3^- accumulation. This could suggest another strain within Clade IID was capable of nitrite reduction coupled with P uptake but lacked the *nar* gene. Indeed, while Ca. Accumulibacter necessarius UW12-POB contains both a *nar* and *nir* gene, Ca. Accumulibacter proximus EsbW_BATAC.285, also of Clade IID, encodes *nap* and *nir* genes.

The diverse population of Accumulibacter in all pilot systems under low-DO conditions led us to search for cytochromes cbb_3 and aa_3, known cytochrome *c* oxidases which catalyze the reduction of oxygen to water[69], within the non-redundant Accumulibacter species set and the

lower quality MAGs assembled in this study. Cytochrome *aa*$_3$-type oxidases are known to have a low affinity for oxygen and have been shown to be upregulated in aerobic stage, specifically following oxygen contact [61, 70]. A complete *cta* operon encoding the *aa3*-type oxidase was encoded in all but 5 MAGs. Conversely, cytochrome *cbb*$_3$-type oxidases are known to have a high affinity for oxygen and are induced under low-DO conditions in Accumulibacter [61, 70]. This enzyme has also been shown to be widespread within the Accumulibacter lineage and is likely why these species has a high affinity for oxygen[61]. Only seven MAGs did not encode a complete *cco* operon for the *cbb3*-type oxidase.

4.6.7 Activity under low-DO conditions

To compare the transcriptional activity and the abundance of the non-redundant Accumulibacter species set under changing low-DO conditions, we collected activated sludge samples from the AO-G pilot in tank AO3 at the end of DO phase 4 (day 326; DO), a day after the start of DO phase 5 (day 327), and ~2 months after the start of DO phase 5 (day 385). During each of these time periods, Type I Accumulibacter consisted of nearly half the Accumulibacter community. In general, the most abundant Accumulibacter species were the most transcriptionally active (**Figure 4-9**). On days 326 and 327, Ca. Accumulibacter delftensis was the most transcriptionally active, followed by Ca. Accumulibacter UW15 and Ca. Accumulibacter meliphilus UW-LDO. These same three species were the most abundant and active two months after the DO reduction. Interestingly, Ca. Accumulibacter UW21 increased in abundance and activity from the end of DO phase 4 to DO phase 5, while the opposite was true for Ca. Accumulibacter propinquus UW16.

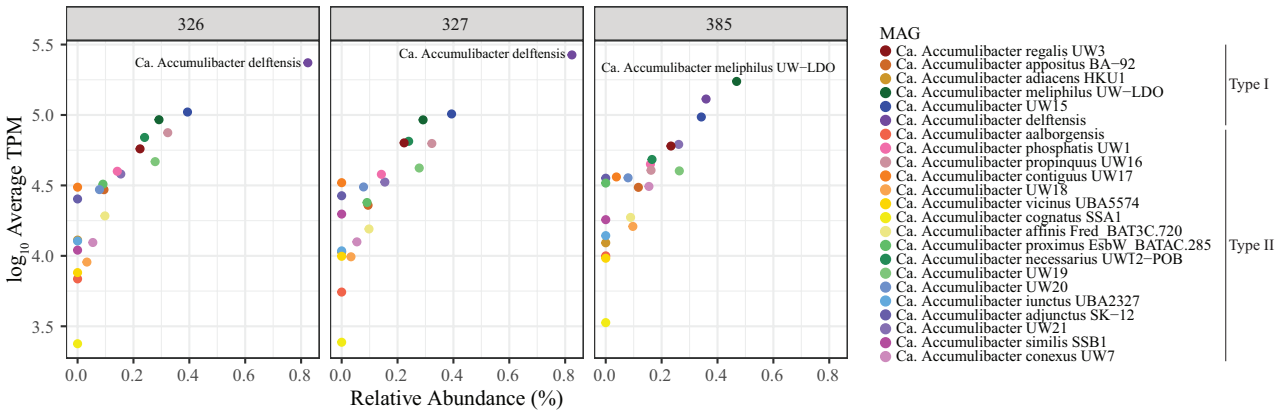

Figure 4-9 Relative abundance and average expression of MAG within the non-redundant Accumulibacter species set. Non-rRNA reads were mapped onto the protein-coding regions of the non-redundant Accumulibacter species set and normalized using transcripts per million (TPM). In general, abundance is a proxy for transcriptional activity

4.7 CONCLUSIONS

In this study, we used a refined database of medium- to high-quality Accumulibacter MAGs to investigate the Accumulibacter population structure and dynamics in pilot-scale BNR systems operated with low-DO conditions. We found that the Accumulibacter community was heterogeneous and highly dynamic. While the presence of some species in any system were consistent throughout time, it is not evident that low-DO was a determining factor for their occurrence. An examination of denitrification potential within the non-redundant Accumulibacter MAG set did not correlate with a significant dominance of any particular species, likely indicating niche differentiating roles which contribute to overall phosphorus and nitrogen removal. Our analyses show that other operational or environmental factors may explain the high microdiversity of the Accumulibacter community, and support evidence that the ability to survive low-DO conditions is widespread within the lineage [22, 61]. Further investigation of transcriptional activity and differential gene expression within a complex microbial community is needed to explain factors leading to functional niche partitioning or community interactions. Overall, this work demonstrates that the advancement of sequencing technology and the ever-growing publicly,

available database of medium- to high-quality reference MAGs can be used to study uncultivated organisms within complex microbial systems. From a wastewater treatment design perspective, this work highlights the resiliency of the Accumulibacter community under low-DO operation for economical and environmentally sustainable treatment.

4.8 Supplementary Figures

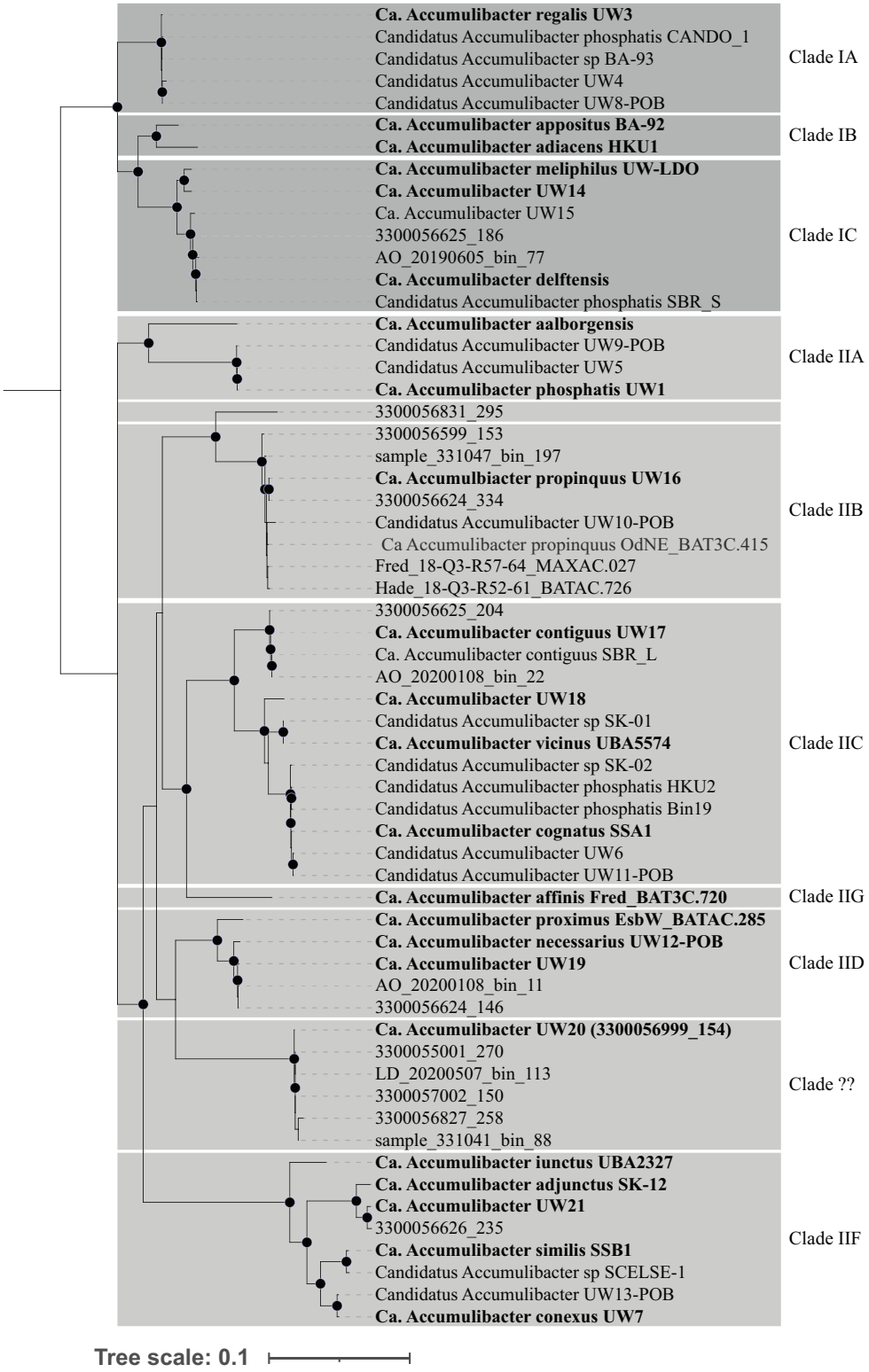

Supplementary Figure 4-1 Maximum-liklihood genome tree of all Accumulibacter MAGs assembled in this study and from Petriglieri et al. (2022)created from the concatenated

alignment of 120 single-copy marker genes using GTDBTk and 200 bootstraps. The tree was visualized in iTOL. Species representatives, which make up the MQ non-redundant Accumulibacter species set, are bolded.

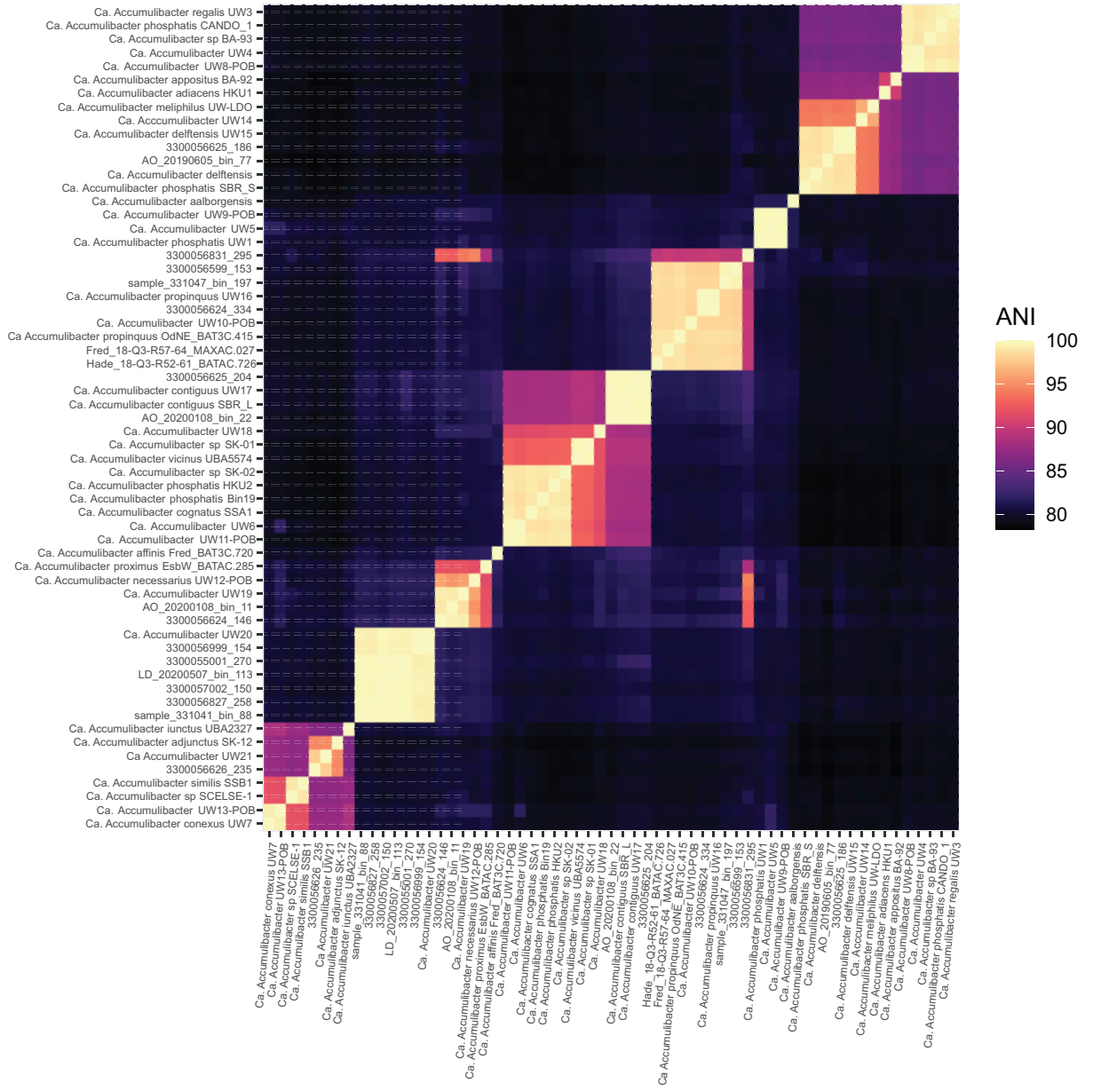

Supplementary Figure 4-2 Pairwise genome-wide ANI comparisons made with fastANI [48] between the 25 MAGs assembled in this study and the 36 HQ Accumulibacter MAGs compiled by Petriglieri, Singleton [12].

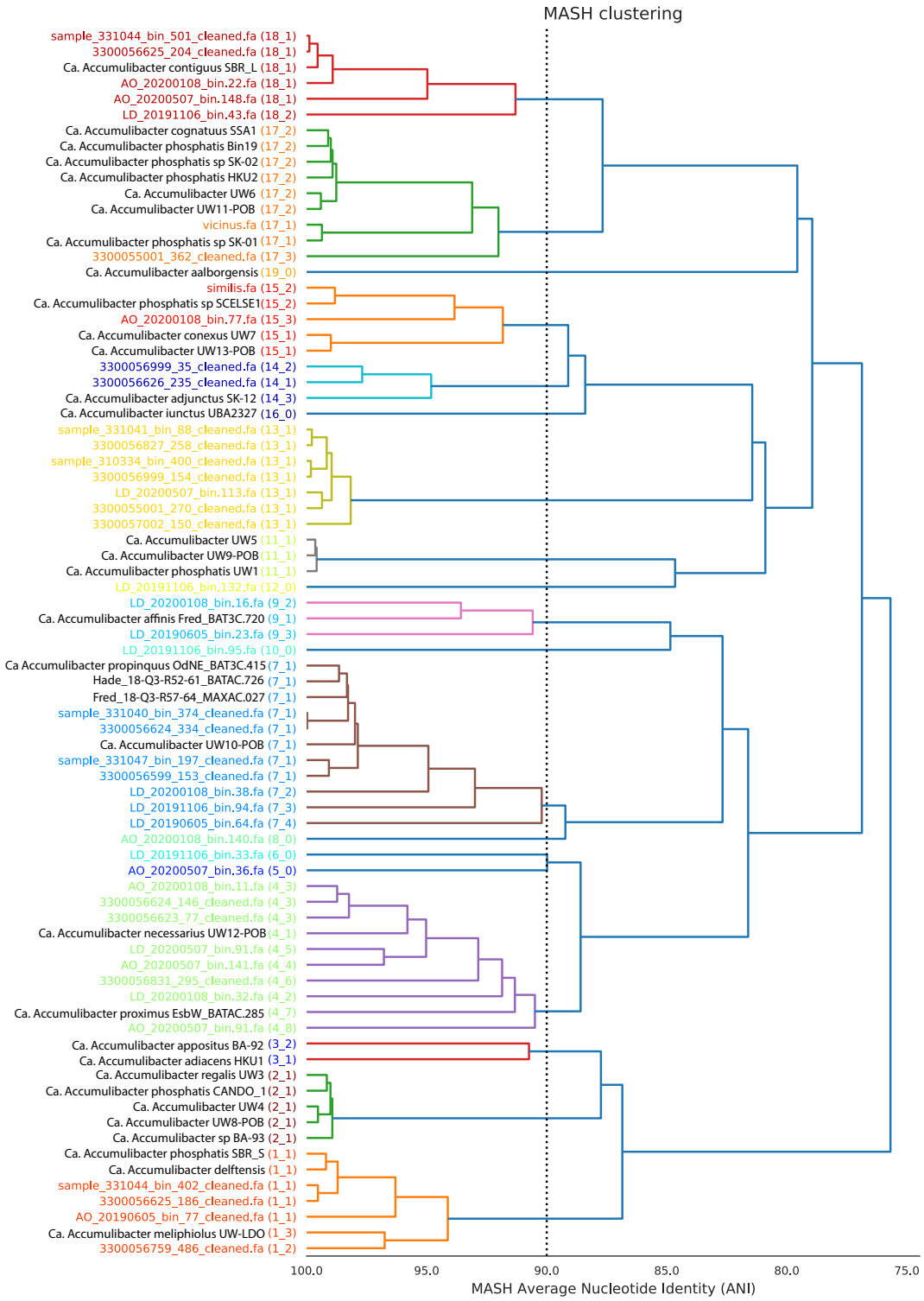

Supplementary Figure 4-3 Clusters of all Accumulibacter MAGs that were assembled from all 34 metagenomes and the 36 HQ MAGs compiled by Petriglieri et al. (2022). This figure was generated by dRep [49].

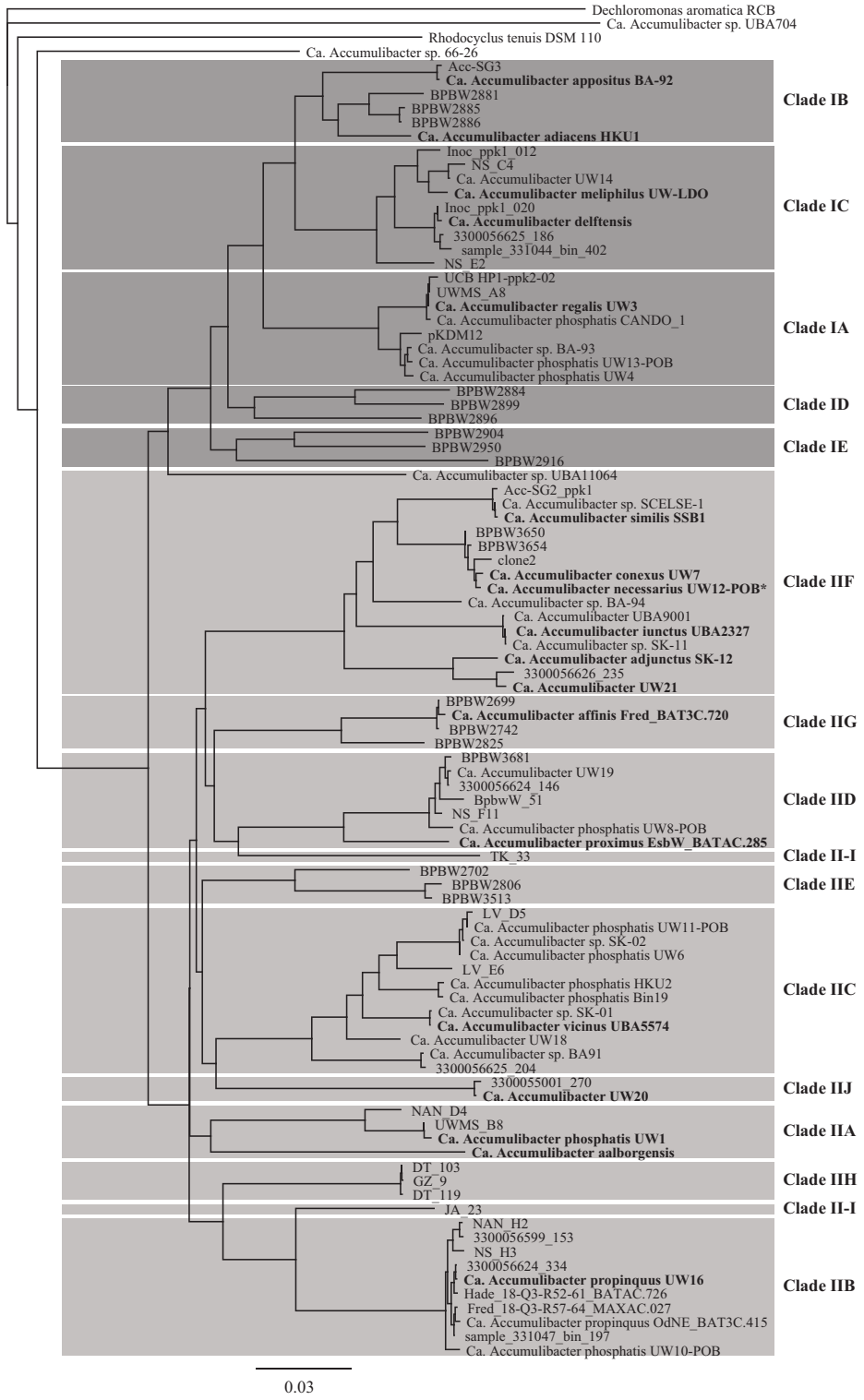

Supplementary Figure 4-4 Phylogenetic tree of non-redundant *ppk1* sequences from a database compiled by McDaniel, Moya-Flores, et al. (2021), supplemented with sequences from Petriglieri et al. (2022) and Accumulibacter MAGs assembled in this study.

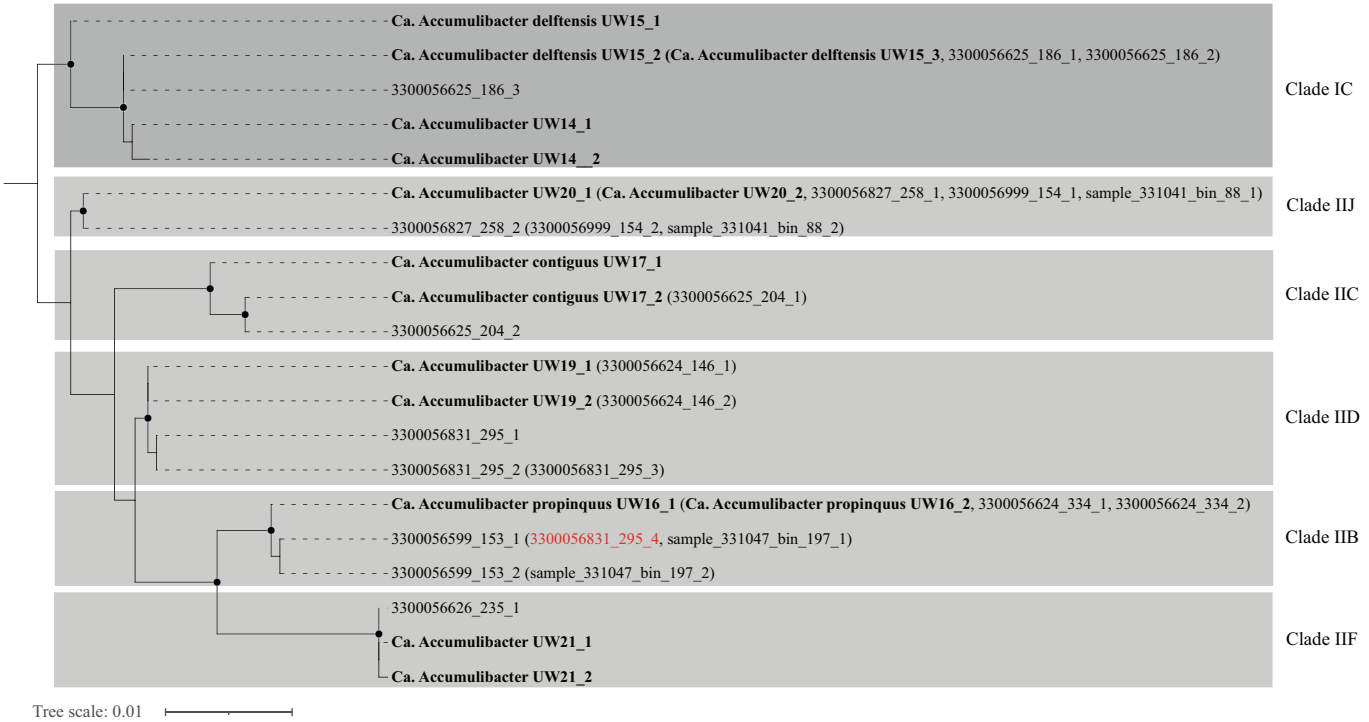

Supplementary Figure 4-5 Phylogenetic tree of all copies of the 16S rRNA sequences from the assembled Accumulibacter MAGs. Identical sequences of a particular branch are in parenthesis. The species representatives of Accumulibacter MAGs assembled from metagenomes of this study are bolded. The 16S rRNA sequence 3300056831_295_4 is likely contamination.

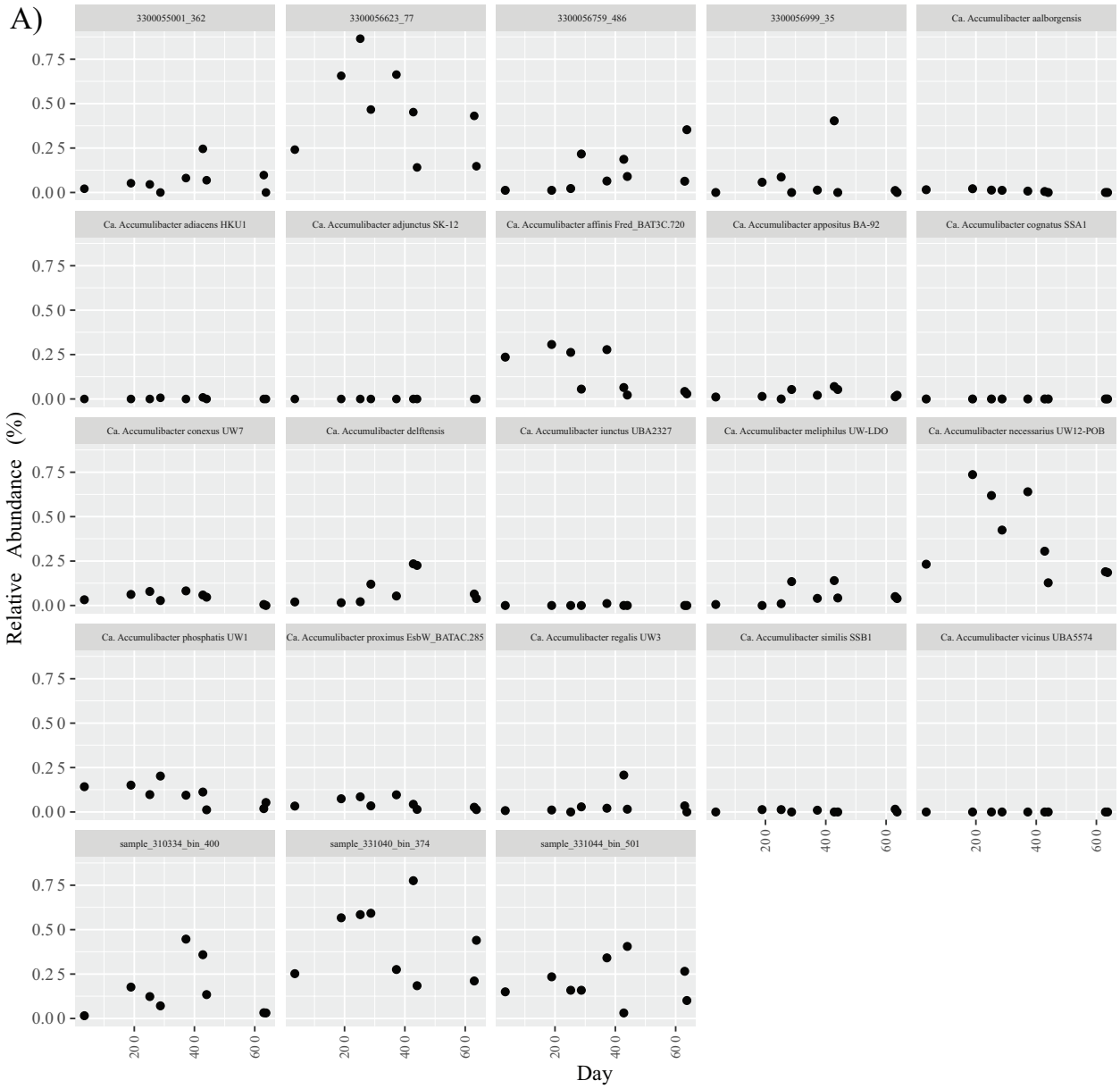
A)
3300055001_362
3300056623_77
3300056759_486
3300056999_35
Ca. Accumulibacter aalborgensis
Ca. Accumulibacter adiacens HKU1
Ca. Accumulibacter adjunctus SK-12
Ca. Accumulibacter affinis Fred_BAT3C.720
Ca. Accumulibacter appositus BA-92
Ca. Accumulibacter cognatus SSA1
Ca. Accumulibacter conexus UW7
Ca. Accumulibacter delftensis
Ca. Accumulibacter iunctus UBA2327
Ca. Accumulibacter meliphilus UW-LDO
Ca. Accumulibacter necessarius UW12-POB
Ca. Accumulibacter phosphatis UW1
Ca. Accumulibacter proximus EsbW_BATAC.285
Ca. Accumulibacter regalis UW3
Ca. Accumulibacter similis SSB1
Ca. Accumulibacter vicinus UBA5574
sample_310334_bin_400
sample_331040_bin_374
sample_331044_bin_501
Relative Abundance (%)
0.75
0.50
0.25
0.00
200
400
600
Day

B)

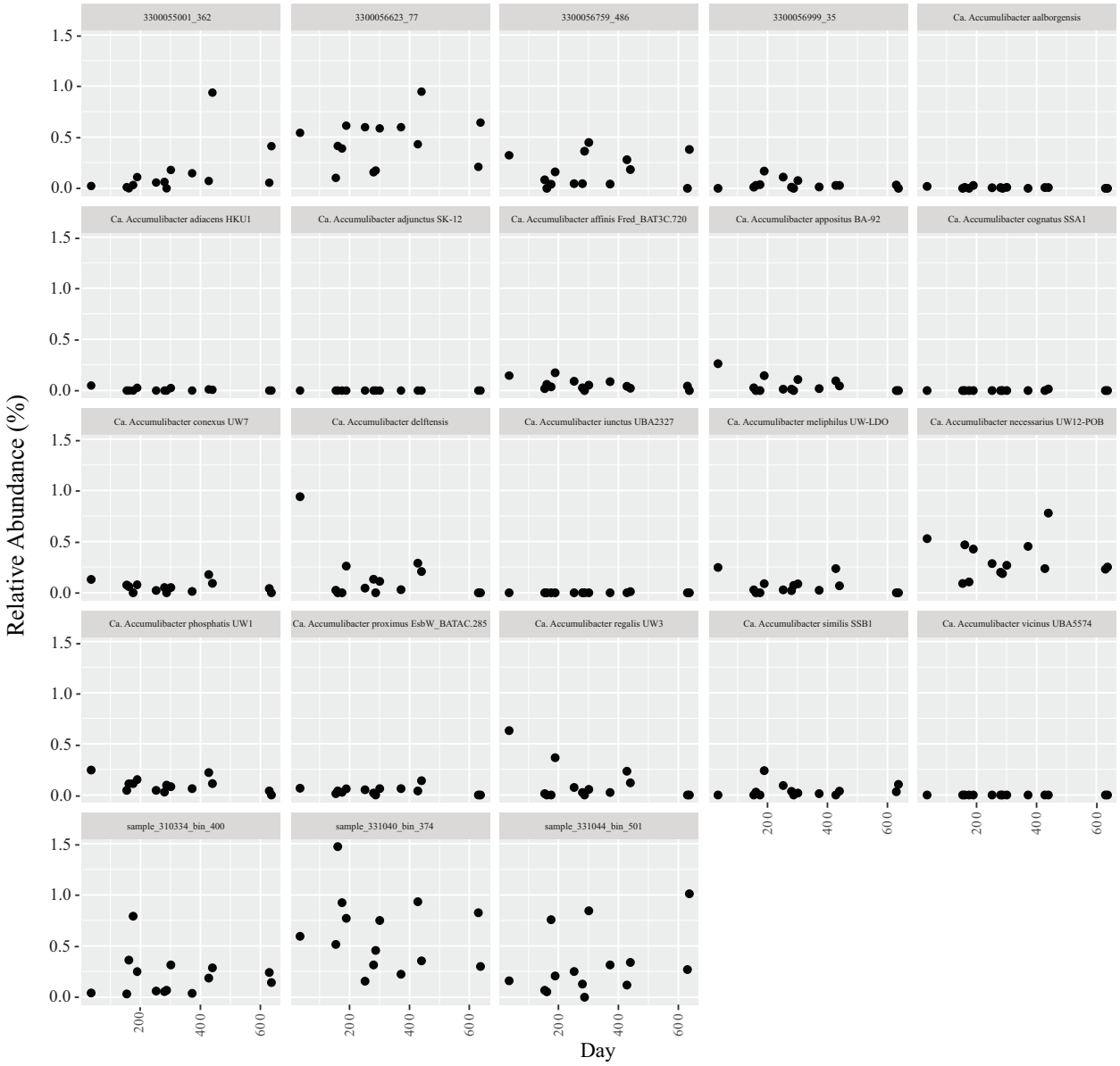
3300055001_362
3300056623_77
3300056759_486
3300056999_35
Ca. Accumulibacter aalborgensis
Ca. Accumulibacter adiacens HKU1
Ca. Accumulibacter adjunctus SK-12
Ca. Accumulibacter affinis Fred_BAT3C.720
Ca. Accumulibacter appositus BA-92
Ca. Accumulibacter cognatus SSA1
Ca. Accumulibacter conexus UW7
Ca. Accumulibacter delftensis
Ca. Accumulibacter iunctus UBA2327
Ca. Accumulibacter meliphilus UW-LDO
Ca. Accumulibacter necessarius UW12-POB
Ca. Accumulibacter phosphatis UW1
Ca. Accumulibacter proximus EsbW_BATAC.285
Ca. Accumulibacter regalis UW3
Ca. Accumulibacter similis SSB1
Ca. Accumulibacter vicinus UBA5574
sample_310334_bin_400
sample_331040_bin_374
sample_331044_bin_501
Relative Abundance (%)
0.0
0.5
1.0
1.5
200
400
600
Day

C)

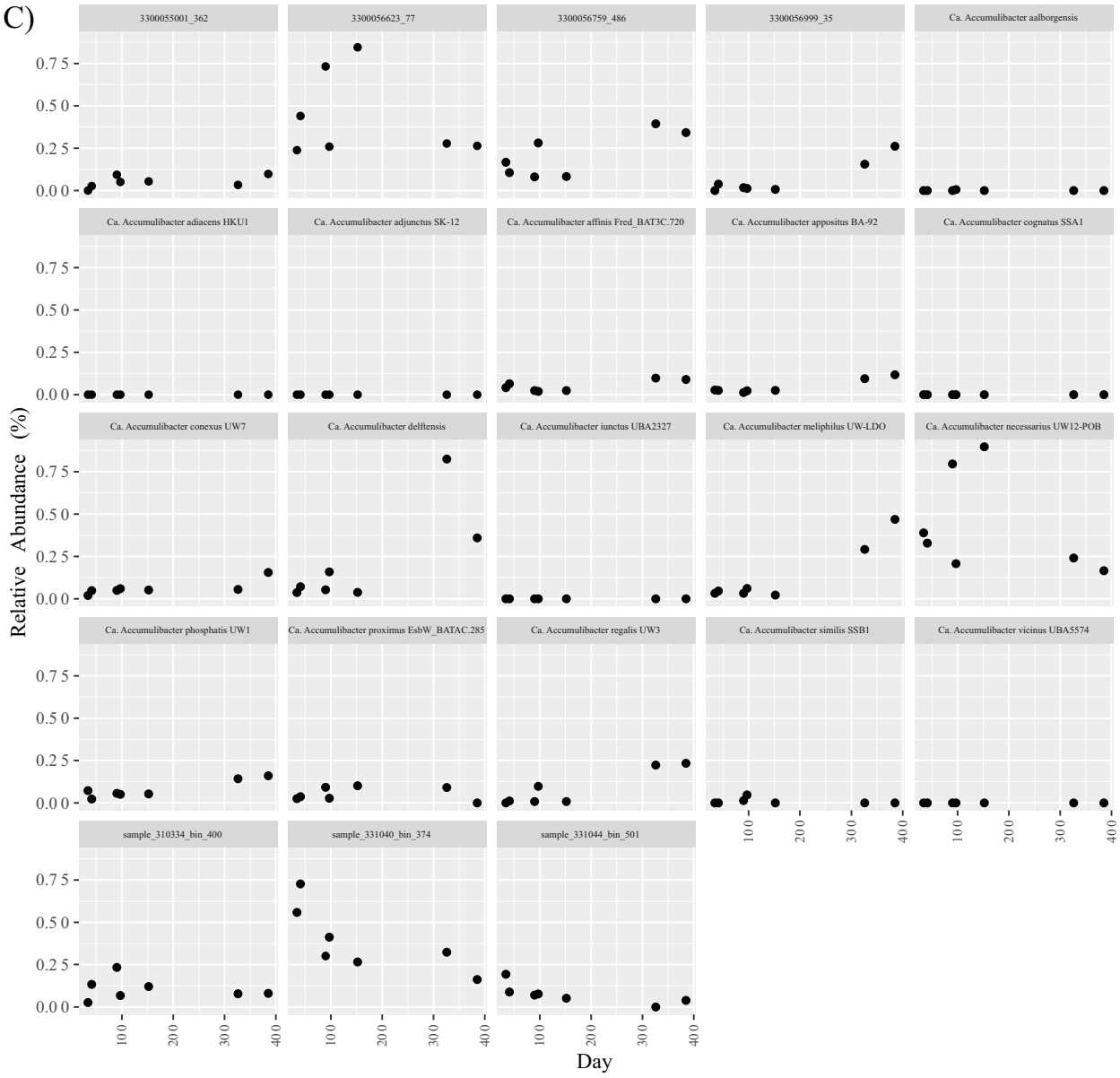
3300055001_362
3300056623_77
3300056759_486
3300056999_35
Ca. Accumulibacter aalborgensis
Ca. Accumulibacter adiacens HKU1
Ca. Accumulibacter adjunctus SK-12
Ca. Accumulibacter affinis Fred_BAT3C.720
Ca. Accumulibacter appositus BA-92
Ca. Accumulibacter cognatus SSA1
Ca. Accumulibacter conexus UW7
Ca. Accumulibacter delftensis
Ca. Accumulibacter iunctus UBA2327
Ca. Accumulibacter meliphilus UW-LDO
Ca. Accumulibacter necessarius UW12-POB
Ca. Accumulibacter phosphatis UW1
Ca. Accumulibacter proximus EsbW_BATAC.285
Ca. Accumulibacter regalis UW3
Ca. Accumulibacter similis SSB1
Ca. Accumulibacter vicinus UBA5574
sample_310334_bin_400
sample_331040_bin_374
sample_331044_bin_501
Relative Abundance (%)
0.75
0.50
0.25
0.00
100
200
300
400
Day

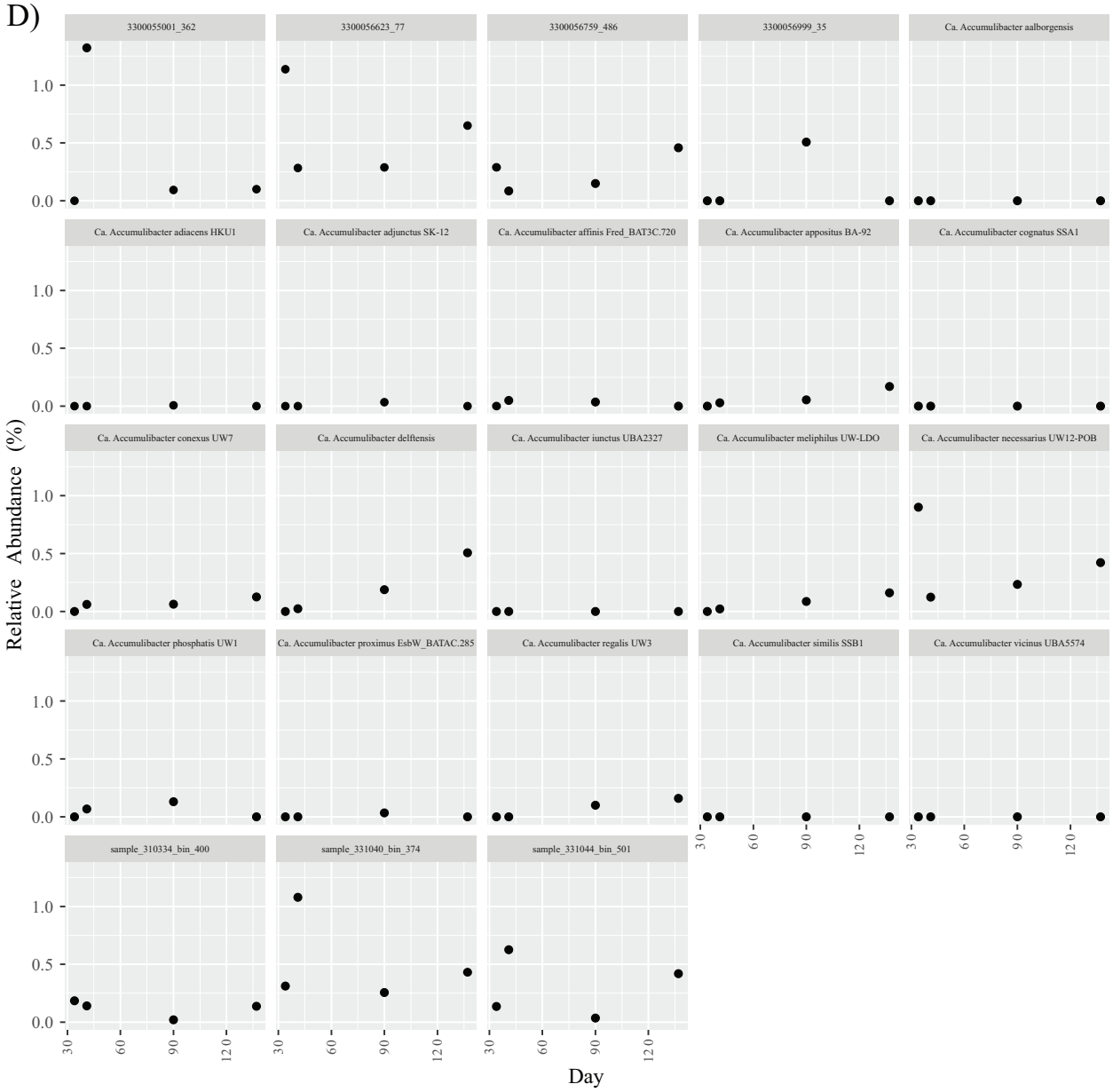

Supplementary Figure 4-6 Time-series relative abundance of each non-redundant Accumulibacter species in the AOia and UCTca pilot-scale plants. (A) UCTca (B) AOia (C) AO-G (D) AO-FF

4.9 Acknowledgments

This work was partially supported by funding from the National Science Foundation (CBET-1803055), the Madison Metropolitan Sewerage District (Madison, WI), and the Great Lakes Bioenergy Research Center (award number DE-SC0018409; U.S. Department of Energy, Office of Science). The author(s) utilized the University of Wisconsin – Madison Biotechnology Center's DNA Sequencing Facility (Research Resource

Identifier – RRID:SCR_017759) to perform quality control of high-molecular weight (HMW) DNA. The work conducted by the U.S. Department of Energy (DOE) Joint Genome Institute (https://ror.org/04xm1d337), a DOE Office of Science User Facility, is supported by the Office of Science of the U.S. DOE operated under the contract DE-AC02-05CH11231.

4.10 References

1. Stensel, H., *Principles of biological phosphorus removal.* Phosphorus and nitrogen removal from municipal wastewater: principles and practice (2nd edition). 1991: p. 141-166.
2. McMahon, K.D., S. He, and A. Oehmen, *The microbiology of phosphorus removal by activated sludge*, in *Microbial ecology of activated sludge*. 2010, IWA Publishers. p. 281-319.
3. Oehmen, A., et al., *Advances in enhanced biological phosphorus removal: from micro to macro scale.* Water Res, 2007. **41**(11): p. 2271-300.
4. Comeau, Y., et al., *Biochemical model for enhanced biological phosphorus removal.* Water Research, 1986. **20**(12): p. 1511-1521.
5. Oehmen, A., et al., *Incorporating microbial ecology into the metabolic modelling of polyphosphate accumulating organisms and glycogen accumulating organisms.* Water Res, 2010. **44**(17): p. 4992-5004.
6. Gao, H., Y.D. Scherson, and G.F. Wells, *Towards energy neutral wastewater treatment: methodology and state of the art.* Environ Sci Process Impacts, 2014. **16**(6): p. 1223-46.
7. Rieger, L., et al., *Ammonia-based feedforward and feedback aeration control in activated sludge processes.* Water Environ Res, 2014. **86**(1): p. 63-73.
8. Åmand, L., G. Olsson, and B. Carlsson, *Aeration control – a review.* Water Science and Technology, 2013. **67**(11): p. 2374-2398.
9. Camejo, P.Y., et al., *Candidatus Accumulibacter phosphatis clades enriched under cyclic anaerobic and microaerobic conditions simultaneously use different electron acceptors.* Water Res, 2016. **102**: p. 125-137.
10. Gao, H., et al., *Complete Nutrient Removal Coupled to Nitrous Oxide Production as a Bioenergy Source by Denitrifying Polyphosphate-Accumulating Organisms.* Environ Sci Technol, 2017. **51**(8): p. 4531-4540.
11. Roy, S., et al., *Denitrification kinetics indicates nitrous oxide uptake is unaffected by electron competition in Accumulibacter.* Water Research, 2021. **189**: p. 116557.
12. Petriglieri, F., et al., *Reevaluation of the Phylogenetic Diversity and Global Distribution of the Genus* mSystems, 2022. **0**(0): p. e00016-22.
13. Roy, S., et al., *Recent advances in understanding the ecophysiology of enhanced biological phosphorus removal.* Current Opinion in Biotechnology, 2021. **67**: p. 166-174.
14. He, S. and K.D. McMahon, *Microbiology of 'Candidatus Accumulibacter' in activated sludge.* Microb Biotechnol, 2011. **4**(5): p. 603-19.
15. Wang, Y., H. Gao, and G. F Wells, *Integrated omics analyses reveal differential gene expression and potential for cooperation between denitrifying polyphosphate and glycogen accumulating organisms.* Environmental Microbiology, 2021. **23**(6): p. 3274-3293.

16. Mao, Y., et al., *Dominant and novel clades of Candidatus Accumulibacter phosphatis in 18 globally distributed full-scale wastewater treatment plants.* Sci Rep, 2015. **5**: p. 11857.
17. McDaniel, E.A., et al., *Metabolic Differentiation of Co-occurring Accumulibacter Clades Revealed through Genome-Resolved Metatranscriptomics.* mSystems, 2021. **6**(4): p. e00474-21.
18. Flowers, J.J., et al., *Denitrification capabilities of two biological phosphorus removal sludges dominated by different 'Candidatus Accumulibacter' clades.* Environmental Microbiology Reports, 2009. **1**(6): p. 583-588.
19. Carvalho, G., et al., *Denitrifying phosphorus removal: linking the process performance with the microbial community structure.* Water Res, 2007. **41**(19): p. 4383-96.
20. Kuypers, M.M.M., H.K. Marchant, and B. Kartal, *The microbial nitrogen-cycling network.* Nature Reviews Microbiology, 2018. **16**(5): p. 263-276.
21. Gao, H., et al., *Genome-centric metagenomics resolves microbial diversity and prevalent truncated denitrification pathways in a denitrifying PAO-enriched bioprocess.* Water Research, 2019. **155**: p. 275-287.
22. Keene, N.A., et al., *Pilot plant demonstration of stable and efficient high rate biological nutrient removal with low dissolved oxygen conditions.* Water Res, 2017. **121**: p. 72-85.
23. Kim, J.M., et al., *Characterization of the denitrification-associated phosphorus uptake properties of "Candidatus Accumulibacter phosphatis" clades in sludge subjected to enhanced biological phosphorus removal.* Applied and environmental microbiology, 2013. **79**(6): p. 1969-1979.
24. Saad, S.A., et al., *Denitrification of nitrate and nitrite by 'Candidatus Accumulibacter phosphatis' clade IC.* Water Research, 2016. **105**: p. 97-109.
25. Zeng, W., et al., *Denitrifying phosphorus removal from municipal wastewater and dynamics of "Candidatus Accumulibacter" and denitrifying bacteria based on genes of ppk1, narG, nirS and nirK.* Bioresource Technology, 2016. **207**: p. 322-331.
26. Stewart, R.D., et al., *Pilot-scale comparison of biological nutrient removal (BNR) using intermittent and continuous ammonia-based low dissolved oxygen aeration control systems.* Water Science and Technology, 2021. **85**(2): p. 578-590.
27. Amstadt, C., *Assessing the effect of selective wasting and fermentation on slduge settleability and biological nutrient removal in two anoxic-oxic pilot-scale treatment plants*, in *Department of Civil and Environmental Engineering*. 2022, University of Wisconsin-Madison: Madison, WI.
28. Garcia Martin, H., et al., *Metagenomic analysis of two enhanced biological phosphorus removal (EBPR) sludge communities.* Nat Biotechnol, 2006. **24**(10): p. 1263-9.
29. Scarborough, M.J., et al., *Metatranscriptomic and Thermodynamic Insights into Medium-Chain Fatty Acid Production Using an Anaerobic Microbiome.* mSystems, 2018. **3**(6): p. e00221-18.
30. Chen, S., et al., *fastp: an ultra-fast all-in-one FASTQ preprocessor.* Bioinformatics, 2018. **34**(17): p. i884-i890.
31. Bankevich, A., et al., *SPAdes: a new genome assembly algorithm and its applications to single-cell sequencing.* J Comput Biol, 2012. **19**(5): p. 455-77.
32. Uritskiy, G.V., J. DiRuggiero, and J. Taylor, *MetaWRAP—a flexible pipeline for genome-resolved metagenomic data analysis.* Microbiome, 2018. **6**(1): p. 1-13.
33. Kang, D.D., et al., *MetaBAT 2: an adaptive binning algorithm for robust and efficient genome reconstruction from metagenome assemblies.* PeerJ, 2019. **7**: p. e7359.

34. Alneberg, J., et al., *Binning metagenomic contigs by coverage and composition.* Nature Methods, 2014. **11**(11): p. 1144-1146.
35. Wu, Y.-W., B.A. Simmons, and S.W. Singer, *MaxBin 2.0: an automated binning algorithm to recover genomes from multiple metagenomic datasets.* Bioinformatics, 2015. **32**(4): p. 605-607.
36. Clum, A., et al., *DOE JGI Metagenome Workflow.* mSystems, 2021. **6**(3): p. e00804-20.
37. Kolmogorov, M., et al., *metaFlye: scalable long-read metagenome assembly using repeat graphs.* Nature Methods, 2020. **17**(11): p. 1103-1110.
38. Li, H., *Minimap2: pairwise alignment for nucleotide sequences.* Bioinformatics, 2018. **34**(18): p. 3094-3100.
39. Vaser, R., et al., *Fast and accurate de novo genome assembly from long uncorrected reads.* Genome research, 2017. **27**(5): p. 737-746.
40. Tennessen, K., et al., *ProDeGe: a computational protocol for fully automated decontamination of genomes.* ISME J, 2016. **10**(1): p. 269-72.
41. Parks, D.H., et al., *CheckM: assessing the quality of microbial genomes recovered from isolates, single cells, and metagenomes.* Genome Res, 2015. **25**(7): p. 1043-55.
42. Seemann, T., *Prokka: rapid prokaryotic genome annotation.* Bioinformatics, 2014. **30**(14): p. 2068-2069.
43. Eren, A.M., et al., *Community-led, integrated, reproducible multi-omics with anvi'o.* Nature Microbiology, 2021. **6**(1): p. 3-6.
44. Kanehisa, M. and S. Goto, *KEGG: Kyoto Encyclopedia of Genes and Genomes.* Nucleic Acids Research, 2000. **28**(1): p. 27-30.
45. Chaumeil, P.-A., et al., *GTDB-Tk: a toolkit to classify genomes with the Genome Taxonomy Database.* Bioinformatics, 2019. **36**(6): p. 1925-1927.
46. Kozlov, A.M., et al., *RAxML-NG: a fast, scalable and user-friendly tool for maximum likelihood phylogenetic inference.* Bioinformatics, 2019. **35**(21): p. 4453-4455.
47. Letunic, I. and P. Bork, *Interactive Tree Of Life (iTOL) v4: recent updates and new developments.* Nucleic acids research, 2019. **47**(W1): p. W256-W259.
48. Jain, C., et al., *High throughput ANI analysis of 90K prokaryotic genomes reveals clear species boundaries.* Nature communications, 2018. **9**(1): p. 5114.
49. Olm, M.R., et al., *dRep: a tool for fast and accurate genomic comparisons that enables improved genome recovery from metagenomes through de-replication.* The ISME journal, 2017. **11**(12): p. 2864-2868.
50. Bushnell, B., *BBMap: a fast, accurate, splice-aware aligner*. 2014, Lawrence Berkeley National Lab.(LBNL), Berkeley, CA (United States).
51. Langmead, B. and S.L. Salzberg, *Fast gapped-read alignment with Bowtie 2.* Nature methods, 2012. **9**(4): p. 357-359.
52. Shen, W., et al., *SeqKit: A Cross-Platform and Ultrafast Toolkit for FASTA/Q File Manipulation.* PLOS ONE, 2016. **11**(10): p. e0163962.
53. Katoh, K., et al., *MAFFT: a novel method for rapid multiple sequence alignment based on fast Fourier transform.* Nucleic Acids Research, 2002. **30**(14): p. 3059-3066.
54. Singleton, C.M., et al., *The novel genus, 'Candidatus Phosphoribacter', previously identified as Tetrasphaera, is the dominant polyphosphate accumulating lineage in EBPR wastewater treatment plants worldwide.* ISME J, 2022. **16**(6): p. 1605-1616.
55. Kopylova, E., L. Noé, and H. Touzet, *SortMeRNA: fast and accurate filtering of ribosomal RNAs in metatranscriptomic data.* Bioinformatics, 2012. **28**(24): p. 3211-3217.

56. Hyatt, D., et al., *Prodigal: prokaryotic gene recognition and translation initiation site identification.* BMC bioinformatics, 2010. **11**(1): p. 1-11.
57. Bray, N.L., et al., *Near-optimal probabilistic RNA-seq quantification.* Nature Biotechnology, 2016. **34**(5): p. 525-527.
58. Bowers, R.M., et al., *Minimum information about a single amplified genome (MISAG) and a metagenome-assembled genome (MIMAG) of bacteria and archaea.* Nat Biotechnol, 2017. **35**(8): p. 725-731.
59. Flowers, J.J., et al., *Comparative genomics of two 'Candidatus Accumulibacter' clades performing biological phosphorus removal.* ISME J, 2013. **7**(12): p. 2301-14.
60. McDaniel, E.A., et al., *Genome-Resolved Metagenomics of a Photosynthetic Bioreactor Performing Biological Nutrient Removal.* Microbiology Resource Announcements, 2021. **10**(18): p. e00244-21.
61. Camejo, P.Y., et al., *Integrated omic analyses provide evidence that a "Candidatus Accumulibacter phosphatis" strain performs denitrification under microaerobic conditions.* Msystems, 2019. **4**(1).
62. McDaniel, E.A., et al., *Signatures of Microbial Diversity at Multiple Scales of Resolution within Engineered Enrichment Communities.* bioRxiv, 2022: p. 2022.10. 01.510452.
63. Lanham, A., et al., *Long-term operation of a reactor enriched in Accumulibacter clade I DPAOs: performance with nitrate, nitrite and oxygen.* Water science and technology, 2011. **63**(2): p. 352-359.
64. Rubio-Rincon, F.J., et al., *"Candidatus Accumulibacter delftensis": A clade IC novel polyphosphate-accumulating organism without denitrifying activity on nitrate.* Water Res, 2019. **161**: p. 136-151.
65. Oyserman, B.O., et al., *Community Assembly and Ecology of Activated Sludge under Photosynthetic Feast-Famine Conditions.* Environ Sci Technol, 2017. **51**(6): p. 3165-3175.
66. Stokholm-Bjerregaard, M., et al., *A Critical Assessment of the Microorganisms Proposed to be Important to Enhanced Biological Phosphorus Removal in Full-Scale Wastewater Treatment Systems.* Front Microbiol, 2017. **8**: p. 718.
67. Kong, Y., J.L. Nielsen, and P.H. Nielsen, *Identity and ecophysiology of uncultured actinobacterial polyphosphate-accumulating organisms in full-scale enhanced biological phosphorus removal plants.* Applied and environmental microbiology, 2005. **71**(7): p. 4076-4085.
68. Zeng, W., et al., *Influence of nitrite accumulation on "Candidatus Accumulibacter" population structure and enhanced biological phosphorus removal from municipal wastewater.* Chemosphere, 2016. **144**: p. 1018-25.
69. Richardson, D.J., *Bacterial respiration: a flexible process for a changing environment1999 Fleming Lecture (Delivered at the 144th meeting of the Society for General Microbiology, 8 September 1999).* Microbiology, 2000. **146**(3): p. 551-571.
70. He, S. and K.D. McMahon, *'Candidatus Accumulibacter' gene expression in response to dynamic EBPR conditions.* ISME J, 2011. **5**(2): p. 329-40.

5 Conclusions and Future Directions

5.1 Summary

Minimizing aeration inputs for biological nutrient removal (BNR) is a promising strategy to reduce energy demands and operational costs for wastewater treatment plants without the need for major construction upgrades. This work builds upon prior pilot-scale BNR treatment systems conducted in collaboration with the Madison Metropolitan Sewerage District (Madison, WI) in which the overarching goal of achieving successful BNR under low dissolved oxygen (DO) has been demonstrated. In this work, we aimed to understand the implications of low-DO on the overall BNR process and the microbial community structure. We showed that effective BNR can be achieved using ammonia-based aeration control (ABAC) using either continuous or intermittent aeration at low-DO (Chapter 2). Modelling efforts led us to adjust the solids retention time to improve slower nitrification rates in the winter, however increasing the solids retention time led to a reduction in solids setting performance. With improved nitrification performance year-round and an increase in total nitrogen removal, we then evaluated the long-term effect of low-DO on nitrous oxide emissions (Chapter 3). We found that reductions in DO were followed by an increase in nitrous oxide production and emission, however emissions decreased after prolonged exposure to low-DO. Aside from reductions in DO, process nuisances caused performance deviations, such as incomplete nitrification and nitrite accumulation, which corresponded with the highest production of nitrous oxide. We then use genome-resolved metagenomics and metatranscriptomics to compare the Accumulibacter community across pilot-scale BNR systems operating at low-DO. We found that the Accumulibacter community in low-DO BNR environments is diverse, indicating the ability to survive low-DO conditions is widespread amongst the lineage (Chapter 4). The coexistence of multiple Accumulibacter

species with the genetic capability to perform various steps of the dentification pathway, could mean that they occupy niche-differentiating roles. Our results highlight challenges that remain to be resolved before implementation of low-DO aeration strategies in conventional wastewater treatment plants. To this end, we have identified future research areas that address these challenges and further our knowledge the microbial community performing BNR for better operation.

5.2 Explore the limit to which DO does not impact sludge settleability

In an effort to improve sludge settleability, under low-DO conditions, we have explored three options to densify the activated sludge flocs detailed in Amstadt [1]. During the operation of the pilot-scale systems described in Chapter 2, we reconfigured the anaerobic zones of both treatment trains to include multiple tanks in series, which improves the plug-flow conditions. It has been suggested that proper plug-flow conditions are necessary to achieve an optimal organic loading rate[2], a factor that is known to impact sludge settleability[3]. Second, we compared the impact of a return activated sludge fermentation zone, which simultaneously supplements influent organic carbon for N and P removal and impacts the organic loading rate. Third, we implemented sludge selective wasting through size- and gravity-based methods. Despite, these efforts we did not observe any significant improvements to sludge settleability. We did make a preliminary conclusion that DO should not be lowered beyond specific setpoints[1], however these limits need to be further explored. For example, a comparison between cascading DO setpoints in each aerobic zone (as designed in Amstadt (2022)) as opposed the same DO setpoints in the entire aerobic zone (as designed in Chapter 2) could be me made. Evaluation of selective sludge wasting methods should also investigate the minimum amount of sludge flow to

the selective wasting device needed to make a significant impact. However, this strategy must be optimized to maintain the necessary solids retention time to maintain BNR performance. Finally, the impact of increasing the DO should be evaluated to see if settleability can be recovered from low-DO conditions.

5.3 Improve nitrous oxide sampling campaigns

To best capture nitrous oxide emission dynamics, we recommend a high-frequency and long-term sampling campaign. In addition to spatial and temporal measurements, this campaign should include diurnal measurements as nitrous oxide has been observed to be dynamic with varying influent load[4]. Multiple, year-long campaigns should be prioritized as short-term monitoring periods are likely to miss seasonal variations increasing the variability in the recorded nitrous oxide emissions. A rigorous campaign is best implemented using online, continuous measurements. The contribution and kinetics of the various nitrous oxide production pathways to the overall generation over varying operational and environmental conditions (e.g. DO, nitrite concentration, process configuration, etc.) should be evaluated to aid in modelling efforts and mitigation strategies. Isotopic, molecular, and 'omic techniques such as qPCR, qFISH, and metatranscriptomics, could aid in this effort.

5.4 Further analysis of BNR microbial community dynamics under low-DO conditions

Our evaluation of the Accumulibacter community revealed that most Accumulibacter members are equipped to survive low-DO conditions, as has been noted by other studies. It has also been observed that the Accumulibacter community adapts to low-DO conditions by increasing P uptake rates rather than oxygen affinity [5]. Efforts to explore the regulatory mechanisms of these

organisms would improve our understanding of Accumulibacter in low-DO systems, particularly under changing conditions such as intermittent aeration. An in-depth investigation of the nitrifier communities under low-DO conditions using ‘omic methods is also needed to answer the question of adaptation or shift in community members (e.g. canonical NOBs to comammox bacteria). With improving sequencing technology, bioinformatic algorithms, and growing databases of high-quality microbial genomes, we are more equipped to answer these questions. Applying these insights allows for improved process predictions and operation.

5.5 References

1. Amstadt, C., *Assessing the effect of selective wasting and fermentation on slduge settleability and biological nutrient removal in two anoxic-oxic pilot-scale treatment plants*, in *Department of Civil and Environmental Engineering*. 2022, University of Wisconsin-Madison: Madison, WI.
2. Sun, Y., et al., *Feast/famine ratio determined continuous flow aerobic granulation.* Science of The Total Environment, 2021. **750**: p. 141467.
3. Sezgin, M., D. Jenkins, and D.S. Parker, *A Unified Theory of Filamentous Activated Sludge Bulking.* Journal (Water Pollution Control Federation), 1978. **50**(2): p. 362-381.
4. Ahn, J.H., et al., *N2O Emissions from Activated Sludge Processes, 2008−2009: Results of a National Monitoring Survey in the United States.* Environmental Science & Technology, 2010. **44**(12): p. 4505-4511.
5. Keene, N.A., et al., *Pilot plant demonstration of stable and efficient high rate biological nutrient removal with low dissolved oxygen conditions.* Water Res, 2017. **121**: p. 72-85.